



**University of
Zurich**^{UZH}

Modeling the influence of traffic infrastructure characteristics on e-scooter accidents in the city of Zurich

GEO 511 Master's Thesis

Author
Yelu He
21-739-404

Supervised by
Dr. Cheng Fu
Prof. Dr. Robert Weibel
Dr. Wernher Brucks (wernher.brucks@zuerich.ch)

Faculty representative
Prof. Dr. Robert Weibel

30.04.2024
Department of Geography, University of Zurich



**Universität
Zürich**^{UZH}

Modeling the influence of traffic infrastructure
characteristics on e-scooter accidents
in the city of Zurich

GEO511 Master's Thesis

Author

Yelu He, University of Zurich
Mat. Nr. 21-739-404

Supervised by

Dr. Cheng Fu¹

Prof. Dr. Robert Weibel¹

Dr. Wernher Brucks²

¹Department of Geography, University of Zurich

²Department of Road Safety, City of Zurich

Zurich, April 30, 2024

Department of Geography, University of Zurich

Abstract

Rapid emergence of shared electric scooter (e-scooter) services has posed new challenges to road safety issues over the last few years as a serious worldwide public concern. Previous studies have investigated e-scooter accidents from multiple perspectives. However, research gaps still exist in understanding the role of infrastructure-related factors in e-scooter accidents, especially in the city of Zurich. The overarching aim of this thesis is to investigate and model the relationship between the characteristics of traffic infrastructure and electric scooter accidents. To address the lack of knowledge of electric scooter safety issues, a spatial-temporal analysis was first conducted for an overview of the pattern of accident distribution. Curb extraction was achieved by applying the Segment Anything Model to Google Street View images as a supplement to existing infrastructure data. A comprehensive dataset including curb variables, infrastructure entropy, and traffic transport was constructed. With random pseudo points being generated, a correlation between e-scooter accidents and traffic infrastructure was eventually determined by regression analysis. Results from this study indicate a strong correlation exists between the presence of e-scooter accidents and traffic infrastructure features such as speed limit and the presence of curbs. Significant variables related to the severity of electric scooter accidents were determined, including distance to road and curb width type. Although there are limitations in data size, coverage, quality, and approaches. Overall, this study offers insights into e-scooter safety, introduces an analysis process to extract infrastructure from street view images, and confirms the important influence of traffic infrastructure on e-scooter accidents.

Keywords: E-scooter accidents, Infrastructure, Road safety, Segment Anything Model, Google Street View, Traffic network

Acknowledgements

I would like to express my sincere gratitude to all the help, guidance and encouragement I gained during the progress of my master thesis. Specifically, I am grateful to:

- Dr. Cheng Fu and Prof. Dr. Robert Weibel for their insights, guidance and feedback.
- Dr. Wernher Brucks for the support in datasets.
- Gregory Biland for insights in generation of pseudo points and helps in collection of variables.
- Martine Besse and Qi Ying for their proofreading.
- Simona Di Vincenzo and other friends for encouragement and help.
- Yidi Ji for always supporting me.
- My family for support and belief.

Contents

List of Figures	iii
List of tables	iv
List of abbreviations	v
1 Introduction	1
1.1 Motivation and Background	1
1.2 Research Goals	3
2 Related Work	5
2.1 Literature Review	5
2.1.1 E-scooter Studies	5
2.1.2 Effects of traffic-infrastructure characteristics on road accidents	9
2.1.3 Usage of Street View Images in studies of road accidents	11
2.1.4 Application of Segment Anything Model	12
2.2 Research Gaps	13
2.3 Research Questions	14
3 Study Area and Data Preprocessing	15
3.1 Study Area	15
3.2 Data Preprocessing	16
3.2.1 E-scooter accident data	16
3.2.2 Google Street View Images	19
3.2.3 Traffic network and transport-related data	20
4 Methodology	23
4.1 Spatial-temporal Analysis	23
4.1.1 Spatial analysis	23
4.1.2 Temporal analysis	23
4.2 Curb extraction using SAM on GSV	24
4.2.1 Application of SAM	24
4.2.2 Visual interpretation	25
4.2.3 Calculating properties of masks	25
4.2.3.1 Spectral features	26
4.2.3.2 Geometric attributes	27
4.2.4 Classification model using Random Forest	28
4.3 Variables generation	29
4.3.1 Curb variables	29
4.3.2 Entropy variables	30
4.3.2.1 Image entropy	30
4.3.2.2 Whole scene entropy	30
4.3.2.3 Ground scene entropy	31
4.3.3 Traffic-transport variables	31
4.4 Regression Analysis	32
4.4.1 Generation of Pseudo-Absence Points	32
4.4.2 Variables generation for random pseudo points	32
4.4.3 Preparation for regression analysis	33

4.4.3.1	Independent variables preparation	33
4.4.3.2	Dependent variables in regression for accident presence	34
4.4.3.3	Dependent variables in regression for accident severity	34
4.4.4	Regression method	34
4.5	Prediction Modelling	34
5	Results	36
5.1	Spatial-temporal distribution of e-scooter accidents	36
5.1.1	Spatial distribution	36
5.1.2	Temporal distribution	38
5.2	Descriptive statistics of accident causes	40
5.3	Curb extraction	40
5.4	Variables generation of accident points	42
5.4.1	Curb variables	42
5.4.2	Entropy variables	44
5.4.2.1	Image entropy	44
5.4.2.2	Whole scene entropy	44
5.4.2.3	Ground scene entropy	44
5.4.3	Traffic-transport variables	47
5.5	Variables generation of random pseudo-absence points	48
5.5.1	Random pseudo-absence points	48
5.5.2	Variables generation	48
5.5.2.1	Curb variables	49
5.5.2.2	Entropy variables	50
5.5.2.3	Traffic-transport variables	50
5.6	Regression analysis	50
5.6.1	Regression for accident presence	50
5.6.2	Regression for accident severity	51
5.6.2.1	Regression for person injury	52
5.6.2.2	Regression for property damage	56
5.7	Prediction Model	59
5.7.1	Person injury	59
5.7.2	Property damage	60
5.7.3	Grid-based aggregation of prediction result	62
6	Discussion	64
6.1	Overview of E-scooter accidents of Zurich	64
6.2	Curb extraction with SAM	65
6.3	Importance of infrastructure-related variables	65
6.4	Comparison with previous studies	66
6.5	Assessment of SAM performance	67
6.6	Limitations	68
6.6.1	Data availability, coverage and quality	68
6.6.2	Methodological approach	68
7	Conclusions	70
7.1	Main findings	70
7.2	Contributions and insights	70
7.3	Outlook and future research	71

List of Figures

3.1	Study area - City of Zurich	15
3.2	E-scooter accidents distribution overview	16
3.3	Example of GSV images in one location	19
3.4	Distribution of valid and invalid GSV images	20
3.5	Traffic network data overview	21
4.1	Output masks example of SAM	25
4.2	Illustration of color distance using example of pixels of curb mask	28
4.3	Histogram example of spectral features between curb and others	28
4.4	Histogram example of attributes between curb and others	29
4.5	Example of infrastructure features allocation	32
4.6	Illustration of random pseudo points	33
5.1	Spatial distribution overview	36
5.2	Kernel density estimation of accidents in each year	37
5.3	Accidents count per road segment in each year	38
5.4	Brief time series exploration	39
5.5	Time series analysis	40
5.6	Classification result for curb extraction	42
5.7	Example of curb extraction	43
5.8	Distribution of curb extraction results for accident locations	43
5.9	Classification result for whole scene entropy	45
5.10	Classification result for ground scene entropy	46
5.11	Entropy variables generation results for accident locations	47
5.12	Distribution of random pseudo-absence points and valid GSV images	49
5.13	Distribution of curb extraction results for random pseudo-absence points	49
5.14	Entropy variables generation results for random pseudo-absence points	50
5.15	Prediction result for presence of person injury	59
5.16	Prediction result for presence of severe person injury	60
5.17	Prediction result for presence of light person injury	60
5.18	Prediction result for number of lightly injured person	61
5.19	Prediction result for presence of property damage	61
5.20	Prediction result for value of property damage	62
5.21	Aggregated prediction results	63

List of Tables

2.1	Summary of previous e-scooter related review studies	7
3.1	Variables and their brief distributions - General information and involvement . .	17
3.2	Variables and their brief distributions - Infrastructure and circumstances	18
3.3	Parameters setting for GSV API	19
3.4	Datasets source for traffic and transport network	21
4.1	Parameters setting for SAM	24
4.2	Label list of manual interpretation	26
4.3	Variables of spectral features	27
4.4	Variables of geometric attributes	27
4.5	Label groups for whole scene entropy	30
4.6	Label groups for ground scene entropy	31
5.1	Top four main causes of e-scooter accidents	40
5.2	Top four main causes for skidding or self-inflicted accident	40
5.3	Label group statistics for curb extraction	41
5.4	Evaluation metrics of RF classification - Curb extraction	41
5.5	Generated curb variables	43
5.6	Label group statistics for whole scene entropy	44
5.7	Evaluation metrics of RF classification - Entropy of whole scene	45
5.8	Label group statistics for ground scene entropy	46
5.9	Evaluation metrics of RF classification - Entropy of ground scene	47
5.10	Generated entropy variables	47
5.11	Generated traffic-transport variables	48
5.12	OLS regression model for accident presence - Model metrics	51
5.13	OLS regression model for accident presence - Significant variables	51
5.14	Dependent variables for accident impact	52
5.15	OLS regression model for the presence of person injury	53
5.16	GAM regression model for presence of person injury	53
5.17	OLS regression model for presence of severe person injury	54
5.18	GAM regression model for presence of severe person injury	54
5.19	OLS regression model for presence of light person injury	55
5.20	GAM regression model for presence of light person injury	55
5.21	OLS regression model for number of lightly injured person	56
5.22	GAM regression model for number of lightly injured person	56
5.23	OLS regression model for presence of property damage	57
5.24	GAM regression model for presence of property damage	57
5.25	OLS regression model for value of property damage	58
5.26	GAM regression model for value of property damage	58

List of abbreviations

ACF Autocorrelation Function. 23, 39

ARIMA Autoregressive Intergrated Moving Average. 23

FOV Field of view. 19

GAM Generalized Additive Model. 34, 52–55, 57–62, 66

GSV Google Street View. 19, 24, 30, 40, 41, 44, 48, 49, 65, 68–70

KDE Kernel Density Estimation. 23, 64, 68

LOESS Locally Estimated Scatterplot Smoothing. 23

MCC Matthews correlation coefficient. 41

OLS Ordinary Least Squares. 34, 52, 54–56, 58–61, 66

OSM Open Street Map. 20

PACF Partial Autocorrelation Function. 23, 39

RF Random Forest. 28–31, 41, 44, 49, 65

RGB Red Green Blue. 26

SAM Segment Anything Model. 3, 4, 12–14, 24, 25, 28, 30, 40, 41, 44, 49, 65, 67, 69–71

SVI Street view imagery. 3, 11, 12, 14, 19, 27, 29, 65, 68, 71

1. Introduction

1.1 Motivation and Background

Road safety issues cause massive casualties and considerable economic losses globally. According to statistics from the World Health Organization (WHO), road traffic crashes lead to approximately 1.3 million deaths each year worldwide, which is the leading cause of death for children and young adults aged 5-29 years. Moreover, in most countries, road traffic crashes cost 3% of their gross domestic product (World Health Organization, 2023). As for Switzerland, road accidents caused an average of 230 people died and 21258 people injured annually over the past decade (Bundesamt für Statistik, 2023b; Federal Roads Office, 2023). In 2018, road crashes resulted in an estimated economic cost of 16.5 billion CHF, which was 2.4% of GDP (International Transport Forum, 2021).

Recognizing the increasing importance of road safety issues, governments from all over the world are dedicated to solving this problem. According to the 2030 Agenda for Sustainable Development, the United Nations (UN) General Assembly has set several targets concerning road safety issues (United Nations, 2015). Target 3.6 indicates halving the number of global deaths and injuries from road traffic accidents by 2020. Target 11.2 specifies providing access to safe, affordable, accessible, and sustainable transport systems for all, improving road safety, notably by expanding public transport, with special attention to the needs of those in vulnerable situations, women, children, persons with disabilities, and older persons. The UN General Assembly adopted Resolution 74/299 “Improving global road safety” (United Nations, 2020) proclaiming the Decade of Action for Road Safety 2021-2030, with the ambitious target of preventing at least 50% of road traffic deaths and injuries by 2030 in September 2020. A Global Plan for the Decade of Action developed by WHO, the UN regional commissions, and other partners in the UN Road Safety Collaboration was released in October 2021.

A wide range of factors affects road accidents, which are usually related to traffic and road characteristics, behaviours of drivers and other road users, vehicles, and environmental conditions (C. Wang et al., 2013). One of the most critical factors impacting road safety outcomes is road infrastructure and environment (Elvik et al., 2009). In previous studies, road accidents have been studied in the context of infrastructure characteristics, including roadway geometries (Shankar et al., 1995), road elements (e.g., number of lanes and lane widths, shoulder width (Noland & Oh, 2004), road curvature (Haynes et al., 2007), road infrastructure improvements (e.g., road upgrading and pavements (Navin et al., 2000)), roundabout design (Hels & Orozova-Bekkevold, 2007), intersections design (Tanishita et al., 2023), and signalisation (Abdel-Aty & Wang, 2006). However, most studies on road safety use official statistics data from the government, survey data, observational data collected through on/off-board devices or sensors, social media, simulation models, as well as open-source data, which is generally labor-intensive and time-consuming with a general requirement of high technical cost and specialized equipment

(Sohail et al., 2023). Furthermore, using the aforementioned traditional data collection methods, a detailed description of specific road infrastructure features (e.g., curbs) may be hard or expensive to extract. Detection and extraction of curbs, which has attracted research attention over the last two decades, is regarded as fundamental for autonomous vehicle navigation related to road safety. The data acquisition methods can be classified into vision, LiDAR, ultrasonic, or a combination of these sensors (Romero et al., 2021), which may have relatively low coverage and complexity issues. Thereby, in order to understand the relationships between road infrastructure features and accidents comprehensively, novel methods with lower cost, less complexity, and higher coverage to extract up-to-date data on detailed road infrastructure (e.g., curbs) are required.

The growing presence of micro-mobility is identified as an emerging challenge to road safety based on the WHO’s Global Plan for the Decade of Road Action 2021-2030 (World Health Organization, 2021). There has been a rapid emergence of shared electric scooters (e-scooters) in recent years. As a micro-mobility service, it provides an efficient and environmentally friendly mode of first- and last-mile transportation (Ma et al., 2021), which also gives users the freedom to make optimal use of road infrastructure and the ability to cut through traffic because of its small size. However, as e-scooters grow in popularity, increasing road accidents that involve them are reported, which have created additional crash risks and caused great concern regarding the road safety of e-scooters by the authorities worldwide. Researchers have studied e-scooter issues in more than 15 countries with a wide range of research topics (Kazemzadeh & Sprei, 2022), including road-safety related issues (safety concerns, accident patterns and issues, traffic enforcement (Kazemzadeh et al., 2023), accident factors (Bjmskau & Karlseo, 2022)), injury patterns (Kleinertz et al., 2021; Niemann et al., 2023), users’ profile and usage pattern (Reck & Axhausen, 2021), system characteristics (Pobudzei et al., 2023), and impacts (Şengül & Mostofi, 2021). In Switzerland, only user characteristics (Reck & Axhausen, 2021), usage, competition, and mode choice (Reck et al., 2021) were studied. A study that considers and investigates more perspectives on e-scooter accidents in the city of Zurich would be of interest.

Previous studies indicate that adverse environmental conditions, risky behaviour of riders (such as alcohol consumption and drug use before riding, smartphone use, and wearing no helmet while riding), hazardous surface features, reduced visibility during nighttime, and infrastructure-related factors all contribute to e-scooter accidents (Azimian & Jiao, 2022; Karpinski et al., 2022; Pobudzei et al., 2023; Stigson et al., 2021; White et al., 2023). Nonetheless, the understanding of how specific road infrastructure features affect e-scooter accidents is insufficient. There is still a lack of comprehensive and factual data-based analysis of e-scooter accidents and their causes, especially considering the impact of traffic-infrastructure characteristics. Moreover, e-scooter users experience more severe vibration impact compared to other road users like cyclists while riding on the same infrastructure facilities (Ma et al., 2021). Small infrastructure features like curbs are likely to cause a higher risk for road accidents of e-scooters. Further data collection of curbs is required to better analyze the impacts of road infrastructure features on e-scooter accidents.

Street view imagery (SVI) has become an important and prevalent data source for urban analysis

and geographic information science in recent years. It is used across a wide range of fields with various applications, including spatial data infrastructure, greenery, health, urban morphology, transportation and mobility, walkability and bikeability, real estate, urban perception, and socioeconomic studies (Biljecki & Ito, 2021). SVI provides valuable large-scale data for urban areas, allowing examination of the visual environment from a human perspective. Numerous studies have attempted to detect, identify or extract objects on road infrastructure from SVI, like traffic signs (Balali et al., 2015; Campbell et al., 2019), road lanes (Mamidala et al., 2019), sidewalks (Ning et al., 2022), road safety barriers (Rahman et al., 2021), signalized intersections (X. Li et al., 2022), pavement marking (Kong et al., 2022) and pavement damage (Ren et al., 2023). Despite this, no studies have investigated curbs extraction from SVI, which is worthwhile to complement current data collection methods.

Image segmentation, which can be defined as classifying pixels with semantic labels or partitioning individual objects or both, plays an important role in computer vision and image processing (Minaee et al., 2022). Numerous image segmentation techniques and algorithms have been applied in feature extraction, among which Segment Anything Model (SAM) stands out as a promptable zero-shot image segmentation model trained with over 1 billion masks on 11 million images (Kirillov et al., 2023). Studies have indicated that SAM has made significant progress in segmentation (C. Zhang et al., 2023) and offered promising solutions for extensive objects detection, which includes features in built environment (civil infrastructure defect (Ahmadi et al., 2023), structural damage (Balaji et al., 2024), mobility infrastructure (Sultan et al., 2024; Xia et al., 2023), safety-related architectural features (Di & Gong, 2024)), remote sensing (tree species (Ferreira et al., 2024), land use and land cover (T. He et al., 2024), rooftop photovoltaics (R. Yang et al., 2024), water extent (Zheng et al., 2023)), medical images (Y. Zhang et al., 2024), other fields (tunnel water leakage (Chen et al., 2024), animal behaviour analysis (C. Yang et al., 2023)). Considering the task of SVI segmentation to extract curbs, SAM has the potential to address this challenge.

1.2 Research Goals

Road safety is increasingly recognised as a serious worldwide public concern, which faces an emerging challenge of micro-mobility, in particular, e-scooters. In the countless studies on e-scooters, much uncertainty still exists about the relationship between e-scooter accidents and traffic infrastructure characteristics, which is likely to be different from that of other road users' accidents. As infrastructure is proven to be one of the key factors impacting road crashes, the lack of data collection methods with lower cost and less complexity for detailed infrastructure features remains a problem. With rapid development of image processing and segmentation techniques, applying advanced AI-based models on SVI to extract specific infrastructure features has become a potential solution.

The major objective of this master's thesis is to understand how traffic infrastructure characteristics affect e-scooter accidents in the city of Zurich. To fill the lack of knowledge on e-scooter accidents in Zurich, other than descriptive statistics, spatial-temporal analysis combined with

geographical information system data is applied. Additionally, with a focus on specific infrastructure features, this study proposes to extract detailed information about curbs from street view images of e-scooter accident locations by using SAM and to classify detected objects considering perspectives of spectral properties and geometric attributes. Curb-related variables are therefore generated based on the results of extraction and classification as a supplement to traffic-infrastructure variables obtained from government data. Regression analysis is then performed aiming to investigate the relationship between traffic infrastructure characteristics and e-scooter accidents. Moreover, with generation of pseudo-absence points, a prediction model for the presence and severity of e-scooter accidents is built, which provides an insight into high risk locations of e-scooter accidents in the city of Zurich.

2. Related Work

2.1 Literature Review

2.1.1 E-scooter Studies

The shared e-scooter has rapidly gained popularity as a novel type of micro-mobility worldwide since its introduction in the USA in 2017 (Hosseinzadeh et al., 2021), of which recent research outputs have covered multiple aspects. The main themes of e-scooter studies can be classified into the following five categories: system characteristics, user profile and behavior, data and technology, health and safety, impact, policy, and regulation.

- **System characteristics:** It has been demonstrated that shared e-mobility is predominantly used for short trips. While e-bike sharing is found to be mostly used for commuting trips, other sharing e-mobility systems are mainly for leisure trips. Moreover, the service demand is significantly affected by attributes of shared e-mobility system, socio-demographic characteristics, land use pattern, level of transport connectivity of the locations, and also psychological variables and travel patterns of the individual (Liao & Correia, 2022).
- **User profile and behavior:** Previous research has indicated that current users of shared e-mobility are mostly male, middle-aged people with relatively high income and education (Liao & Correia, 2022). In Zurich specifically, users tend to be young, university-educated, full-time employed males who live in affluent households without children or cars (Reck & Axhausen, 2021). The mode choice of micro-mobility is nested and determined by distance and time of day, and the relationship between fleet density and usage is concluded as a "plateau effect," which means the fleet densities increase as marginal utility decreases (Reck et al., 2021).
- **Data and technology:** Different data collection methods have been applied, and the data sources are: medical records from emergency/trauma center in hospitals (Frank et al., 2023; Harbrecht et al., 2022; Linhart et al., 2024); local authorities, transport modeling tools, statistics, census; public transport or micro-mobility providers; survey, observation, interview, and experiment; open source databases (Kazemzadeh & Sprei, 2022; Ma et al., 2021; Oeschger et al., 2020; O'Hern & Estgfaeller, 2020). Also, supporting technologies for e-scooter have been investigated, such as on-board charger arrangement for installation (Solero, 2001).
- **Health and safety:** E-scooter accidents led to extra burden on the emergency capacities (Harbrecht et al., 2022). Numerous studies with a focus on injury patterns of e-scooter accidents have found that head, face, and upper limbs are the most commonly affected

parts. Compared to other road user accidents, e-scooter accidents occur more on weekends with alcohol use (Kleinertz et al., 2021). Several studies have suggested helmet use, strict alcohol controls, and locking periods could be an effective way to prevent serious injury from e-scooter crashes (Frank et al., 2023; Linhart et al., 2024). The observed injury pattern and severity should also take into account the differences in age, gender, and driving behavior between e-mobility services (Niemann et al., 2023). A large and growing body of literature has investigated e-scooter accidents. E-scooters are more vulnerable to potholes and road obstacles because of their small wheel diameter, thickness, and wheel type combined with speeds of 20-50 km/h (International Transport Forum, 2020). E-scooter crashes mostly take place at intersections or driveways, on the transition between sidewalk and roadway (Shah et al., 2021), arterial roads/streets (H. Yang et al., 2020), while the riders are most frequently injured on sidewalks (Cicchino et al., 2021). Most accidents are recorded as single crashes (Stigson et al., 2021), without the involvement of other road users (International Transport Forum, 2024). The main causes and factors that contribute to e-scooter accidents have been particularly analyzed, which is summarized in the forthcoming paragraph.

- **Impact:** Attention has also focused on the impact of e-scooter from diverse perspectives, which could be categorized into environment, society-users, economy, transport, and safety (Mitropoulos et al., 2023). It has been suggested that shared e-mobility services can potentially cause positive effects on transportation and environment, such as reducing car use, car ownership, and greenhouse gas emissions (Liao & Correia, 2022). The environmental burdens associated with charging e-scooters are found to be small relative to materials and manufacturing burdens as well as the impacts of transporting scooters to overnight charging stations. A net reduction in environmental impacts could be nearly realized when e-scooter ride replaces average personal automobile travel (Hollingsworth et al., 2019). Moreover, studies indicate a great potential for a modal shift from other transport modes to e-micro-mobility vehicles in travel behaviors (Şengül & Mostofi, 2021) and an alternative and asset to avoid public transport and to promote social distancing, for example, during COVID-19 pandemic time (Dean & Zuniga-Garcia, 2023; Dias et al., 2021). As for economic impact, using e-scooters together with public transport is highly beneficial. The single use of e-scooters is reasonable compared to other means of transport, except bike and walking. E-scooter combined with public transport offers considerable savings in comparison with car use, which reduces user cost by 69%. But the combination of e-scooters with a train, subway, or bus increases the cost by 35% in contrast to exclusive use of public transport (Edel et al., 2021). Another dominant field is the impact on safety, in which a large number of studies have analyzed e-scooter incidents and examined them, summarized in the previous point.
- **Policy and regulation:** E-scooter safety regulations on minimum age, maximum speed, maximum power, limit for drink-ride, requirement of helmet, mandatory insurance and riding on sidewalk varies from countries (International Transport Forum, 2024), and many places do not have policies for e-scooter usage. Researchers have attempted to discuss the regulations on micro-mobility, such as sidewalk and curb management policies, equitable

service standards and equity programs, enforcement and data standards (Shaheen & Cohen, 2019), economic regulation (Button et al., 2020), trending policy strategies like using pilot programs and vendor limits or caps (Riggs et al., 2021).

Table 2.1: Summary of previous e-scooter related review studies

Main focus	Research topics covered	Main conclusion(s) or recommendation(s)	Paper
Integration of micro-mobility and public transport systems	Data sources, system characteristics, users, impacts	The main gaps that could be identified are the impacts of integrating micro-mobility and public transport on different aspects of society, the environment, and the economy.	Oeschger et al., 2020
Current research status	User behavior, vehicle technology, planning, policy, health, and safety	A proliferation of research in the field of powered micro-mobility is identified. Safety issue is important, particularly when using shared micro-mobility systems.	O'Hern and Estgfaeller, 2020
Knowledge from sustainability aspects on micro-mobility	Benefits, technology, policy, behavioral mode-choice	The findings demonstrate the importance of micro-mobility as a low-carbon mobility and sustainable transport mode in urban areas.	Abduljabbar et al., 2021
Current knowledge	Uses and users, health and environmental impacts, policy issues	E-scooter renters' profiles highly match that of other micro-mobility service users. E-scooters are frequently related with a high perception of risk from the public. Further investigation into environmental impact of shared e-scooters and policy changes are required.	Bozzi and Aguilera, 2021
Impacts of e-micromobility	Travel behaviors, energy consumption, environmental impacts, safety, and related regulations	An overview of impacts of e-micromobility on urban transport is provided. Surplus energy demands and impacts of land use parameters, urban forms, and population density on citizens' e-micromobility mode choice are advisable to investigate.	Şengül and Mostofi, 2021
E-scooter user experience	Data collection methods, e-scooter (non) users, trip characteristics, infrastructure characteristics	The findings suggest a lack of studies to evaluate e-scooter level of service. Research gaps in e-scooters remain in their travel demand, practice in existing infrastructure, and traffic characteristics.	Kazemzadeh and Sprei, 2022
E-scooter user behavior	Usage pattern, demand estimation and potential impacts (in transportation, environment, health, social and land use)	Shared mobility services are mainly used for short-distance trips, with users of mostly male, middle age, well education and high income. The service demand is significantly related to operational attributes of shared mobility system, socio-demographic characteristics, land use patterns, and level of transport connectivity of the locations.	Liao and Correia, 2022
E-scooter injuries	Demographic characteristics, most common injuries, management of patients	Upper limb fractures are the leading injuries from e-scooters. And the major mechanism of injury is falling.	P. Singh et al., 2022
Psycho-social characteristics of e-scooter riders	Behavioral and risk-related features	Improvement and enforcement of traffic laws, and training processes for e-scooter users are in growing need.	Useche et al., 2022
Current knowledge	Use patterns, consumer perception, environmental impact	Knowledge needs in deep comprehension of use patterns; e-scooter functions in transport system; policies, designs, and operations.	Badia and Jenelius, 2023
E-scooter safety with focus on transport and medical research domains	Safety concerns of e-scooting, accident patterns, and issues, traffic enforcement	Analysing interactions of e-scooters with other road users, and adopting surrogate safety measures for e-scooters is in a dire need. In e-scooters involved collisions, head and face injuries are found to be the most common injury types.	Kazemzadeh et al., 2023
Attributes and impacts of e-scooter operations and services	Attributes in service, infrastructure type, and operation of e-scooters. Impacts on environment, society-users, economy, transport performance, and safety.	The study concludes that the selection of e-scooter type and role within the transport system should be guided by the community. The findings suggest a need for the development of e-scooter impact estimation and investigation of the relationship between user characteristics, impacts, and e-scooter attributes.	Mitropoulos et al., 2023

Previous literature review studies on e-scooters are summarized in Table 2.1, which overall indicate a proliferation in this field. Collectively, these studies outline the main gaps in the following areas: functions and impacts of integrating e-scooter and public transport, operation in existing infrastructure related to safety issues, improvement and enforcement of traffic laws and regulations, e-scooter usage patterns, traffic characteristics, travel demand, as well as investigation into interactions between e-scooter and other road users.

There is a consensus among researchers that safety is one of the most crucial topics in micro-mobility studies, particularly e-scooter studies. A large number of articles have analyzed the characteristics of e-scooter accidents and attempted to model the causes and factors contributing to them. Regarding the crash type, most accidents are recorded without the participation of other road users (International Transport Forum, 2024). A study on e-scooter fatalities in the United States from 2018 to 2020 using media and police reports found that 86% of e-scooter crashes involved motor vehicles, and 28% of them were hit-and-runs. Two main crash types of fatal crashes are found: an e-scooter was stuck by a motor vehicle from behind, and an e-scooter rider lost control of the e-scooter (Karpinski et al., 2022). Another article collected crash-related reports based on web content mining in German found that approximately half of the crashes are due to solo rider failure (Brauner et al., 2022). Analyses in Sweden showed that most of the injuries occurred in single crashes, while another road user was injured in 13% of the cases because of interactions with e-scooters or due to a parked e-scooter (Stigson et al., 2021). As for the spatial distribution, e-scooter accidents are identified to happen at intersections or driveways, transition areas between sidewalk and roadway (Shah et al., 2021), while their collision with vehicles mainly took place on arterial roads/streets and intersections (H. Yang et al., 2020). E-scooter riders are mostly often injured on sidewalks (Cicchino et al., 2021). Compared to bicycle collisions, e-scooter crashes occur predominantly in the city center, and concentrate next to traffic signals on primary roads with adjacent intersections and a mix of land use (Pobudzei et al., 2023). Considering the temporal factors, the majority of e-scooter accidents took place at night (Brauner et al., 2022; Karpinski et al., 2022) or in the evenings. E-scooter accidents happened more commonly on Fridays or during weekends (Pobudzei et al., 2023; Stigson et al., 2021). In terms of user behavior, abundant studies have shown that behavior, experience and other rider-related factors significantly correlate with micro-mobility safety. Young, male riders are generally over-represented among all users of e-scooter accidents (Azimian & Jiao, 2022; Bjsmskau & Karlseo, 2022; International Transport Forum, 2020, 2024), as revealed in studies that user attributes like age and gender are related to travel behavior (Gioldasis et al., 2021). Driving under drug influence or alcohol consumption is an indispensable factor for e-scooter accidents (Brauner et al., 2022; Gioldasis et al., 2021). Misuse of e-scooters is another common cause, such as riding e-scooters in pairs, in the wrong directions or on forbidden terrain (Brauner et al., 2022), not following traffic rules, and being distracted by smart mobile devices (Bjsmskau & Karlseo, 2022). Additionally, environmental conditions have been proven to be another factor for e-scooter crashes. Unfavorable environmental surroundings like precipitation and fog (Karpinski et al., 2022), lighting and surface condition, direction of traffic flow and level of demand (White et al., 2023), road with pothole or low friction (Stigson et al., 2021) were revealed as risk factors. Finally yet importantly, infrastructure-related factors are indicated to

contribute to e-scooter accidents. Several studies have revealed that e-scooter accidents mostly occurred in dense urban settings (Azimian & Jiao, 2022). However, e-scooter riders experience more severe vibration impact than other road users from the same facilities regardless of the pavement types, which is caused by e-scooters' quick changes in acceleration (Ma et al., 2021), smaller wheel diameter and thickness (International Transport Forum, 2020). Infrastructure factors, including surface transitions, riding surface type, and riding locations (White et al., 2023) were therefore examined to be one of the most crucial precipitating factors. Studies also indicated that street length and type, number of street nodes, and traffic signals were statistically significant factors (Pobudzei et al., 2023), while collision between e-scooters and curbs is another common cause (Stigson et al., 2021). In view of all the literature that has been mentioned so far, factors of e-scooter accidents are summarised as risky behavior of users, reduced visibility during nighttime, adverse environmental conditions, and infrastructure-related factors.

2.1.2 Effects of traffic-infrastructure characteristics on road accidents

Road safety generally involves a variety of different aspects, including road infrastructure, road user behaviors, traffic characteristics, environmental circumstances (Sohail et al., 2023), and vehicles (C. Wang et al., 2013). Concerning road user behaviors, several studies have revealed how driver and pedestrian behaviors affect road accidents. Driving behaviors include mainly two categories, inattentive driving, and aggressive/reckless driving, which are often the primary causes of traffic crashes (Chan et al., 2020; Iio et al., 2021; Jahangiri et al., 2016; Paleti et al., 2010). Also, drivers were found to decrease their speed and increase headway as compensatory measures to reduce the workload imposed in general, during distracting activity or disadvantageous weather conditions (H. Singh & Kathuria, 2021). Additionally, pedestrian risk behaviors such as using electronic gadgets and mobile phones and non-using pedestrian crosswalks are reported to be frequently involved in road accidents (Levulytė et al., 2017; Narváez et al., 2019). Regarding environmental circumstances, it has been proven in several papers that lighting and weather conditions have an impact on crash severity. For instance, one research focusing on accidents in Saint Petersburg from 2015 to 2021 has found that missing road illumination had the highest influence on crash severity, which increased fatality in the range of 10.3% to 13.9%. Besides, precipitations are one of the most contributing factors that negatively affect crash severity, causing a rise in fatality and severe injuries (Rodionova et al., 2022). As for vehicle-related factors, determined vehicle handling and stability characteristics that lead to loss of control or proneness to overturning are identified (JONES, 1976). Besides, the association between accident severity and vehicle type has been examined to be significant (George et al., 2017; Manap et al., 2021).

Another crucial factor for road accidents is traffic conditions, which mainly include speed, traffic density, traffic flow as well as traffic congestion. First, speed is a vital factor exerting a decisive influence on road accidents concerning both occurrence and severity (Elvik, 2004; Harms, 1993). With controlling traffic exposure and road infrastructure characteristics, it has been demonstrated that there is a positive relationship between mean speed and injury accidents (Gitelman et al., 2017). Second, the impact of traffic density on accidents has been investigated by using variables such as Volume over Capacity (V/C) ratio index. An interstate study in Detroit

found that the correlation between accident rates and V/C values suits a U-shaped pattern, which indicates that accident rates in a very low hourly V/C range are the highest, decrease with rise of V/C and increase again while V/C continues to increase (Zhou & Sisiopiku, 1997). Another research focusing on single and multi-vehicle highways revealed a negative-exponential relationship between single-vehicle accidents and density (Ivan et al., 2000). Accident risk and number of crashes increase with higher traffic density and V/C, but prediction models that consider traffic volume as the only explanatory covariate may not be adequate to describe accident process on freeway segments (Lord et al., 2005). Third, traffic flow also has an influence on accidents. Previous studies investigated the relationship between traffic flow and accidents and found that incidence rates for both property damage-only crashes and injury crashes are the highest when the traffic flow is the lightest (under 400 vehicles per hour). And incidence rates are the lowest when the traffic flow is at a rate of 1000 to 1500 vehicles per hour (Martin, 2002). Moreover, by providing tools to monitor real-time safety level of traffic flow on an urban freeway, a strong relationship between traffic flow conditions and accidents has been demonstrated (Golob et al., 2004). Fourth, traffic congestion is another problem which leads to risky situations. One study using a disaggregate spatial analysis in London has examined how congestion affects traffic safety and found that congestion as a mitigation of accident severity may be less inclined to occur in urban surroundings but may still be a contributing factor on higher speed roads and motorways (Noland & Quddus, 2005). Also, a study on urban multi-lane freeways in Colorado revealed that accident total rates together with injury and fatal crash rates increase with an increase in congestion (Kononov et al., 2008). It has been suggested that increased traffic congestion is associated with more fatal/killed and serious injury accidents, while congestion only has little impact on slight injury accidents (Chao Wang & Ison, 2013). Moreover, it has conclusively been shown that traffic congestion levels interact with road infrastructure effects for road crashes (Noland & Quddus, 2005).

A great number of existing studies have emphasized the important influence of infrastructure characteristics in road accidents. The road infrastructure and built environment-related factors include roadway geometry, road surface, road complementary, roadside equipment as well as intersection and roundabout design. First and foremost, findings from numerous studies support that road geometry plays a vital role in road accidents. A study focusing on principal arterial roads in Washington State revealed that an increase in section length and number of lanes tend to increase accident frequency, while narrower lanes less than 3.5 meters decrease accident frequency (Milton & Mannering, 1998). However, a study in low-volume non-urban roads found that accident rates decrease with increasing lane width (less than 3 to 3.25 meters) and increase with further extension of lane width (Gitelman et al., 2014). As for shoulder width, an initial increase in shoulder width, up to 2 to 2.5 meters, is related to an increase in accidents, while a further increase in shoulder width leads to a decrease in accidents (Gitelman et al., 2014). In addition, an increase in the number of lanes has also been found to be associated with an increase in both accidents and fatalities (Noland & Oh, 2004). In terms of curvature, horizontal and vertical alignments have been investigated to affect the frequency of accident occurrence. The number and average spacing of horizontal curves, as well as curvature radius designed for road segments with different speed limits, have various impacts on accidents of different

types (Shankar et al., 1995). Also, increasing the percentage of horizontal curve length per kilometer is likely to increase the probability of possible injury relative to property damage only (Shankar et al., 1996). The association between curvature measures and the number of fatal, serious, and slight collisions was studied in the United Kingdom, and the result shows that collision numbers negatively relate to road curvature. Cumulative angle is the most strongly curvature measure that relates to fatal crashes. For instance, an increase of 1° in cumulative angle per kilometer is linked with approximately a 0.5% decrease in crashes (Haynes et al., 2007). Similarly, an increase in minimum horizontal radius is found to be related to injury accident reduction (Gitelman et al., 2014). A non-linear relationship between curve radius and crash risk has been reported, that the crash risks increase exponentially as curve radius decrease (B. Wang et al., 2017). Regarding road surface, previous studies have proven that crash risk increases due to road surface with inadequate friction, uneven pavement, ice, snow, oil, and leaves (Papadimitriou et al., 2019). Furthermore, road complementary and roadside installations such as median barriers, sidewalks, bus bay, and signalization are considered to be another factor for road accidents (Abdel-Aty & Wang, 2006; Hanson et al., 2013; Vlahogianni et al., 2012). Researchers have found that bus stops, parking spaces as well as object units are positively correlated to pedestrian accidents (Pljakić et al., 2022). Several studies reported that curb ramps and the presence of a roadside curb increase the likelihood of safety-critical events for road accidents (Stigson et al., 2021; B. Wang et al., 2017). Infrastructure improvement has also been suggested to reduce the frequency of rear-end collisions (Navin et al., 2000). Last but importantly, the relationship between junction type, roundabout and intersection design, and road accidents has also been demonstrated (Hels & Orozova-Bekkevold, 2007; Tanishita et al., 2023; Vlahogianni et al., 2012).

2.1.3 Usage of Street View Images in studies of road accidents

Street view imagery (SVI), as one of the most important and entrenched data sources, is been applied in countless papers in the field of urban studies (Biljecki & Ito, 2021). The biggest application domain is using SVI to create and maintain spatial data infrastructure, such as mapping buildings (Ogawa & Aizawa, 2019; L. Zhang et al., 2020), extracting characteristics of buildings and cities (Y. Li et al., 2018; Q. Yu et al., 2020), constructing 3D model (Bruno & Roncella, 2019; Kim et al., 2020), predicting land use (Shivangi Srivastava & Tuia, 2020). Another dominating area is urban greenery, like measurement of near road greenery and greenery networks (B. Y. Cai et al., 2018). Further applications include health and well-being (Keralis et al., 2020), urban morphology (Middel et al., 2019), walkability (Y. Li et al., 2022; Steinmetz-Wood et al., 2020; Yenchu, 2019), bikeability (Ito & Biljecki, 2021), real estate (Hanibuchi et al., 2019), urban perception (Gong et al., 2019), visual quality (Ye et al., 2019), as well as socioeconomic studies (Diou et al., 2018).

Another major application area is in transportation and mobility studies, where numerous papers focus on detecting and extracting specific objects on road infrastructure from SVI. Lane detection algorithms combined SVI with a convolutional neural network model have been developed (Mamidala et al., 2019). Combined with aerial imagery, sidewalk extraction from SVI is

also realized (Ning et al., 2022). Likewise, previous studies have detected, classified, and mapped the traffic signs from SVI and combined them with their sizes and positions (Balali et al., 2015; Campbell et al., 2019). As for specific road surface information, authors have attempted to detect pavement marking defects and damage like cracks, potholes, manhole cover as well as patch (Kong et al., 2022; Ren et al., 2023). Concerning road complementary, detecting signalized intersections and road safety barriers such as concrete barriers, metal crash barriers, and rumble strips from SVI become a reality (X. Li et al., 2022; Rahman et al., 2021). Furthermore, researchers have proposed approaches to classify street context and segment roads (Alhasoun & Gonzalez, 2019; Chacra & Zelek, 2016).

So far, SVI has also provided important insights into our current knowledge on road safety. Data derived from SVI is used to obtain pedestrian and road infrastructure features for analysis on the severity of pedestrian casualty (Hanson et al., 2013). House features annotated by using SVI were found to be able to improve car accident risk prediction (Kita-Wojciechowska & Kidziński, 2019). Features of built environment derived from SVI were found to be strongly associated with perceived crash risk among school-aged children (Kwon & Cho, 2020). An automatic approach to extract and map road safety features from SVI was found to largely improve model performance (Sainju & Jiang, 2020). One study using indices of drivers' visual environment calculated from SVI revealed that the proportion of trees and the proportion of road length with trees are related to the frequency of speeding crashes (Q. Cai et al., 2022). Additionally, another research defined several types of street spaces visible to drivers by using SVI and examined that an open road type of street space (with more visible sky, roadway, and signage) is significantly associated with the greatest increase in road crashes (Stiles et al., 2022). Moreover, hazard scenarios for non-motorized transportation identified using SVI provide insights for new methods to improve vehicle safety (Y. Wang et al., 2022). Streetscape elements extracted from SVI have been used to investigate their relationship with vehicle accidents, and the findings suggest that they could effectively describe built-environment information at road-segment level (Hu et al., 2023). Besides, SVI was also used to address the identification of risk factors for cyclist safety, such as tram and train rails (Rita et al., 2023). Furthermore, pedestrians' perceived road safety detected by SVI was proposed (Hamim & Ukkusuri, 2024). Possible misperception of road safety from SVI has also been investigated (X. Yu et al., 2024).

2.1.4 Application of Segment Anything Model

With the rapid evolution of artificial intelligence (AI) in the past few years, an advanced AI model developed by Meta AI in 2023, Segment Anything Model (SAM) has made great progress in breaking the boundaries in image segmentation (C. Zhang et al., 2023). Trained with the largest segmentation dataset to date (over one billion masks on eleven million images), consisting of three components (an image encoder, a prompt encoder, and a mask decoder), SAM is able to produce high-quality object masks from simple input prompts and to generate masks for all objects in an image with outstanding zero-shot performance on various segmentation tasks (Kirillov et al., 2023). Plenty of studies have applied SAM in a wide range of fields to improve object detection from images. One of the dominating fields is segmenting medical images (Y. Zhang et al., 2024).

In the field of civil infrastructure and built environment, studies presented that SAM provides an effective solution with more accurate and comprehensive results for detecting features such as cracks in concrete structures (Ahmadi et al., 2023), assessing the impact of earthquakes on buildings and infrastructure (Balaji et al., 2024), and generating spatial inventory of architectural features (Di & Gong, 2024). Besides, researchers have also proposed a SAM-based framework combined with aerial or satellite imagery data to obtain road infrastructure (Sultan et al., 2024) and pedestrian infrastructure (Xia et al., 2023), which further enhanced SAM's effectiveness and efficiency in segmentation tasks. Furthermore, another burgeoning application area is remote sensing. Recent studies have employed SAM on satellite and aerial images to improve tree species classification (Ferreira et al., 2024), map urban flooding (Y. He et al., 2024), extract rooftop photovoltaics (R. Yang et al., 2024), as well as to detect scalable water extent (Zheng et al., 2023). In an evaluation study focusing on land use and land cover segmentation in remote sensing imagery, SAM was examined to detect objects of various sizes accurately, presenting rich content and high consistency with reference polygons (T. He et al., 2024). In addition, SAM has also been applied for inspection of tunnel water leakage (Chen et al., 2024), extraction of landmarks from old drawings and photos (David et al., 2023), and tracking animal behaviors (C. Yang et al., 2023).

Researchers have also shown an interest in quality assessment and performance evaluation of SAM. It has been demonstrated that SAM has an excellent performance in the discernment of well-circumscribed objects in certain imaging modalities (Y. Zhang et al., 2024). By investigating SAM applications in different fields, it was observed that SAM performs excellently in common scenes, but requires prior knowledge of manual prompts for complex scenes. The effectiveness decreases in low-contrast applications, while small and irregular objects may still be challenging for SAM (W. Ji et al., 2023). Also, SAM was found to segment occluded objects into several separated masks (G.-P. Ji et al., 2023). In application of remote sensing imagery, SAM resulted in reduction of manual annotation (Osco et al., 2023), and was found to excel in apprehending contextually similar regions (Yilmaz & Kavzoglu, 2024). However, studies have shown that SAM has limitations in complex scenarios with lower spatial resolution images (Osco et al., 2023), as well as constraints in specific scenarios such as excessive segmentation in areas with rich texture information or inadequate segmentation in areas with small differences (Yilmaz & Kavzoglu, 2024).

2.2 Research Gaps

In view of all the literature that has been mentioned so far, several research gaps are identified as follows:

- With an increasing concern on the safety issue of e-scooters, previous research has investigated e-scooter accidents from various perspectives in different countries. However, there have been few studies about e-scooter accidents in the city of Zurich, Switzerland.
- Abundant evidence emphasized the important impact of traffic-infrastructure character-

istics on road accidents. What is not yet clear is the influence of specific infrastructure features such as curbs, of which the details are hard or expensive to obtain by using traditional data collection methods. Extraction curb information using SAM from SVI is worth further investigation.

- Although numerous studies have indicated that one of the most contributing factors for e-scooter accidents is infrastructure-related, much uncertainty still exists about the relationship between traffic-infrastructure characteristics and e-scooter accidents.

2.3 Research Questions

The aim of this master's thesis is to analyze e-scooter accidents and to identify the influence of traffic-infrastructure characteristics on them in the city of Zurich. Research questions are formulated as follows, which serve as an initial foundation and provide guidance for further analysis during this project.

RQ1 What are the spatio-temporal patterns of e-scooter accidents in Zurich? What are the main causes of the accidents?

RQ2 How could infrastructure features be extracted from SVI by using SAM?

RQ3 How do traffic-infrastructure characteristics relate to e-scooter accidents?

3. Study Area and Data Preprocessing

3.1 Study Area

This thesis focuses on the city of Zurich, which is located in the northeastern part of Switzerland. As the largest city and one of the economic and cultural centers in Switzerland, it has over 447,000 inhabitants at the end of 2023 with a total area including water of 91.9 square kilometers (Präsidualdepartement, 2024). In Switzerland, the average daily distance traveled per person is around 30 kilometers. The overall transport modal split is: 69% by car, 16% by railway, 5% for travel on foot, 3% by public road transport (bus, tram), 3% by bike (including e-bike), and 1% with motorized two-wheeler. Compared to 2015, travel distances of almost all means of transport decreased, while the travel distance of e-bikes is the only one to be recorded an increase. In 2021, the share of vehicle-like devices including e-scooter is 0.1% in daily travel distance and 0.7% in daily time spent on road (Bundesamt für Statistik, 2023a). Zurich has an extensive, modern public network with high quality with a traffic area of 12.8 square kilometers (Präsidualdepartement, 2022). Since 2019, several shared micro-mobility providers have started operating dockless e-scooters in the city of Zurich, such as Lime, Bird, Tier, and Voi (Reck & Axhausen, 2021).

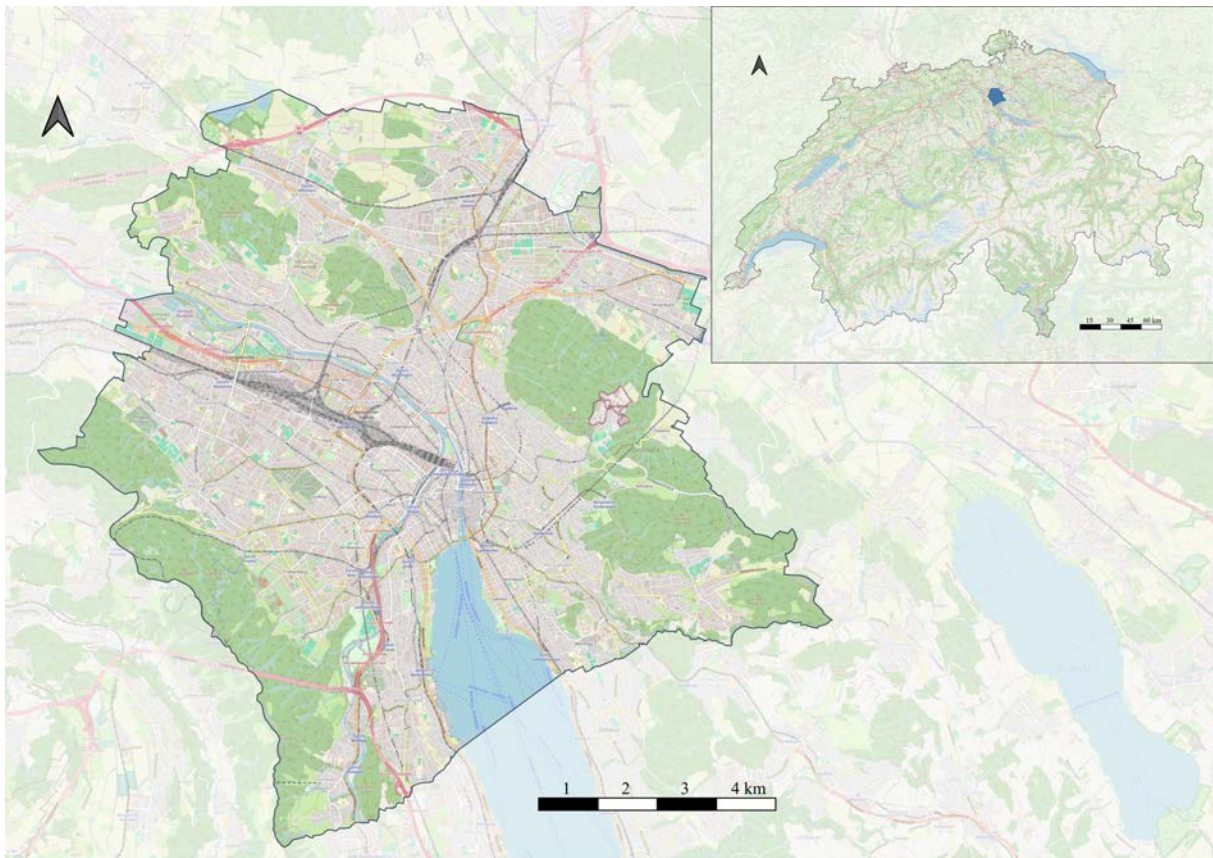


Figure 3.1: Study area - City of Zurich

3.2 Data Preprocessing

3.2.1 E-scooter accident data

The e-scooter accident dataset was provided by the transportation department (Dienstabteilung Verkehr, DAV) of the security department (Sicherheitsdepartment) in the city of Zurich. Each road accident involving e-scooters that occurred between 2019 and 2022 in the city of Zurich was recorded and reported by the city police based on an accident recording protocol of Federal Roads Office (Bundesamt für Strassen ASTRA, 2018b). Each accident is identified by an accident ID, and a total of 350 e-scooter accidents are recorded. This dataset contains several main categories of information for each accident: general information, involving objects and persons, infrastructure, and circumstances. Concerning general information, in addition to the date, time, coordinates, and accident type together with the main cause, are also determined according to the official instructions for accident assessment protocol (Bundesamt für Strassen ASTRA, 2018a). In terms of involving objects and persons, vehicle type, person type and detailed information of persons are included, such as age, blood/breath alcohol concentration. As for infrastructure, this dataset focuses on the characteristics of the occurring location site and road elements, consisting of location sites, in/out of town, right of way, road type, maximum speed as well as street lighting. Also, circumstances like weather, light, road, and traffic are included. Furthermore, accidents involving children and senior citizens are specifically recorded. The overall distribution of all recorded e-scooter accidents is displayed in Figure 3.2.

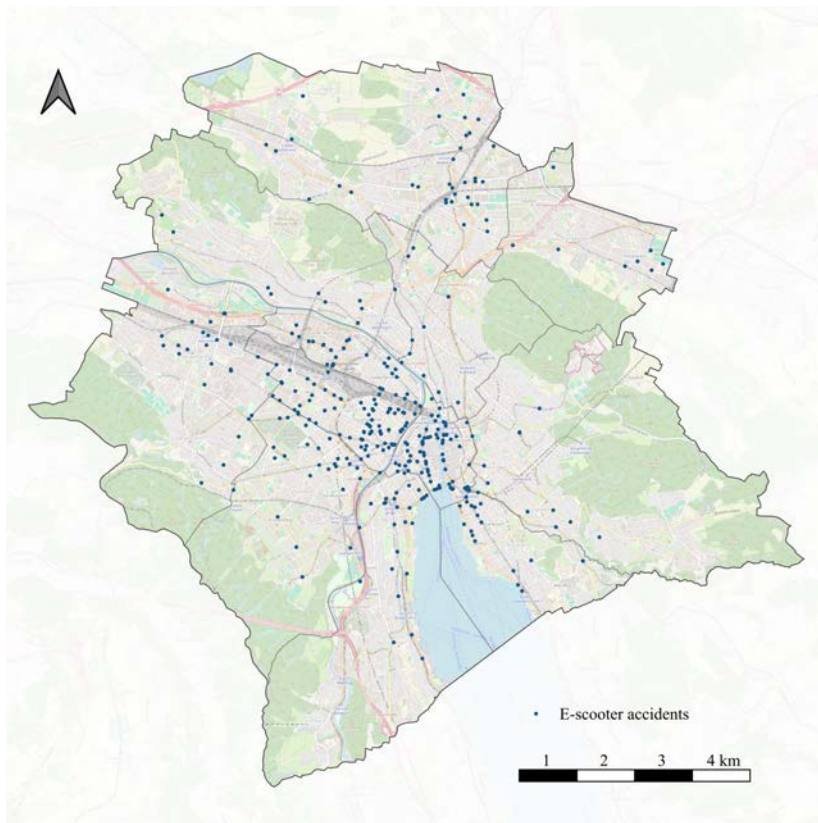


Figure 3.2: E-scooter accidents distribution overview

Table 3.1: Variables and their brief distributions - General information and involvement

	Variable	Category	N	%
General information	Accident type group	Skidding or self-inflicted accident	198	56.6
		Overtaking accident or lane change	10	2.9
		Rear-end collision	10	2.9
		Turning out accident	19	5.4
		Turning in accident	19	5.4
		Crossing the carriageway	48	13.7
		Head-on collision	11	3.1
		Parking accident	3	0.9
	Pedestrian accident	32	9.1	
	Person injury		Fatality	0
Seriously injured			59	16.9
Lightly injured			245	70.0
No injury (Property damage only)			46	13.1
Property damage*		0-100	207	59.1
		100-250	29	8.3
		250-500	23	6.6
		500-1000	16	4.6
		1000-2000	19	5.4
		2000-5000	43	12.3
		5000-10000	12	3.4
> 10000	1	0.3		
Drivers**	Age*	0-14	18	5.2
		15-24	82	23.7
		25-34	114	32.9
		35-64	104	30.1
		>65	2	0.6
		Unknown	26	7.5
Alcohol level*		0	59	17.0
		0-0.49‰(blood) or 0-0.24 mg/l(exhaled)	10	2.9
		0.50-0.79‰(blood) or 0.25-0.39 mg/l(exhaled)	13	3.8
		>0.80‰(blood) or >0.40 mg/l(exhaled)	104	30.1
		Unknown	160	46.2
Objects	Vehicle type	E-scooter only	193	55.1
		E-scooter + Pedestrian	28	8.0
		E-scooter + Bicycle	15	4.3
		E-scooter + Passenger Car	76	21.7
		E-scooter + Other vehicle***	22	6.3
		E-scooter + Vehicle-like devices	2	0.6
		E-scooter + Vehicles of mixed types	6	1.7
Unknown and other	8	2.3		

* Specific value was recorded for each accident (Property damage, participants' age, and alcohol level). The value category here in the table is just to provide an overview of their distributions.

** Involving persons are recorded for each accident, including pedestrians, drivers, and passengers. Only drivers of involving e-scooters are included in the table.

*** Other types of vehicles include delivery van, truck, motorbike, slow e-bike, bus, and tram.

Other than date, time and coordinates, general information and involvement parameters are shown in Table 3.1 above. Further details on infrastructure and circumstances are shown in the following Table 3.2.

Table 3.2: Variables and their brief distributions - Infrastructure and circumstances

	Variable	Category	N	%
Infrastructure	Location site	Straight section	202	57.7
		Curve section	14	4.0
		Junction	113	32.3
		Roundabout	1	0.3
		Square	15	4.2
		Parking place	3	0.9
		Other	2	0.6
	In/out of town	In town	350	100.0
		Out of town	0	0.0
	Road type	Main road	67	19.2
		Secondary road	272	77.7
		Other	11	3.1
	Maximum speed	60	2	0.6
		50	255	72.8
		30	87	24.8
20		3	0.3	
8		3	0.3	
Street lighting	In operation	191	54.6	
	Out of operation	156	44.5	
	No lighting	3	0.9	
Circumstances	Weather	Sunny	209	59.7
		Cloudy	101	28.9
		Rainy	35	10.0
		Snowfall	1	0.3
		Other	4	1.1
	Light	Day	159	45.4
		Night	177	50.6
		Dawn or dusk	14	4.0
	Road surface	Dry	277	79.1
		Damp	28	8.0
		Wet	41	11.7
		Icy	1	0.3
		Snow-covered	1	0.3
		Other	2	0.6
	Traffic volume	Normal	89	25.4
Weak		221	63.1	
Strong		30	8.6	
Stationary congestion		2	0.6	
Halting congestion		1	0.3	
Other		7	2.0	

3.2.2 Google Street View Images

Google Street View (GSV) is one of the most well-known services capturing, processing, and serving global-scale SVI. Panoramic imagery is captured from a vehicle or device mounted with multiple cameras and sensors accompanied by computers (Anguelov et al., 2010). And the vast majority of them offer omnidirectional coverage taken on public roadways (Biljecki & Ito, 2021). The GSV service could be accessed through a web interface integrated with Google Maps, phone apps, and application programming interface (API). Here in this thesis, SVI data was requested in an HTTP (Hyper Text Transfer Protocol) URL (Uniform Resource Locator) form using GSV static API provided by Google Maps Platform. Request for each GSV image was set with customized parameters such as latitude and longitude of the locations, heading of cameras, Field of view (FOV), pitch as well as output image size, as listed in Table 3.3. To have a comprehensive knowledge of the surrounding environment for each accident, four directions are identified by four headings of cameras (0° , 90° , 180° , 270°). Besides, it's necessary to note that the API only provides imagery at a lower resolution compared to the web service. Here the output image size was set to be the maximum value for the API service, which is 640 x 640 pixels. An example of four-direction GSV images for each e-scooter accident point is given in Figure 3.3.

Table 3.3: Parameters setting for GSV API

Parameter	Description	Setting value
Location	Latitude and longitude	Coordinates value
Heading	Heading of camera	0, 90, 180, 270
FOV	Horizontal field of view for the image	120
Pitch	Up and down angle of camera	0
Size	Output image size in pixels	640 x 640

After downloading GSV imagery, images with invalid content of null, indoor, rooftop, and sky are filtered manually, which are regarded as no help of providing infrastructure information in this work. Out of 350 e-scooter accident locations, 295 with images of valid content are obtained to build the GSV dataset for further investigation. The distribution of locations with valid GSV images is shown in Figure 3.4 below.



Figure 3.3: Example of GSV images in one location

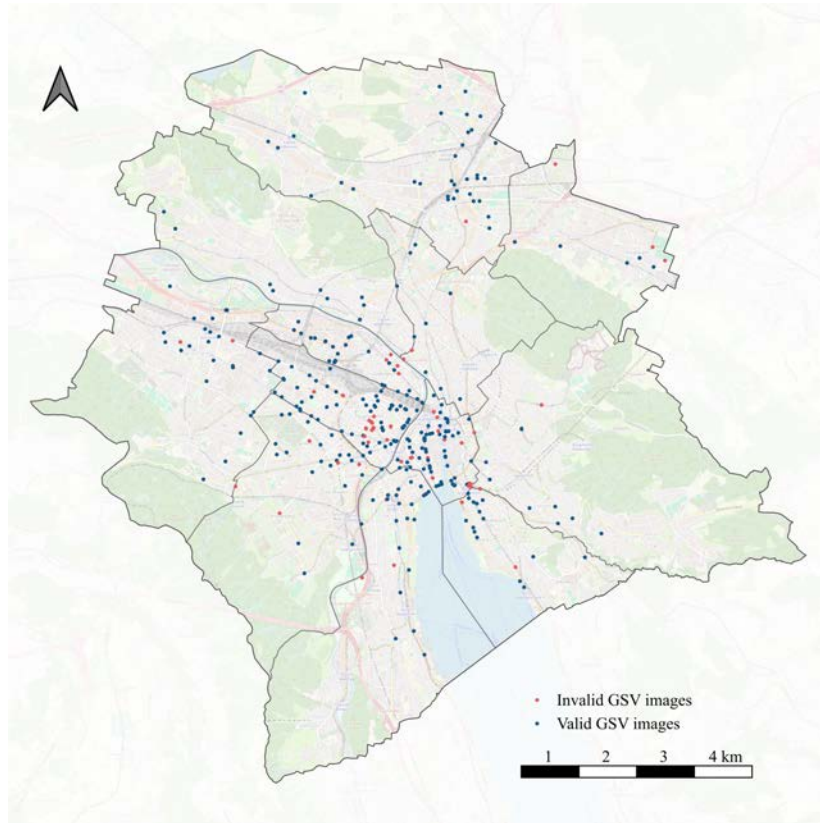


Figure 3.4: Distribution of valid and invalid GSV images

3.2.3 Traffic network and transport-related data

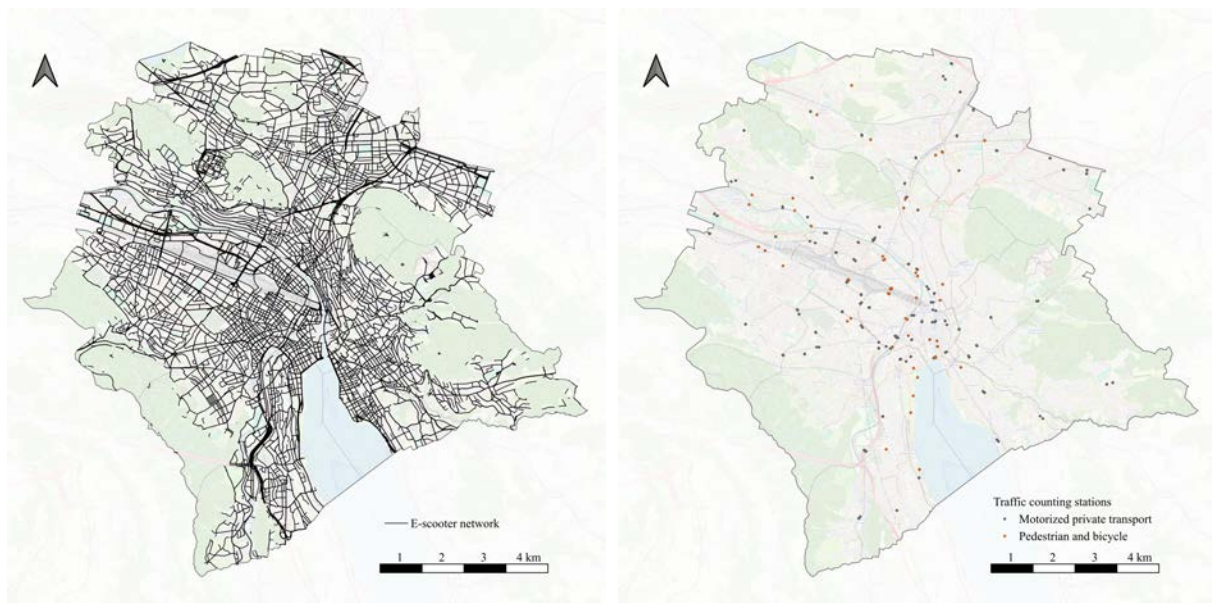
Additionally, road infrastructure and transport network data are also collected for this thesis, from the published datasets from Open Data Zurich, traffic department (Dienstabteilung Verkehr, DAV) along with Open Street Map (OSM). Main source datasets are listed in the following table 3.4.

Considering the usage pattern and travel characteristics of e-scooters, as well as the concentrated distribution of dockless e-scooters in urban areas, the e-scooter network was built by merging the street network, footpaths, bicycle paths and filtering out the natural areas such as forest. An overview of the e-scooter network is presented in Figure 3.5a.

Regarding the traffic datasets, values denoting traffic characteristics were recorded in different counting stations and measuring points. Each vehicle traffic counting station contains several measuring points, recording the traffic volume of motorized private transport vehicles. As for bicycle and pedestrian counting stations, bicycle traffic was recorded using induction loops embedded in the road surface, while pedestrian traffic was counted using passive infrared radiation. Traffic count data for each e-scooter accident point was represented by records from the nearest counting stations and closest time. The counting stations are displayed in Figure 3.5b. In addition to traffic count data, traffic density data was acquired from the traffic model dataset (GVM-ZH 2018), which contains traffic forecast data such as average daily traffic, traffic demand during morning and evening rush hours. Based on traffic supply and traffic

Table 3.4: Datasets source for traffic and transport network

	Dataset	Description
Network	Strassennetz	Road network
	Kommunaler Richtplan Verkehr	Traffic plan
	Linien des öffentlichen Verkehrs	Public transport lines
	Haupt- und Nebenstrassen	Main and secondary roads
	Veloinfrastruktur Radwege und Radstreifen	Bicycle network
	Velonetzplanung	Bicycle network plan
	Fuss- und Velowegnetz	Foot and cycle path network
Traffic	Gesamtverkehrsmodell-ZH	Passenger traffic model for Canton of Zurich
	Daten der Verkehrszählung zum motorisierten Individualverkehr	Traffic census data for individual motorized transport
	Daten der automatischen Fussgänger- und Velozählung - Viertelstundenwerte	Automatic pedestrian and bicycle counting data
Zone	Stadtkreise	Urban districts
	Statistische Zonen	Statistical zones
	Statistische Quartiere	Statistical districts
	Tarifzonen des öffentlichen Verkehrs	Public transport traffic zones
Infrastructure	Haltestellen des öffentlichen Verkehrs	Public transport stops
	Fussgängerstreifen	Pedestrian crossing
	Randabschlüsse Konzeptplan	Curb concept plan
	Öffentliche Beleuchtung der Stadt Zürich	Public lighting
	Öffentlich zugängliche Parkhäuser	Publicly accessible parking garages
	Öffentlich zugängliche Strassenparkplätze	Publicly accessible street parking spaces
	Zweiradparkierung	Two-wheeler parking spaces
Other	Kantonaler Richtplan	Structural plan for land use areas



(a) E-scooter network

(b) Traffic counting stations

Figure 3.5: Traffic network data overview

zones, source/destination matrices for public transport, motorized private transport as well as non-motorized transport (consisting of pedestrian and bicycle traffic) are estimated for average weekday traffic.

4. Methodology

4.1 Spatial-temporal Analysis

4.1.1 Spatial analysis

To gain an overview of the spatial distribution of e-scooter accidents, two methods were employed, including visualizing a Kernel Density Estimation (KDE) heat map and a road network map with aggregated number of e-scooter accidents per road segment.

Heat maps were created with the purpose of visualizing the underlying spatial patterns of e-scooter accidents with KDE. Analogous to a histogram, KDE estimates and smooths the data by using a continuous probability density curve. Results of KDE are self-explanatory, unlike many other visualization methods (Lord et al., 2021). One of the most influential parameters in KDE is bandwidth, which denotes the standard deviation of the smoothing kernel. An inappropriate parameter specification of bandwidth could lead to an incorrect or distorted representation of the data distribution. Here in this thesis, KDE was performed with function `Kdeplot` from Python package `seaborn` (Waskom, 2021), of which the smoothing bandwidth values were selected by Scott's Rule (Scott, 2015) and smoothing algorithm used was Gaussian kernel.

Besides, a road network map with the aggregated number of accidents per road segment was generated by three steps. Firstly, with the e-scooter road network, lines from each accident point to the closest road segment were gained by using the 'shortest line between features' algorithm provided in QGIS. Secondly, with the intersection between the lines dataset and road network data, the numbers of e-scooter accidents per segment were assigned to road segments. Thirdly, the total number of accidents for each segment was visualized on a network represented by color gradients.

4.1.2 Temporal analysis

To intuitively visualize the potential temporal pattern of e-scooter accidents, the number of accidents on different time scales was plotted as a line graph, including year, month, day of week, and hour. Furthermore, the Seasonal-Trend decomposition method provided in the Python package, `statsmodels`, was applied to decompose the e-scooter accident time series into three components, trend, season, and residual with Locally Estimated Scatterplot Smoothing (LOESS). While the trend component illustrates a relative long-term increase or decrease, the season component presents whether there is a certain cycle and a fixed frequency. Additionally, the residual component helps to determine whether the time series is stationary or non-stationary. Moreover, Autocorrelation Function (ACF) and Partial Autocorrelation Function (PACF) were performed in order to explore the number of autoregressive and moving average lags for Autoregressive

Intergrated Moving Average (ARIMA) model, which could offer a comprehensive understanding of the time series and forecast for the upcoming series.

4.2 Curb extraction using SAM on GSV

In general, three processes were designed to extract curbs from GSV images, which are obtaining image segmentation with the application of SAM, calculating properties of output masks, and building a classification model with a visual interpretation of masks.

4.2.1 Application of SAM

As introduced in Section 2.1.4, SAM has made great progress in image segmentation with an overall excellent performance. Since SAM is suggested to install with CUDA support and requirement on an advanced version of machine learning packages, Pytorch 2.0.1 and Torchvision 0.15.2 were utilized. An automatic mask generation was applied with SAM, which required a `SamAutomaticMaskGenerator` class including SAM settings for checkpoint (model version), model type, and device. Parameters setting for SAM are listed in Table 4.1 as follows.

Table 4.1: Parameters setting for SAM

Parameter	Setting
Checkpoints	sam_vit_h_4b8939.pth
Model type	vit_h
Device	CUDA

SAM was applied to images of four directions in each e-scooter accident location for automatic mask generation. Figure 4.1 shows an example from the segmentation output of SAM. Mask information was subsequently extracted from the output dictionary with a segmentation key and stored in a standard binary file format for the Python package Numpy. Each segmentation result from each image was represented by a binary mask of all pixels.

In addition, with the binary masks, the contours of each mask were then identified by the function `findContours` provided in the Python OpenCV library. Each individual contour is a Numpy array of (x,y) coordinates of boundary points of the input mask, which makes further shape analysis and object recognition possible. Furthermore, after examining the performance of SAM with test images, several problems were found. First, since the mask sometimes was an object that had several separate parts, selecting the representative one or more contours or merging them into an integrated one is crucial to analyze the properties of contours. Second, some contours were fairly small with a limited number of pixels, which might hardly contribute to object extraction and largely increase workload in subsequent analysis. Third, excessive segmentation was found in areas with rich texture information, namely there were overlaps or repeats of contours, which probably resulted in duplicated contours. Therefore, several filtering functions were written to solve these problems. For each mask, contours with an area size of less than 6 pixels were removed, and all other maintained contours were then considered as part of



(a) Input original image



(b) Segmentation output masks

Figure 4.1: Output masks example of SAM

the contour collection for further analysis. Additionally, masks that were totally located inside one of the others, as well as masks with a large portion of the intersection with the others, were removed.

4.2.2 Visual interpretation

To prepare classes for the classification model, manual interpretation was conducted for SAM output of 20 randomly selected locations. Seven label groups of objects in total are presented in the following Table 4.2.

4.2.3 Calculating properties of masks

To distinguish masks of different objects and to prepare variables for classification, properties of mask contours were calculated, including geometric attributes and spectral features.

Table 4.2: Label list of manual interpretation

Label group	Label name	Label group	Label name
Sky	Sky		Road
Vegetation	Vegetation		Bicycle lane
Curb	Curb		Manhole
Building	Building		Zebra crossing
	Vehicle		Blind way
	Train		Chimney
Means of transportation	Tram		Tile stone
	Bus		Electric pole
	Bicycle		Light pole
	Motorbike		Pavement
	Other		Railway
	Tag	Infrastructure	Road bridge
	Human		Road sign
	Building part		Road part
Other	Mountain		Stairs
	River		Street wire
	Shadow		Trash bin
	Light		Tower crane
	Post mailbox		Traffic light
			Street light
		Tram/bus station	
		Warning post	
		Road ground sign	

4.2.3.1 Spectral features

Considering the characteristics of curb colors, which could be described as grey consistently. Spectral features with a focus on color value were acquired with a total number of 17, as listed in Table 4.3. Other than statistics of values in three channels (green, red, and blue), variables related to color distance were also designed to quantify the difference between pixel colors and standard grey. By plotting RGB values in 3D plots by regarding red channel, green channel, and blue channel as the three axes (x, y, z) ranging from 0 to 255 separately, each color could be represented with a point in these space. Besides, it was assumed in this thesis that a standard grey point would be located at the body diagonal line of this cubic color space, from (0,0,0) to (255,255,255). Therefore, the difference between color and grey could be expressed as the distance between the color point and the grey line. Figure 4.2 illustrates the color distance of mean values of RGB color channels to grey for all pixels in one curb mask.

Differences in spectral features between the curb and other masks were subsequently examined for feature filtering and selection. For example, a histogram of median values in green color as well as a histogram of mean value in red color were given as follows (in Figure 4.3).

Table 4.3: Variables of spectral features

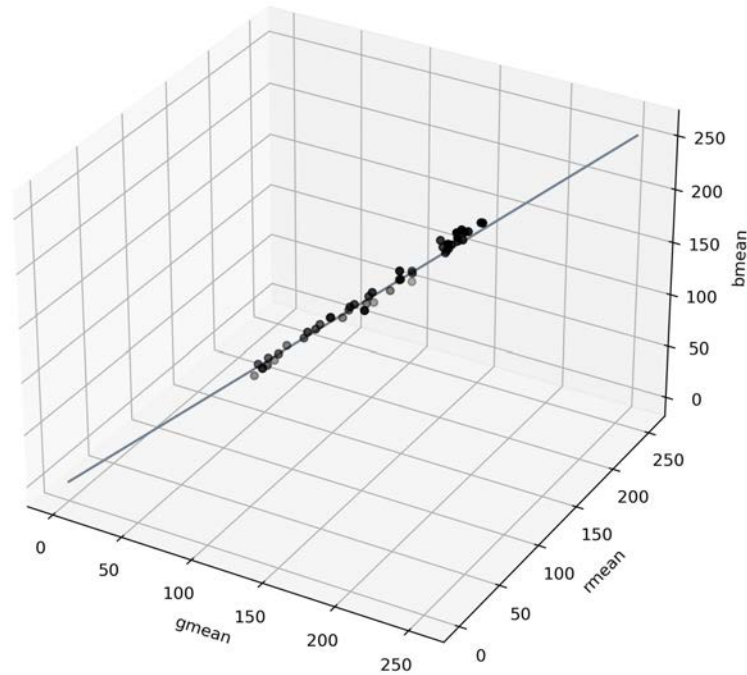
Variable	Description
gmedian	median value of green color
rmedian	median value of red color
bmedian	median value of blue color
gmean	mean value of green color
rmean	mean value of red color
bmean	mean value of blue color
gstd	standard deviation of green color
rstd	standard deviation of red color
bstd	standard deviation of blue color
gq25	25th percentile of green color
gq75	75th percentile of green color
rq25	25th percentile of red color
rq75	75th percentile of red color
bq25	25th percentile of blue color
bq75	75th percentile of blue color
cdmean	mean value of color distance to grey
cdstd	standard deviation of color distance to grey

4.2.3.2 Geometric attributes

Another typical characteristic of curb is its relatively long narrow shape, small size as well as low position in SVI. Additionally, calculating geometric attributes, including contour features and properties, was completed by using functions provided in the Python OpenCV library. As shown in Table 4.4, 18 variables of geometric attributes were considered.

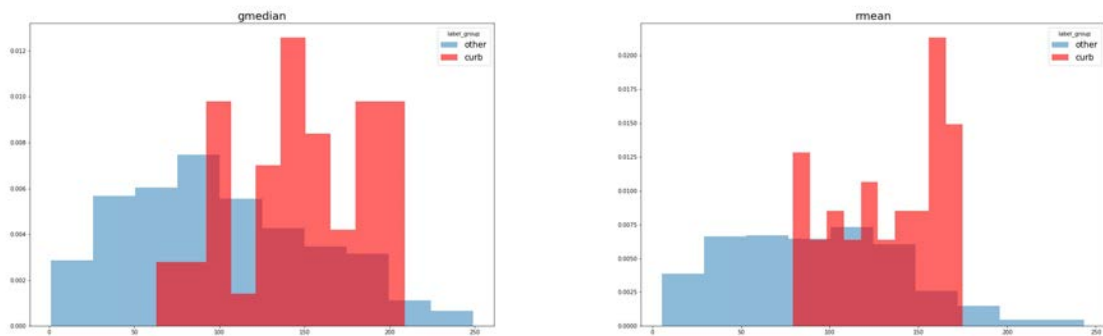
Table 4.4: Variables of geometric attributes

Variable	Description
isconvex	convex or not
area	area size
aspect_ratio_wh	ratio of width to height in rotated bounding rectangle
extent	ratio of area to rotated bounding rectangle area
solidity	ratio of area to its convex area
aspect_ratio_wh_s	ratio of width to height in straight bounding rectangle
extent_s	ratio of area to straight bounding rectangle
orien_re	angle of rotation of rotated bounding rectangle
orien_ell	orientation of fitting ellipse
ed	diameter of the circle with same area
ratio_ell	ratio of minor axis length to major axis length
perimeter	curve length or a closed contour perimeter
is_mce_inside	center of mass inside or not
is_cen_inside	centroid inside or not
leftm	x of leftmost points
rightm	x of rightmost points
topm	y of topmost points
bottomm	y of bottommost points



Pixel colors (black points) and grey color (grey diagonal line)

Figure 4.2: Illustration of color distance using example of pixels of curb mask



(a) Median value of green color

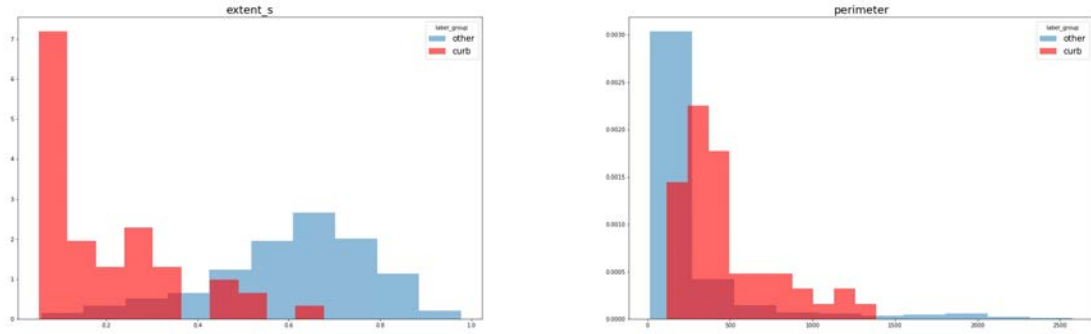
(b) Mean value of red color

Figure 4.3: Histogram example of spectral features between curb and others

Likewise, each spectral feature was then evaluated with histograms and checked if there were differences between curbs and other masks. Figure 4.4 presents the histogram of the ratio of area to straight bounding rectangle along with a histogram of perimeter or curve length as an instance.

4.2.4 Classification model using Random Forest

By calculating both spectral features and geometric attributes of every mask identified and extracted from SAM output in all e-scooter accident locations, input variables for RF were



(a) Ratio of area to straight bounding rectangle

(b) Perimeter or curve length

Figure 4.4: Histogram example of attributes between curb and others

generated. For the purpose of extracting curbs better, instead of including all masks in the entire image, only masks located in the lower part of images were selected, considering the typical pattern of the curb's position in SVI. Besides, two label groups (other and means of transportation) were merged for simplicity of classification.

Random Forest (RF) method is an ensemble-based machine learning technique that combines predictions of several base estimators built with a provided learning algorithm for improving predicting performances. Forests of this method denote a combination of tree predictors, and each tree is dependent on values of an independently sampled random vector, which has the same distribution as all trees in the forest (Breiman, 2001). Compared to other machine learning algorithms, this approach was confirmed with high accuracy and advantages in dealing with imbalanced datasets (More & Rana, 2017). RandomForestClassifier provided by Python library scikit-learn was employed in this thesis for building RF classification model. Parameters such as the number of trees were selected after checking prediction accuracy within a wide range of setting values.

4.3 Variables generation

For subsequent regression and prediction, variables with a broad coverage of traffic infrastructure characteristics were generated for e-scooter accident locations, considering three aspects of variables, including curb, entropy, and traffic infrastructure.

4.3.1 Curb variables

Following curb extraction achieved by RF classification model in Section 4.2, the presence or absence of curbs, along with the number of curbs, were obtained for all four images in each e-scooter accident location. Overall numeric curb variables per location point were summarized into mean, maximum, and minimum of curb counts.

4.3.2 Entropy variables

Entropy in information theory was introduced to measure information contained in a system, and Shannon entropy was designed to represent an absolute mathematical limitation on how the data from the system could be compressed onto a perfectly noiseless channel without loss (Shannon, 1948). In the field of image processing, entropy is regarded as one of the metrics for describing the complexity of a given image (Hayashi et al., 2023). With the purpose of comprehensively extracting information from GSV images, three entropy variables were calculated. In this thesis, these entropy variables were considered to reflect the complexity of surrounding infrastructures in drivers' visual environments. In addition to fundamental image entropy regarding only pixel values, the entropy of objects in visual view could be obtained with the application of SAM and classification model. Two article entropy variables were built for considering the objects of the entire image and considering only infrastructure objects located at the lower part of the image.

4.3.2.1 Image entropy

The first entropy variable generated was image entropy, which represents the randomness of colors. An image with higher entropy denotes its complexity in pixel color values. To acquire image entropy, a function was written and executed, including converting the image to gray scale, computing the histogram of pixel value, as well as calculating the entropy of the distribution from the histogram. For each accident location, there were four image entropy values from GSV images of four directions. Mean, maximum, and minimum values of image entropy were then attained.

4.3.2.2 Whole scene entropy

Regarding entropy of objects in the whole image, similar to Section 4.2, another RF classification model was trained with properties dataset of masks as well as labels defined by visual interpretation. For each image, mask labels classified by the RF model corresponded to object groups, which overall constituted the distribution of objects in the whole scene of input GSV image. All label groups identified during visual interpretation were included as target values for classifying the entire image, as shown in Table 4.5.

Table 4.5: Label groups for whole scene entropy

Class	Label group
0	Building
1	Curb
2	Infrastructure
3	Means of transportation
4	Other
5	Sky
6	Vegetation

4.3.2.3 Ground scene entropy

With a central focus on the curb and other infrastructure features located at ground level, an additional classification model was trained with processes akin to methods introduced before. Different from the previous two RF classification models, only objects identified as infrastructure based on the classification result of Section 4.3.2.2 with positions at the lower part of images were used as input for this RF model. Among the infrastructure identified at ground level, seven label groups were used, as seen in Table 4.6.

Table 4.6: Label groups for ground scene entropy

Class	Label group
0	Bike lane
1	Curb
2	Ground sign
3	Manhole
4	Other
5	Pavement
6	Road

4.3.3 Traffic-transport variables

Infrastructure features that are assumed or mentioned in previous literature on road safety are obtained from the published official datasets, including public transport stops, public traffic lines (bus, tram, train), pedestrian crossings, curbs, public lighting, and parking places (parking garages, street parking spaces, two-wheeler parking spaces). For every single infrastructure feature dataset, distances from each e-scooter accident point to the nearest feature are obtained by calculating the shortest line between features in QGIS. Moreover, attributes of the nearest infrastructure feature are also assigned to each accident point, as illustrated in Figure 4.5. Additionally, properties of statistical zones and traffic zones are allocated by intersecting e-scooter accidents and the areas. Furthermore, the traffic count of each e-scooter accident was derived from traffic count datasets (motorized vehicle, bicycle, pedestrian) based on its occurring time and closest counting stations. Traffic count data for both bicycles and vehicles were summarised to a weekly average value. Besides, traffic density and demand were extracted from the passenger traffic model dataset. Missing values for traffic count, density, and demand were replaced by an average number of other records that were measured in the same time period or nearby areas.

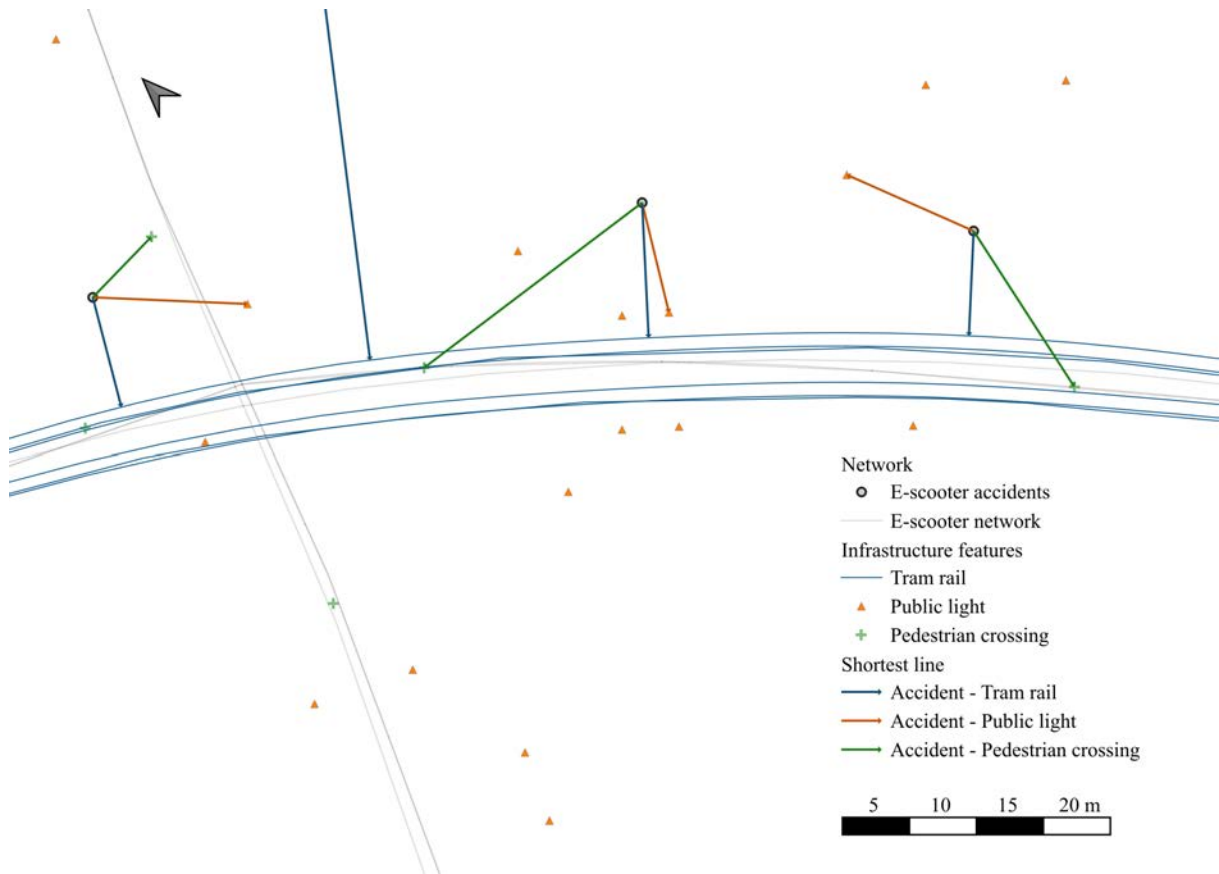


Figure 4.5: Example of infrastructure features allocation

4.4 Regression Analysis

4.4.1 Generation of Pseudo-Absence Points

To investigate the relationship between traffic infrastructure characteristics and e-scooter accidents, random pseudo points were generated along the network at least 10 meters away from location points recorded with accidents. The procedure used was similar to Biland (2023). Specifically, 16,922 random points on the e-scooter network were produced, and out of them, 1015 points were then extracted randomly. Subsequently, by filtering points that were located within a 10-meter distance to accident points and to boundary lines of the city of Zurich. Following this, 995 random pseudo points were created, of which the amount setting was suggested by a previous study (Barbet-Massin et al., 2012). This dataset could be assumed as points with the absence of accidents on the one hand and regarded as points randomly distributed on the e-scooter road network. The distribution of pseudo points with at least a 10-meter distance to accident points is illustrated in Figure 4.6.

4.4.2 Variables generation for random pseudo points

Likewise, the preparation of variable dataset for random pseudo points was conducted with the same processes introduced in Section 4.3.1, Section 4.3.2.1 as well as Section 4.3.3, including

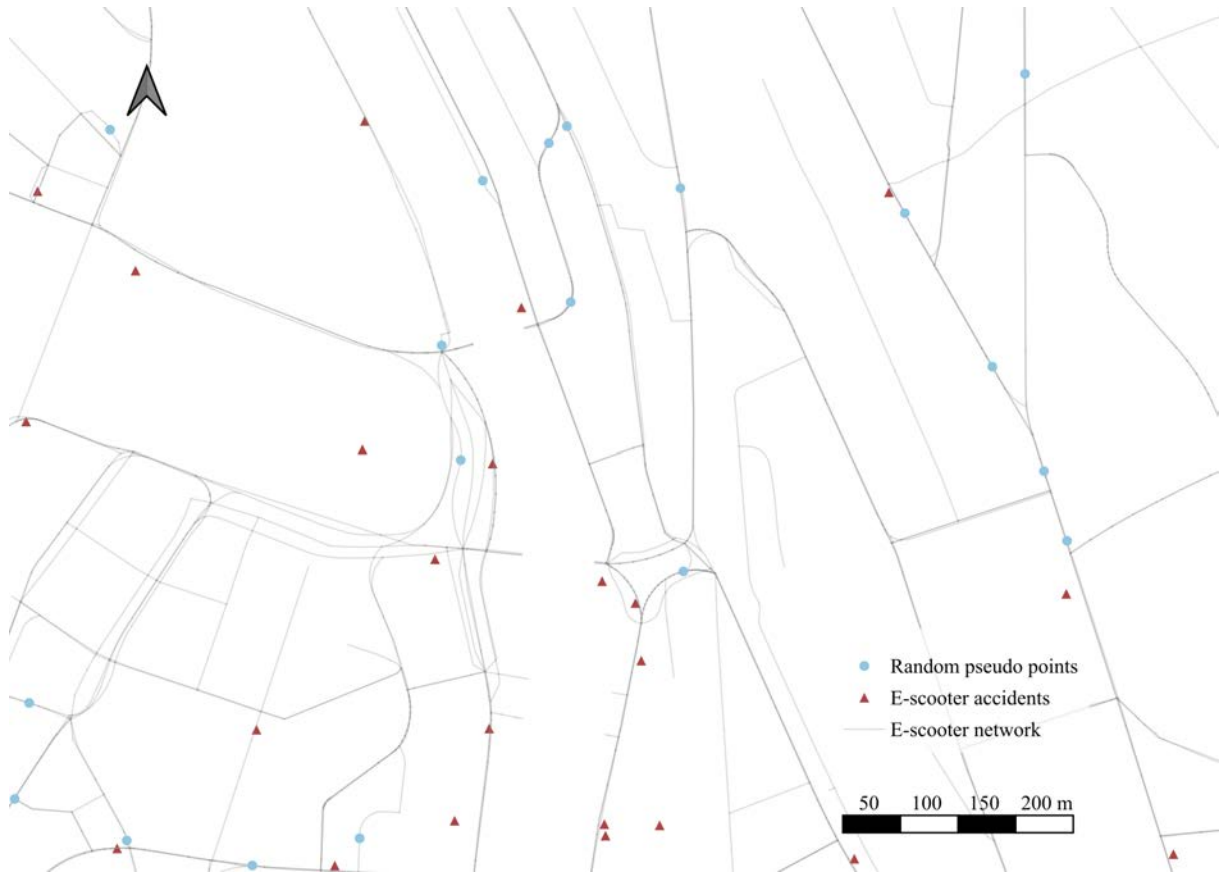


Figure 4.6: Illustration of random pseudo points

curb variables, entropy variables, and traffic transport variables.

4.4.3 Preparation for regression analysis

To determine the influence of traffic infrastructure characteristics on e-scooter accidents, two aspects of accidents were considered: presence and severity. In this thesis, while the presence of an accident denotes the possibility of happening or not, the severity of the accident represents how serious an accident would be when it takes place (namely, the vulnerability). It is important to note that regression analysis on the presence of accidents was conducted on a combination of variables dataset from accident points and random pseudo points, while regression analysis on the severity of accidents was only applied within the variable dataset from accident points.

4.4.3.1 Independent variables preparation

With the combination of variables generated for accident points and random pseudo points, the preparation of independent variables covering a wide range of traffic infrastructure characteristics was completed. Subsequently, two different processes of variable transformation were carried out for numeric variables and categorical variables, respectively. With regard to transforming numeric variables, normalization was achieved by applying a Yeo-Johnson power transformation function (Yeo & Johnson, 2000). The following standardization was completed by computing the

z score of each variable (Huck et al., 1986). Concerning categorical variables, one hot encoding was conducted, which converted each category of one variable into new binary variables.

4.4.3.2 Dependent variables in regression for accident presence

Concerning the presence of accidents, points in the accident dataset were locations with the presence of accidents, and random pseudo points were assumed as locations with the absence of accidents. Furthermore, as a binary dependent variable, the presence of an accident was assigned as 1 to accident points, while it was set as 0 for random pseudo-absence points.

4.4.3.3 Dependent variables in regression for accident severity

Dependent variables were generated according to the recorded impact of e-scooter accidents, which included a number of lightly and severely injured persons, as well as the value of property damage. Here in this thesis, the presence of person injury was therefore assigned as 0 to the accidents with neither lightly injured person nor severely injured person, while it was assigned as 1 for all the other accidents. Likewise, the presence of property damage was assigned as 1 to accidents with a value of property damage more than 0. Additionally, the number of injured persons with different types of injury (light, severe) along with the value of property damage were also included as numeric dependent variables.

4.4.4 Regression method

Two regression methods were applied to determine the correlation between independent and dependent variables generated in the previous sections, Ordinary Least Squares (OLS) and Generalized Additive Model (GAM) linear model. As one of the most prevalent regression methods, OLS regression estimates coefficients of linear regression equations with an aim to minimize the sum of square errors. GAM was also applied as a supplement and comparison to the results of OLS. GAM is a generalized linear model in which the linear response variable is dependent linearly on unknown smoothing functions of several predictor variables (Hastie, 1990). And a linear GAM is a GAM with a normal error distribution. Regression analysis was applied by using OLS function provided by the Python package statsmodels, and LinearGAM from the Python library pyGAM.

4.5 Prediction Modelling

Prediction modelling was performed for the severity of accidents, considering that the pseudo points were locations randomly distributed on a road network exposed to the same risk and possibility of accidents. Regression between traffic infrastructure characteristics and both categorical dependent variables, such as the presence of person injury, light person injury, severe person injury along with the presence of property damage, and numeric dependent variables including

a number of lightly injured persons, severely injured persons, as well as the value of property damage, were performed separately. By using regression models built with a variables dataset of accident points, prediction for the aforementioned dependent variables was then achieved by fitting the model to pseudo points. To improve the visualization of spatial patterns of prediction results, points with different values of prediction results were aggregated to square grids.

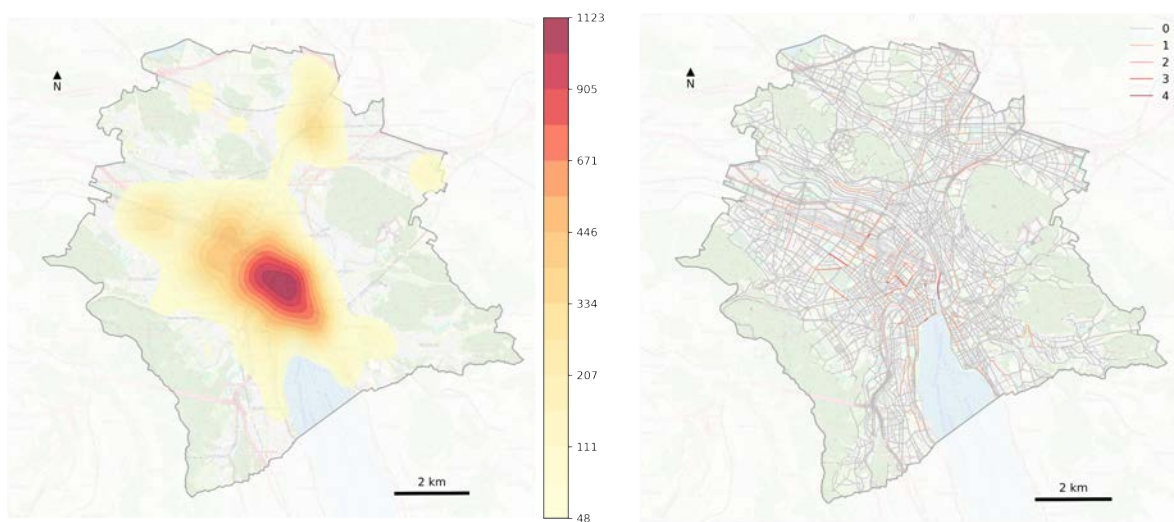
5. Results

5.1 Spatial-temporal distribution of e-scooter accidents

5.1.1 Spatial distribution

The spatial distribution of e-scooter accidents with kernel density estimation is presented in Figure 5.1a. An optimized smoothing bandwidth of about 732 meters determined by Scott's Rule and a Gaussian kernel smoother were used for the estimation. As it shows, the area with the densest distribution of e-scooter accidents is predominately located in the city center, specifically the western area of District 1, together with the junction area of Districts 1 and 4. It is to the southwest of Zurich's main train station, including the most area of the old town. Besides, e-scooter accident locations are also concentrated at three public transport stations, Hardbrücke, Alstetten, and Oerlikon.

Additionally, to have a better overview of the spatial distribution of e-scooter accidents in the road network, Figure 5.1b shows aggregated accidents per road segment. The road segments with the most e-scooter accidents are Limmatquai (from station Central to bridge Münsterbrücke), Bahnhofstrasse (from intersection Bahnhofstrasse-Sihlstrasse to station Rennweg). Other road segments with relatively high frequency of e-scooter accidents are General-Guisan-Quai (from the intersection with Beethovenstrasse to the intersection with Claridenstrasse), Badenerstrasse (from the intersection with Langstrasse to the intersection with Ankerstrasse, from station Albisriederplatz to station Letzigrund), Bäckerstrasse, and Hardstrasse (from station Hardbrücke to intersection with Geroldstrasse).



(a) Kernel density estimation

(b) Aggregated accidents per road segment

Figure 5.1: Spatial distribution overview

Besides, the spatial distribution of e-scooter accidents for each year is shown in the following figures. Regarding the kernel density estimation result, the smoothing kernel bandwidth values for 2019, 2020, 2021, and 2022 are, respectively, about 1019 meters, 948 meters, 916 meters, and 856 meters. As can be seen in Figure 5.2, there has been a slight decrease in the area with a high density of e-scooter accidents from 2019 to 2020 and a constant increase from 2020 to 2022. The highest density area has been maintained to be situated at the city center, while it has extended further to the northwestern direction till station Hardbrücke. Moreover, while there were no main concentrations other than the city center and station Albisriederplatz in 2020, station Oerlikon and station Altstetten have developed to become new centers of highly dense e-scooter accidents since 2021. Furthermore, based on the results of aggregated e-scooter accidents per road segments for each year in Figure 5.3. While no e-scooter accidents took place on the same road segments in 2019, the number of road segments with more e-scooter accidents has been increasing since then. Also, the distribution of road segments with accidents has spread from the city center to suburban areas.

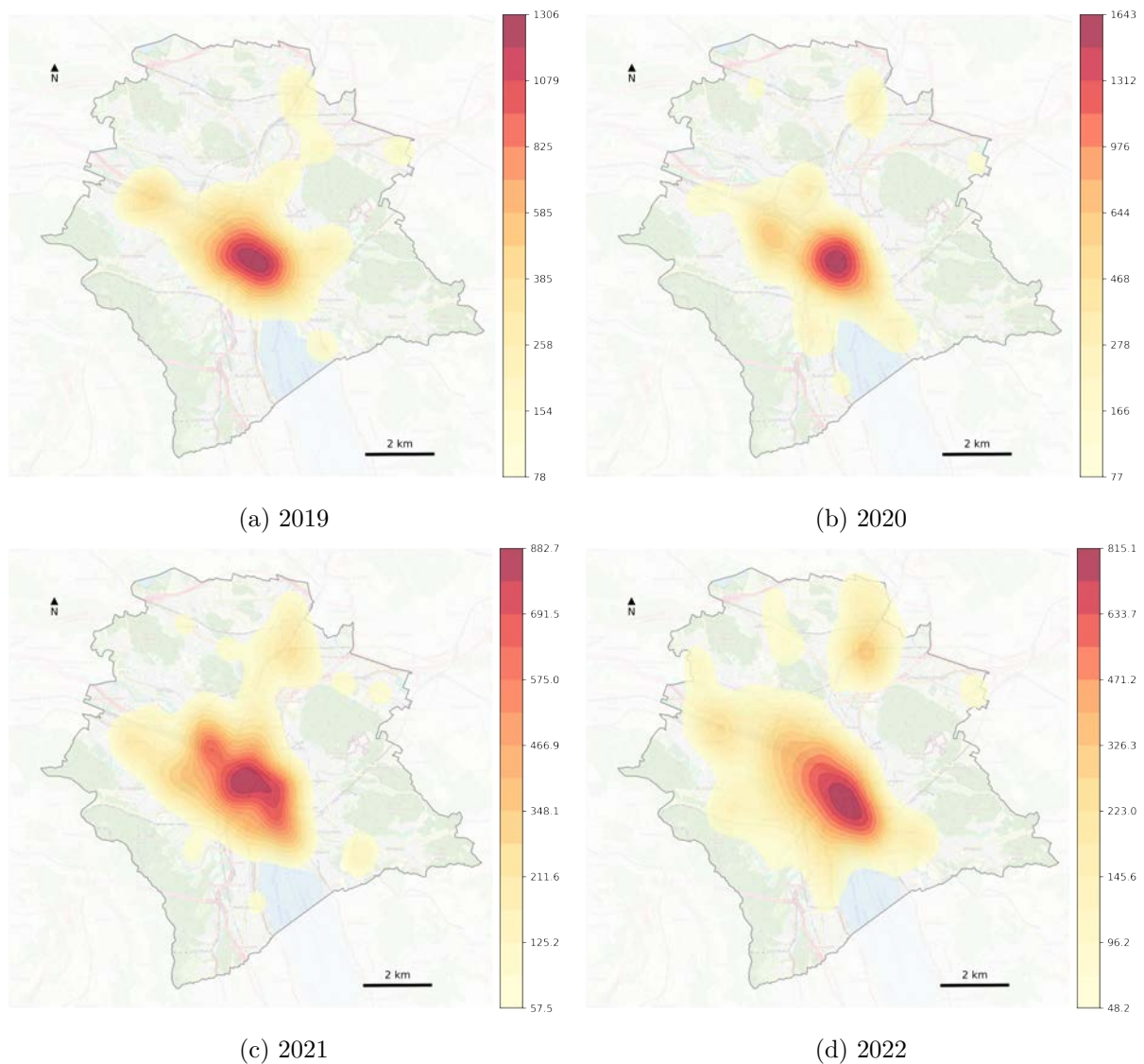


Figure 5.2: Kernel density estimation of accidents in each year

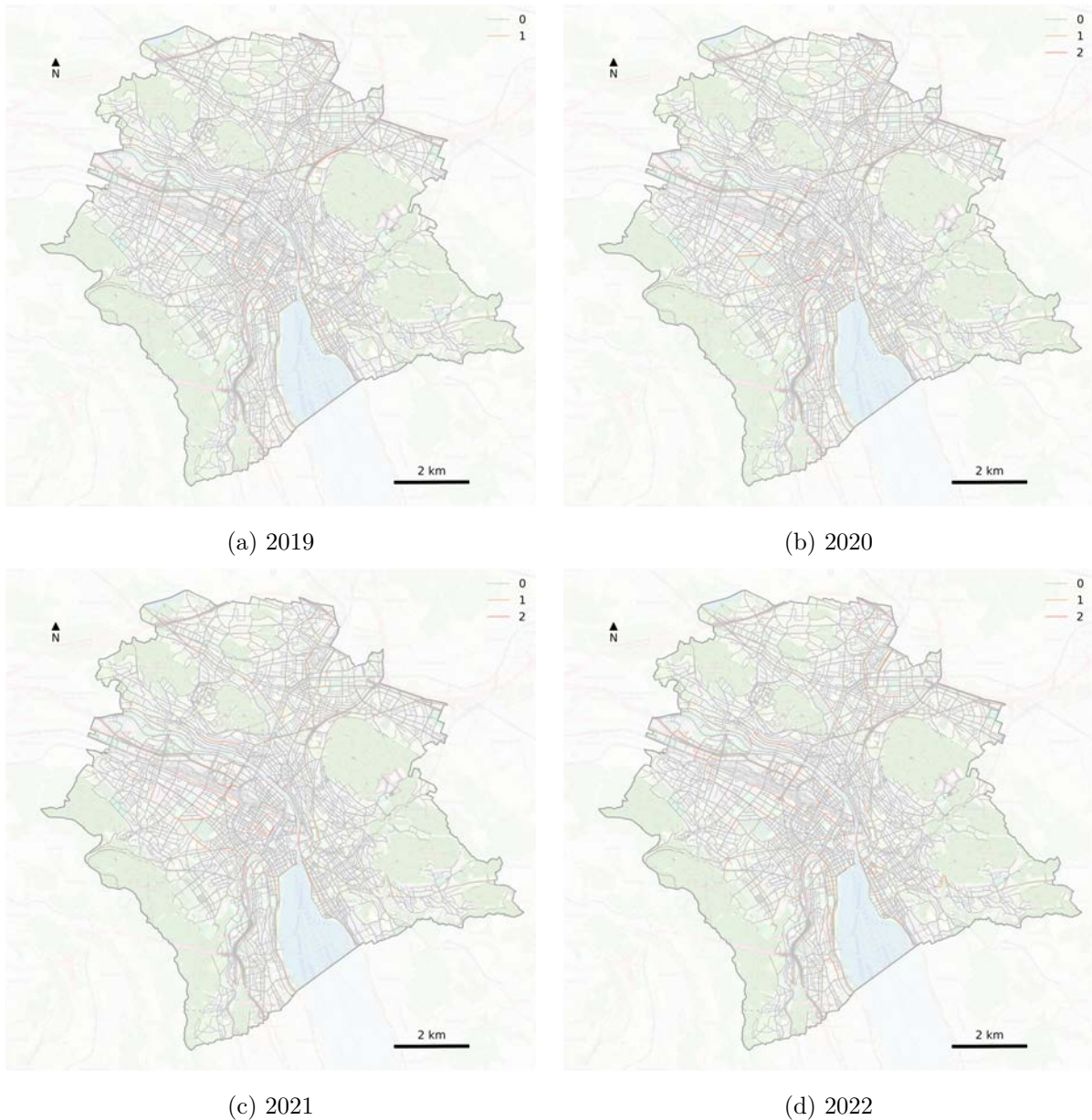


Figure 5.3: Accidents count per road segment in each year

5.1.2 Temporal distribution

A brief exploratory temporal analysis on different time scales is shown as line charts in Figure 5.4a below. Firstly, the graph reveals that there has been a steady rise in the number of e-scooter accidents in the city of Zurich since 2019 annually. The number of e-scooter accidents in 2021 is nearly a three fold increase compared with it in 2019. Secondly, concerning the month, over half of the e-scooter accidents occurred in the four months spanning from summer to early autumn, which are July, August, September, and October. Thirdly, the vast majority of accidents concentrated during the weekend, especially on Saturday. Fourthly and just as importantly, e-scooter accidents took place more commonly from early afternoon and late night (from 14:00 to 3:00). In addition, the temporal patterns of e-scooter accidents are different between weekdays and weekends, as shown in Figure 5.4b. While the accidents on weekdays

mostly happened from late afternoon and evening (from 16:00 to 23:00), accidents on weekends were primarily concentrated from midnight to the early hours of the morning (0:00 to 3:00).



Figure 5.4: Brief time series exploration

Furthermore, to determine the underlying pattern of time series, the seasonal-trend decomposition, ACF and PACF results are shown in the following Figure 5.5. Considering the combination of ACF and PACF plot, a second-order moving average model could be observed. Other than the autocorrelation analysis, as presented in Figure 5.5a, smoothed estimates of three components of the time series (season, trend, and residual) were extracted. It illustrates an increasing trend and the seasonality of an annual cycle.

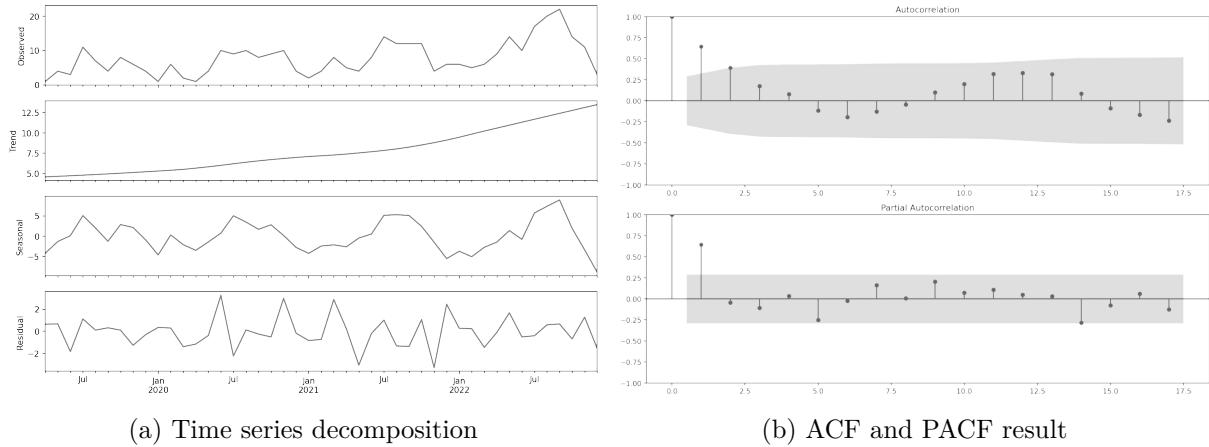


Figure 5.5: Time series analysis

5.2 Descriptive statistics of accident causes

The main causes of e-scooter accidents were recorded in the dataset, among which the top five most common causes are presented in Table 5.1. Additionally, 56.6% e-scooter accidents were determined as skidding or self-inflicted accidents. Table 5.2 shows that the influence of alcohol, as well as other influences related to inattention and distraction, account for the majority of skidding or self-inflicted accidents.

Table 5.1: Top four main causes of e-scooter accidents

Cause	Count	%
Influence of alcohol	120	34.3
Other influence related to inattention and distraction	73	20.9
Unauthorized use of pavement or footpath	29	8.3
Disregarding a red light	14	4.0

Table 5.2: Top four main causes for skidding or self-inflicted accident

Cause	Count	%
Influence of alcohol	103	52.0
Other influence related to inattention and distraction	68	34.3
Crossing the track at an acute angle for two-wheeled vehicles	8	4.0
Unauthorized use of pavement or footpath	8	4.0

5.3 Curb extraction

With the application of SAM to GSV images in e-scooter accident locations, 103373 segmentation masks were produced from 1180 images in total. Subsequently, by identification of contours and filtering out overlaps or repetitions, 57035 mask contours were generated. To prepare training datasets for further mask classification, mask output files of 80 GSV images in 20 e-scooter

accident locations were randomly selected for manual visual interpretation. In total, there were 3934 masks defined and labeled from SAM segmentation result after filtering.

As the result of Section, after calculating properties of mask contours filtering masks in upper part of images, several label groups were then merged as for the purpose of better extracting curbs. Label groups for classification and their counts in the training dataset are presented in Table 5.3.

Table 5.3: Label group statistics for curb extraction

Class	Label group	Count	%
0	Curb	49	2.3
1	Infrastructure	535	24.8
2	Other	1355	62.7
3	Vegetation	221	10.2

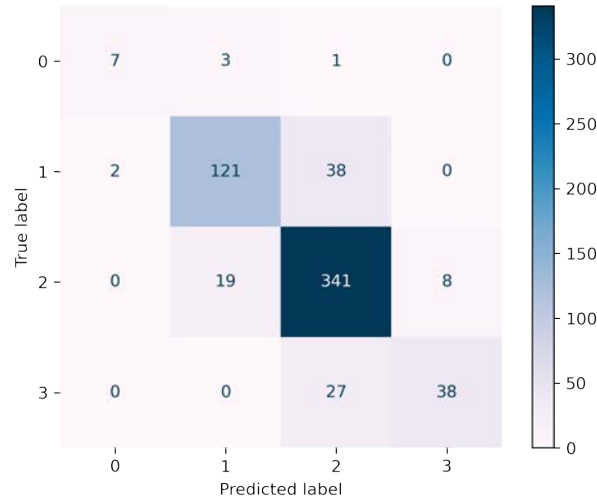
The summary of classification results is provided in the confusion matrix in Figure 5.6a. Moreover, the performance of the RF classification model was evaluated and quantified with metrics of different assessment methods, as presented in Table 5.4. Overall, the classification model has an accuracy score of 0.838, MCC score of 0.693, and Kappa score of 0.688. Label group curb has a precision score of 0.778, a recall score of 0.636, and an F1 score of 0.700. According to the importance ranking of variables illustrated in Figure 5.6b, the top three influential spectral features for curb extraction are the 25th percentile, mean value, and median value in the green color channel ('gq25', 'gmedian', and 'gmean'), while the top three important geometric attributes are contour perimeter, equivalent diameter and bottom position ('perimeter', 'ed', and 'bottomm').

Table 5.4: Evaluation metrics of RF classification - Curb extraction

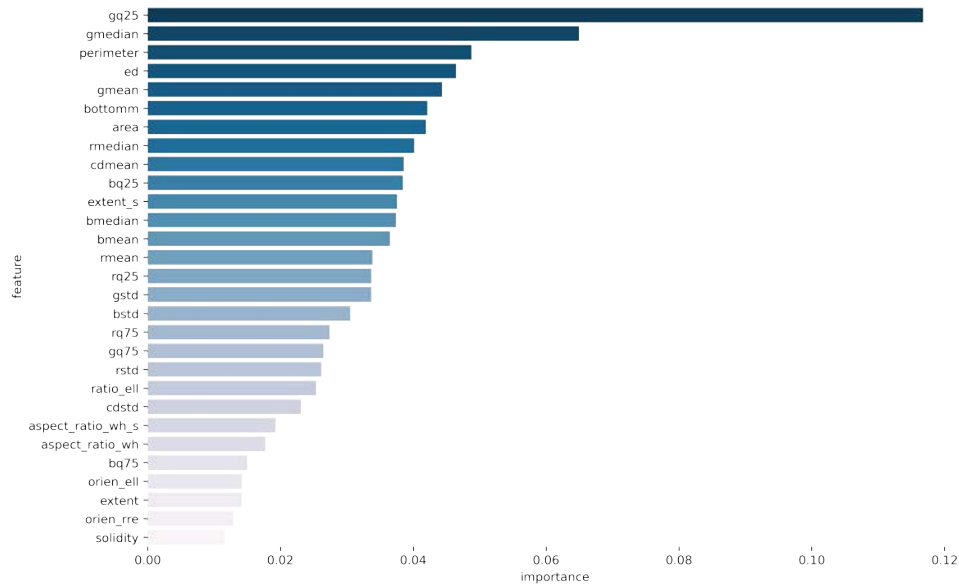
Metrics	0	1	2	3	Overall
Accuracy					0.838
Precision	0.778	0.846	0.838	0.826	0.838
Recall	0.636	0.752	0.927	0.585	0.838
F1	0.700	0.796	0.880	0.685	0.833
MCC					0.693
Kappa					0.688

Subsequently, by applying the classification model to the whole dataset of mask contour properties, curb extraction from GSVimages in e-scooter accident locations was achieved. Figure 5.7 below illustrates an example of curb extraction result at one location.

Both the presence and number of curbs were obtained based on the classification result. Curbs were recognized and extracted from GSV images in over half of the e-scooter accident locations. The number of curbs in locations where curbs were identified is mostly one or two. Distributions of presence and numbers of recognized curbs are shown in the following Figure 5.8.



(a) Confusion matrix



(b) Importance value of variables

Figure 5.6: Classification result for curb extraction

5.4 Variables generation of accident points

5.4.1 Curb variables

With the extraction result illustrated in the previous section, the presence and total numbers for each accident location were regarded as two basic variables for the curb. In addition, to thoroughly describe the detailed curb environment, the average, minimum as well as maximum number of curbs detected from all four directions in each e-scooter location were calculated as a complement. The curb variables are listed in Table 5.5.

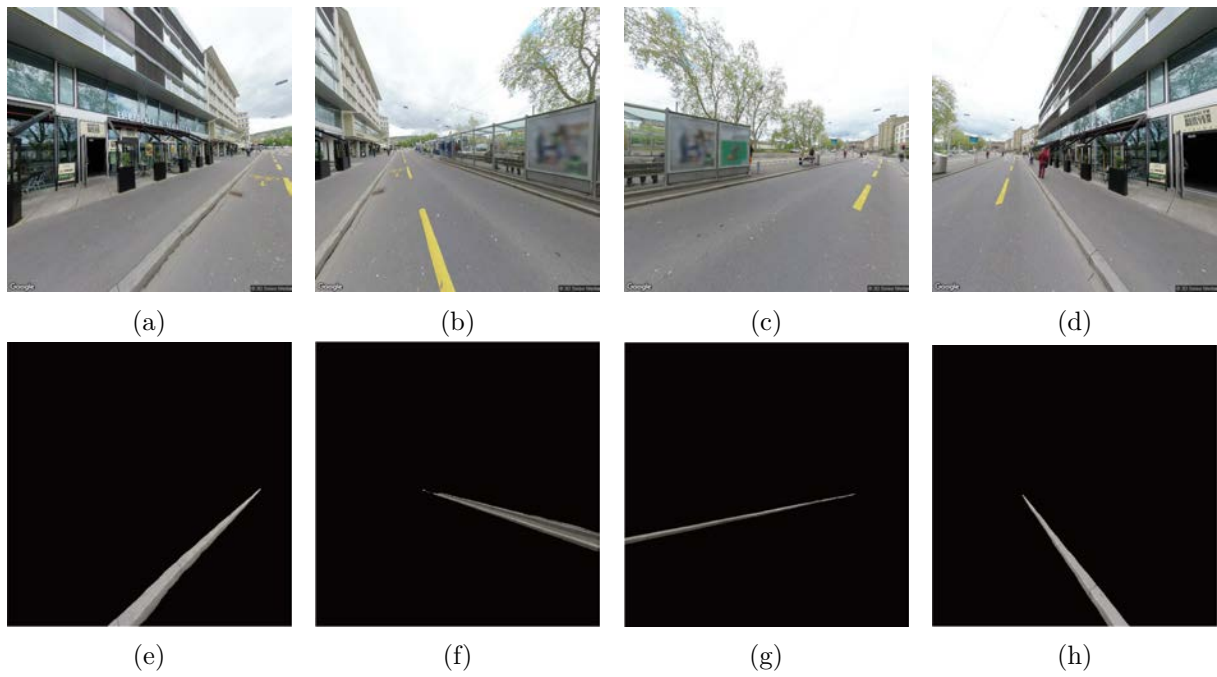
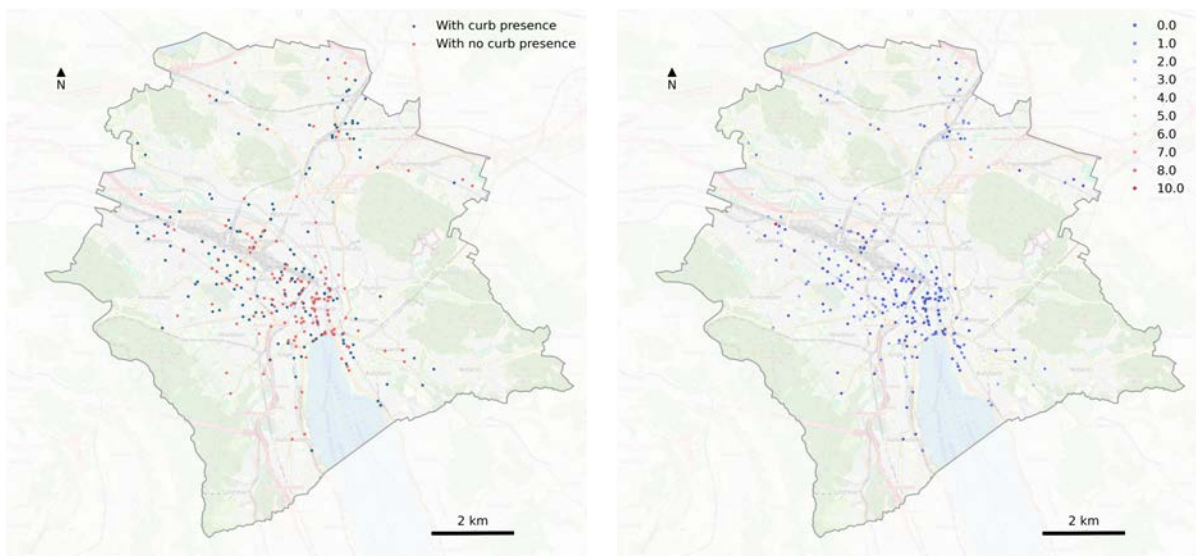


Figure 5.7: Example of curb extraction



(a) Presence of curbs

(b) Numbers of curbs

Figure 5.8: Distribution of curb extraction results for accident locations

Table 5.5: Generated curb variables

Type	Variable	Description
Numeric	cmean	Average number of curb
	cmin	Minimum number of curb
	cmax	Maximum number of curb
Categorical	cp	Presence of curb

5.4.2 Entropy variables

5.4.2.1 Image entropy

For each accident location, there were four image entropy values from GSV images of four directions as the result of Section. Mean, maximum, and minimum values of image entropy were then attained. The distribution map of the mean image entropy value from four directions in each e-scooter accident is shown in Figure 5.11a.

5.4.2.2 Whole scene entropy

Along with the image entropy obtained from the perspective of pixel color values, the entropy of mask objects for the whole scene was also computed in view of semantic segmentation. With the application of SAM and manual interpretation result mentioned in the previous section, classifying objects into different label groups from GSV images could provide insights to describe the complexity of items observed in specific locations. Similar to curb extraction methods, label groups were firstly identified as listed in Table 5.6 below. Another RF classification model was then performed to acquire the distribution histogram of object groups for the whole scene.

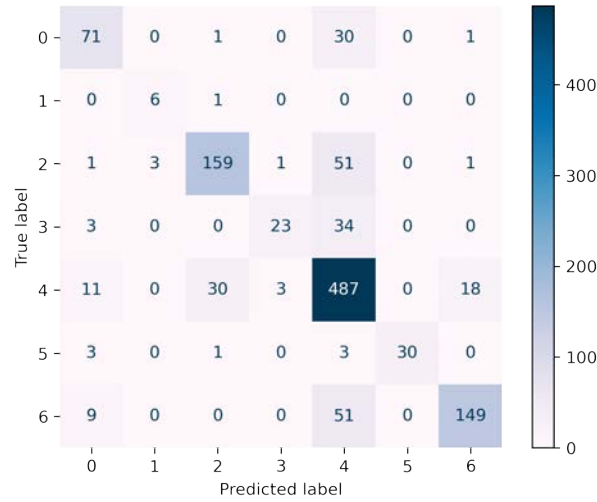
Table 5.6: Label group statistics for whole scene entropy

Class	Label group	Count	%
0	Building	401	10.2
1	Curb	49	1.2
2	Infrastructure	717	18.2
3	Means of transportation	189	4.8
4	Other	1822	46.3
5	Sky	112	2.9
6	Vegetation	644	16.4

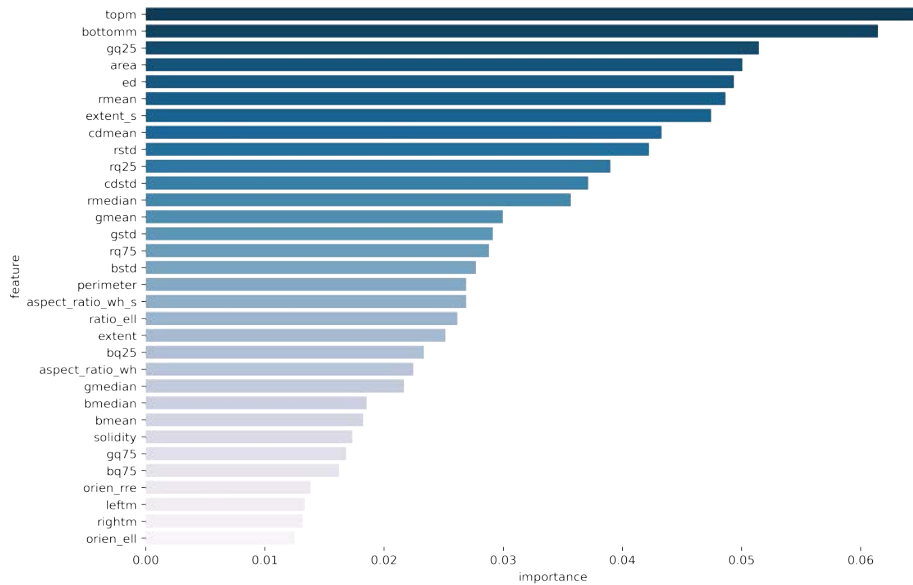
Likewise, the RF classification result summary was shown as the confusion matrix in the following Figure 5.9a. As illustrated in Table 5.7, the model is of good performance with an overall precision score of 0.794 and a recall score of 0.783. By applying the RF classification model, the entropy of objects identified for the whole scene was gained. It can be seen from the Figure 5.9b that the three most important variables are vertical positions ('topm', 'bottomm') and 25 percentile of values in green color channel ('gq25'). And the spatial distribution of the average value of whole scene entropy is presented in Figure 5.11b.

5.4.2.3 Ground scene entropy

Apart from the specific focus on curb, other infrastructure features that are located at ground level were considered to constitute a complete ground scene for e-scooter users. By using the infrastructure segmentation group identified previously, one more classification model was built to detect infrastructure features on the ground. As shown in Table 5.8, seven primary label



(a) Confusion matrix



(b) Importance value of variables

Figure 5.9: Classification result for whole scene entropy

Table 5.7: Evaluation metrics of RF classification - Entropy of whole scene

Metrics	0	1	2	3	4	5	6	Overall
Accuracy								0.783
Precision	0.724	0.667	0.828	0.852	0.742	1.000	0.882	0.794
Recall	0.689	0.857	0.736	0.383	0.887	0.811	0.713	0.783
F1	0.706	0.750	0.779	0.529	0.808	0.896	0.788	0.779
MCC								0.686
Kappa								0.680

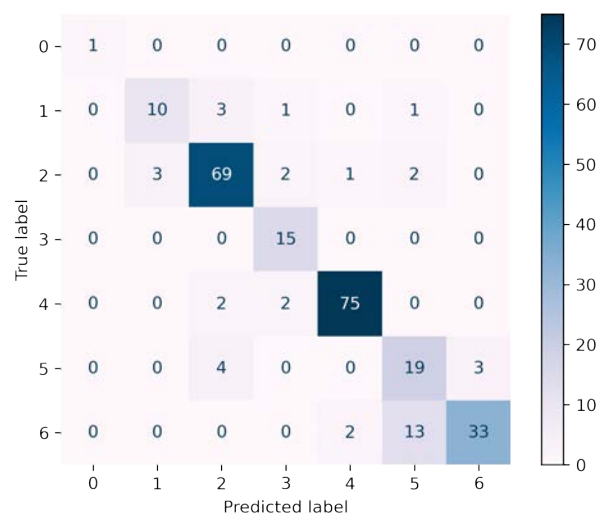
groups were set for the classification. Assessment and result of the built model were presented in the following confusion matrix (5.10a) and evaluation metrics 5.8. Besides, the Figure 5.10b shows that features of highest importance are predominantly geometric attributes, including vertical positions ('topm', 'bottomm') and equivalent diameter('ed'). The entropy of ground

scene results for each accident location were mapped as seen in Figure 5.11c.

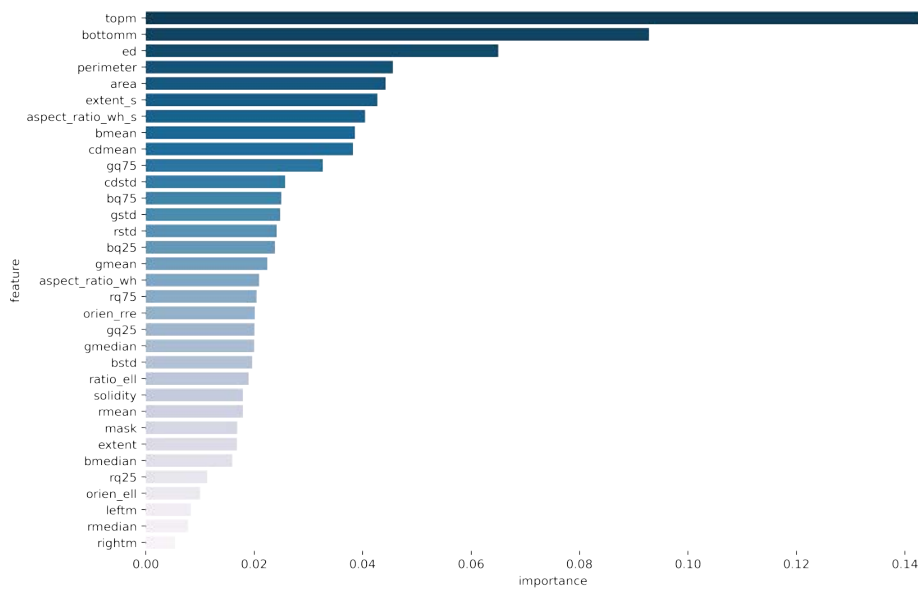
Summary of all three entropy variables generated is provided in Table 5.10.

Table 5.8: Label group statistics for ground scene entropy

Class	Label group	Count	%
0	Bike lane	7	1.0
1	Curb	49	6.4
2	Ground sign	217	28.3
3	Manhole	40	5.2
4	Other	226	29.5
5	Pavement	92	12.0
6	Road	135	17.6



(a) Confusion matrix



(b) Importance value of variables

Figure 5.10: Classification result for ground scene entropy

Table 5.9: Evaluation metrics of RF classification - Entropy of ground scene

Metrics	0	1	2	3	4	5	6	Overall
Accuracy								0.820
Precision	1.000	0.667	0.832	0.731	0.953	0.531	0.900	0.833
Recall	0.500	0.526	0.899	0.950	0.953	0.667	0.610	0.820
F1	0.667	0.588	0.864	0.826	0.953	0.591	0.727	0.819
MCC								0.770
Kappa								0.767

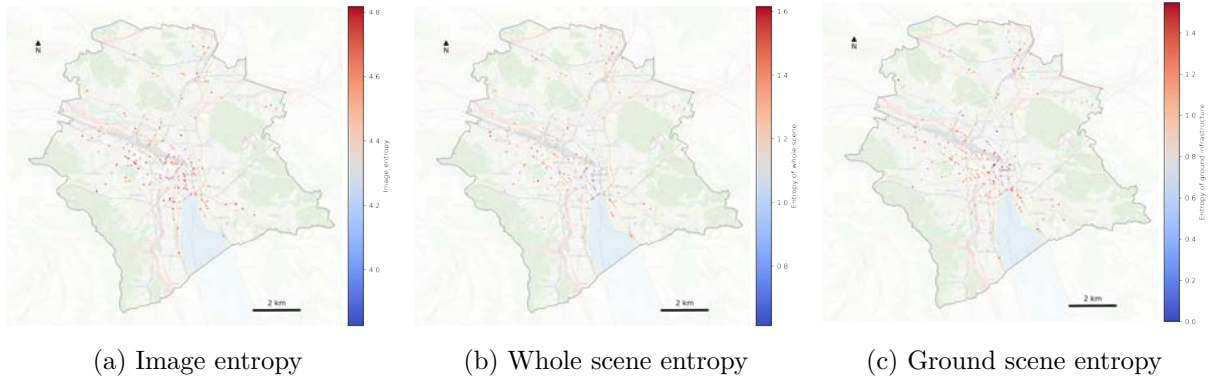


Figure 5.11: Entropy variables generation results for accident locations

Table 5.10: Generated entropy variables

Type	Variable	Description
Image entropy	ie	Average value of image entropy
	iemin	Minimum value of image entropy
	iemax	Maximum number of image entropy
Whole scene entropy	mew	Average entropy value for whole scene
	mewmin	Minimum entropy value for whole scene
	mewmax	Maximum entropy value for whole scene
Ground scene entropy	meg	Average entropy value for whole scene
	megmin	Minimum entropy value for ground scene
	megmax	Maximum entropy value for ground scene

5.4.3 Traffic-transport variables

Traffic-transport variables of three main types were generated, including distance from accident locations to infrastructure features as well as numeric and categorical variables of traffic network characteristics. Table 5.11 below illustrates the list of generated variables. Categorical variables were encoded into one-hot numeric values.

Table 5.11: Generated traffic-transport variables

Type	Variable	Description
Distance to infrastructure features	dbusl	Distance to bus line
	dtraml	Distance to tram rail
	dtrainl	Distance to train rail
	dplight	Distance to public light
	dstation	Distance to public transport station
	dparkcar	Distance to car parking space
	dparktw	Distance to two-wheeler parking space
	dpedcro	Distance to pedestrian crossing
	dstopsign	Distance to stop sign
	dcurb	Distance to curb
dtrafficarea	Distance to traffic area	
droad	Distance to road	
dvfpath	Distance to bicycle and pedestrian route	
Numeric traffic characteristics	speedlimit_value	Speed limit value
	gvm_dvw	Average daily traffic
	gvm_msp	Traffic demand in morning peak hours
	gvm_asp	Traffic demand in evening peak hours
	r_width_value	Road width
Categorical traffic characteristics	curbtype	Curb width type
	z_qnr	Statistical city district
	z_knr	Urban district
	trafficarea	Traffic zone
	r_width	Road width group
	r_surface	Road surface type
	speedlimit	Speed limit group

5.5 Variables generation of random pseudo-absence points

5.5.1 Random pseudo-absence points

Figure 5.12 below presents the distribution of generated random pseudo-absence points. Similar to the process for e-scooter accident location points, GSV images of pseudo points were also retrieved and filtered by their content. In total, 995 pseudo points were generated, of which 792 locations had valid GSV images.

5.5.2 Variables generation

The variable generation process for pseudo points is the same as that for accident locations, including creating curb variables, entropy variables as well as traffic-transport variables. Additionally, number, name, and data format of variables generated for pseudo points are consistent with the previous variable dataset for accident points.

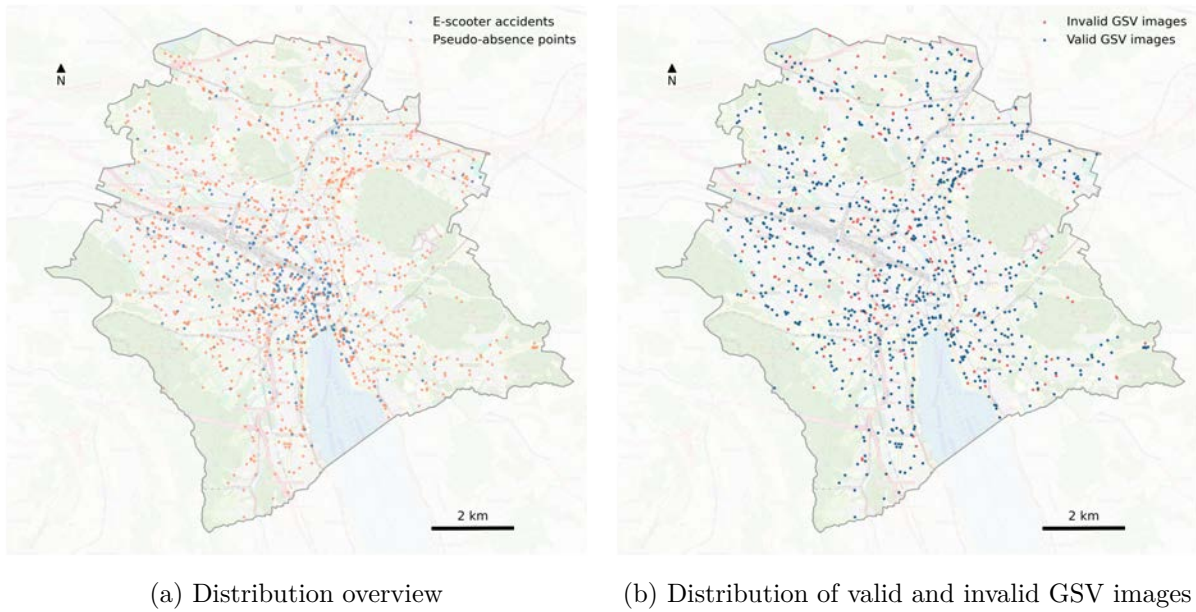


Figure 5.12: Distribution of random pseudo-absence points and valid GSV images

5.5.2.1 Curb variables

By applying SAM on GSV images of pseudo points, calculating properties of output segmentation masks, and building RF classification model, curb variables including presence, number(average, maximum, minimum) were attained. Figure 5.13 illustrates the spatial distribution of two curb variables (presence and average number) for pseudo points.

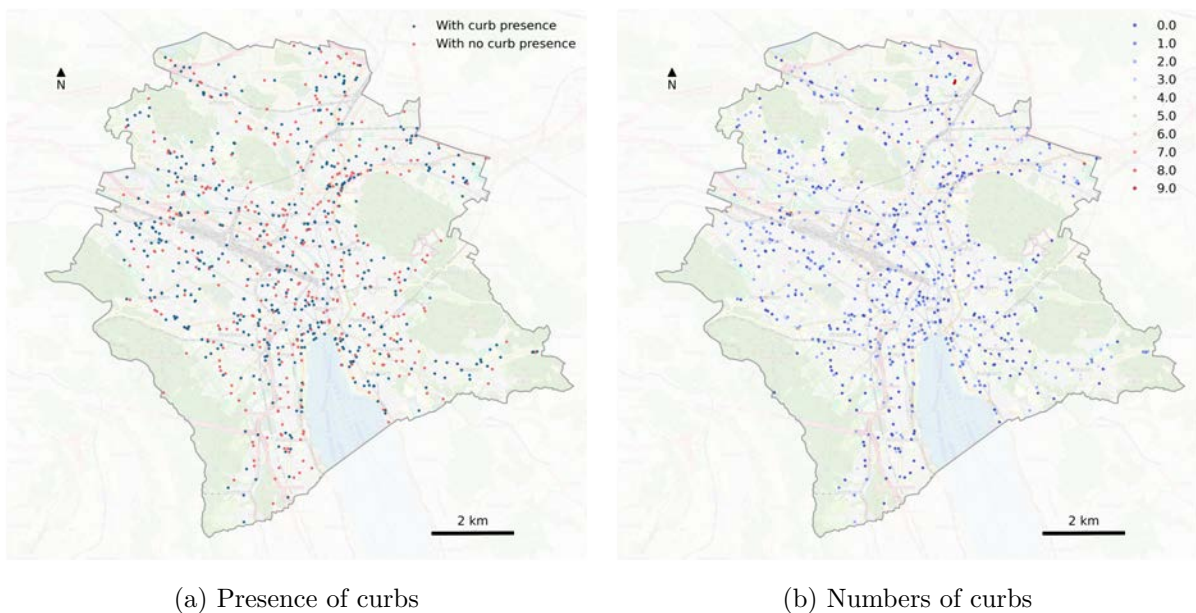


Figure 5.13: Distribution of curb extraction results for random pseudo-absence points

5.5.2.2 Entropy variables

Image entropy, whole scene entropy, and ground scene entropy were produced, of which the average values calculated from four images for each pseudo point location were mapped as shown in the following Figure 5.14.

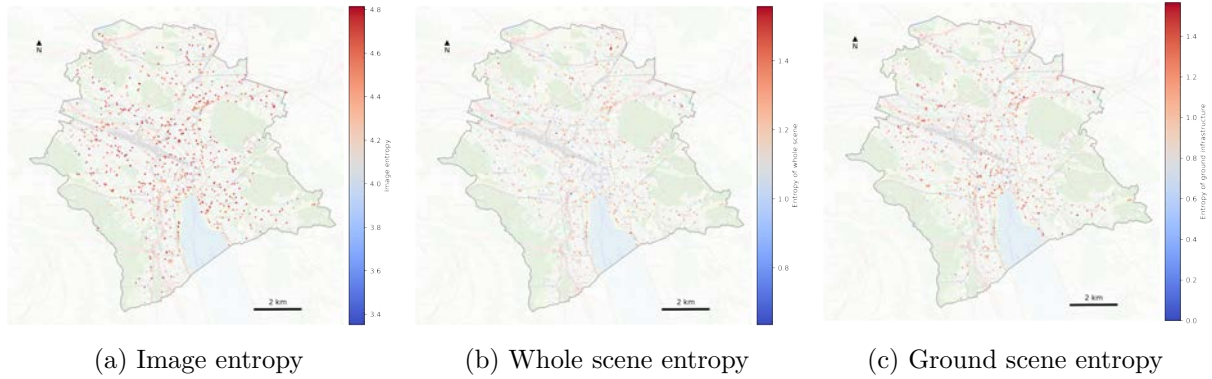


Figure 5.14: Entropy variables generation results for random pseudo-absence points

5.5.2.3 Traffic-transport variables

Likewise, three types of traffic-transport variables for pseudo points were acquired by merging with transport and traffic network infrastructure datasets, including distance to infrastructure features and numeric and categorical traffic network characteristics. It is important to note that several traffic-transport variables generated for pseudo points have more categories than those for accident points, since the pseudo points spread in a larger distribution. These variables were therefore not considered thoroughly in the prediction model. Specifically, they are variables of speed limit and statistical district.

5.6 Regression analysis

5.6.1 Regression for accident presence

The regression result for presence of accident is presented as follows in Table 5.12 and 5.13. Out of the 98 independent variables, 53 variables were determined to be statistically significant. As for numeric variables, speed limit, curb presence, and road width were identified to have a negative correlation with accident presence at the highest significance. Distance to traffic area, train railway, stop sign, and tram rail, as well as maximum number of curbs was positively related to presence of accident. While daily traffic density was found to be negatively correlated with it. Regarding categorical variables, as shown in the table, presence of accidents was associated with speed limit type, urban district, statistical district, road width type.

Table 5.12: OLS regression model for accident presence - Model metrics

Metrics	Value
R-squared	0.672
Adjusted R-squared	0.642
F-statistic	21.91
Prob(F-statistic)	0.000
Log-likelihood	-55.119
AIC	298.200
BIC	767.4

Table 5.13: OLS regression model for accident presence - Significant variables

Variables	P-value	Coefficient	Significance
speedlimit_value	0.000	-0.2709	***
r_width_value	0.000	-0.1306	***
r_width_5,3,6	0.000		***
trafficarea_3,1	0.000		***
z_knr_5,6,12,9,1,3,10	0.000		***
r_surface_1	0.000	0.3428	***
speedlimit_1,2,3	0.000		***
curbtype_1	0.000	0.3251	***
cp	0.000	-0.2680	***
z_qnr_7,8,14,1,11,12,5,15	0.000		***
z_qnr_4,16,31,9,32	0.007-0.001		**
speedlimit_5	0.003	-0.4362	**
dtrafficarea	0.004	0.0399	**
r_width_4	0.005	0.0942	**
dtrainl	0.006	0.0300	**
z_knr_8	0.009	-0.1709	**
z_qnr_3,8,2,6,13,21	0.038-0.010		*
dstopsign	0.011	0.0300	*
r_width_7	0.014	-0.1447	*
dtraml	0.016	0.0290	*
gvm_dwv	0.024	-0.1395	*
curbtype_2	0.030	0.1317	*
z_knr_2, 11	0.048-0.032		*
cmax	0.040	0.0812	*

Significance codes: 0 *** 0.001 ** 0.01 * 0.05

5.6.2 Regression for accident severity

Additionally, to investigate whether there is a correlation between all variables with accident severity, regression analysis was also performed by combining the previously created variable dataset for accident points and severity records from the accident dataset. In total, six dependent variables for severity were set, including person injury and property damage. It is worth noting

that there are three types of personal injury recorded for e-scooter accidents: fatal, light, and severe. However, no e-scooter accidents from 2019 to 2022 in the city of Zurich were involved with person fatality. Therefore, only light and severe personal injury were considered in this thesis. Records related to the impact of e-scooter accidents were selected, containing the number of injured persons (lightly and severely) and property damage value. Dependent variables for the regression model were generated based on both the presence of injury and the number of injured persons. Specifically, binary values of 0 and 1 were added based on the number of injured persons and property damage to represent whether e-scooter accidents involved person injury or property damage. Since the maximum number of severely injured persons recorded in the dataset is 1, the presence variable with a form of binary values is exactly identical to the number of persons for severe injury. As can be seen from the following Table 5.14, the number of severely injured persons is not included.

Table 5.14: Dependent variables for accident impact

	Variable	Description
Person injury	inp	1 for injury and 0 for no injury
	svp	1 for severe injury and 0 for no severe injury
	lvp	1 for injury and 0 for no injury
	lv	Number of lightly injured persons
Property damage	pdp	1 for damage presence and 0 for no damage
	pd	Numeric value of property damage

For all the six dependent variables, regression analysis was performed respectively with OLS linear regression model and GAM linear regression model. Metrics of built models were listed in the following tables to provide a basic outline of regression performance. Moreover, variables identified to be statistically significant were summarised with p-values.

5.6.2.1 Regression for person injury

Presence of injury Table 5.15 and Tale 5.16 illustrate the results of OLS linear regression and GAM linear regression separately. R-squared value of OLS model is 0.291 while pseudo R-squared value of GAM model is 0.547. Variables determined to be correlated with the presence of injury are road surface, curb width type, traffic area, statistical district, and distance to the road in the OLS regression model. Results from GAM regression show that more variables are statistically significant, including presence of curb, minimum and maximum number of curbs, curb width type, road width value and type, speed limit, statistical district, urban district, traffic area, maximum whole scene entropy, bicycle traffic count, distance to pedestrian crossings, distance to road, distance to curb, along with average, minimum, maximum value of image entropy.

Presence of severe injury From Table 5.17 and Table5.18, OLS regression model on the presence of severe injury has an R-squared value of 0.27 while the pseudo R-squared value of GAM is 0.530. Concerning the defined significant variables, OLS regression result shows six

Table 5.15: OLS regression model for the presence of person injury

(a) Model metrics		(b) Significant variables			
Metrics	Value	Variables	P-value	Coefficient	Significance
R-squared	0.291	r_surface_1	0.000000	0.3981	***
Adjusted R-squared	0.048	curbtype_2	0.000011	0.2528	***
F-statistic	1.199	trafficarea_2	0.000064	0.2876	***
Prob(F-statistic)	0.159	curbtype_1	0.007041	0.1453	**
Log-likelihood	-51.645	z_qnr_21	0.023315	-0.2046	*
AIC	255.300	z_qnr_20	0.024801	-0.1995	*
BIC	535.500	droad	0.049077	0.0840	*

Significance codes: 0 *** 0.001 ** 0.01 * 0.05

Table 5.16: GAM regression model for presence of person injury

(a) Model metrics		(b) Significant variables		
Metrics	Value	Variables	P-value	Significance
Pseudo R-squared	0.547	cp	0.000000	***
Log-likelihood	-486.125	cmin	0.000000	***
AIC	1225.083	cmax	0.000000	***
AICc	1417.316	r_width_value	0.000000	***
GCV	0.324	speedlimit_value	0.000000	***
		curbtype [^]	0.000000	***
		z_qnr [^]	0.000000	***
		z_krn [^]	0.000000	***
		trafficarea [^]	0.000000	***
		r_width [^]	0.000000	***
		r_surface [^]	0.000000	***
		speedlimt [^]	0.000000	***
		mewmax	0.000002	***
		bicyclecount	0.000623	***
		dpedcro	0.003813	**
		droad	0.008227	**
		dcurb	0.009403	**
		ie	0.016757	*
		iemin	0.018670	*
		iemax	0.030583	*

[^] All categories of the variable.

Significance codes: 0 *** 0.001 ** 0.01 * 0.05

variables, including urban district, statistical district, road width type, distance to nearby road, and curb width type. And GAM regression finds fourteen variables significant, such as presence of curb, minimum and maximum number of curbs, curb width type, road width value and type, speed limit, statistical district, urban district, traffic area, distance to public light as well as average ground scene entropy.

Table 5.17: OLS regression model for presence of severe person injury

(a) Model metrics		(b) Significant variables			
Metrics	Value	Variables	P-value	Coefficient	Significance
R-squared	0.270	z_knr_2	0.000065	0.3779	***
Adjusted R-squared	0.021	z_qnr_2	0.001087	0.5526	**
F-statistic	1.083	r_surface_1	0.009891	0.1681	**
Prob(F-statistic)	0.325	droad	0.017777	0.1117	*
Log-likelihood	-80.491	r_width_4	0.026391	0.0418	*
AIC	313.000	curbtype_1	0.048491	0.1169	*
BIC	593.200	Significance codes: 0 *** 0.001 ** 0.01 * 0.05			

Table 5.18: GAM regression model for presence of severe person injury

(a) Model metrics		(b) Significant variables		
Metrics	Value	Variables	P-value	Significance
Pseudo R-squared	0.530	cp	0.000000	***
Log-likelihood	-377.075	cmin	0.000000	***
AIC	1006.982	cmax	0.000000	***
AICc	1199.215	r_width_value	0.000000	***
GCV	0.397	speedlimit_value	0.000000	***
		curbtype^	0.000000	***
		z_qnr^	0.000000	***
		z_krn^	0.000000	***
		trafficarea^	0.000000	***
		r_width^	0.000000	***
		r_surface^	0.000000	***
		speedlimit^	0.000000	***
		dplight	0.029018	*
		meg	0.036984	*

^ All categories of the variable.

Significance codes: 0 *** 0.001 ** 0.01 * 0.05

Presence of light injury Regarding the presence of light injury, OLS regression model with R-squared value of 0.252 and GAM regression model with pseudo R-squared value of 0.507 were shown in the following Table 5.19 and Table 5.20. In the OLS regression model, variables of statistical district, urban district, traffic area, speed limit, road surface, road width, curb width type, minimum image entropy are found to have a correlation with the presence of light injury. While the GAM regression model provides results that significant variables include presence of curb, minimum and maximum number of curbs, curb width type, road width value and type, speed limit, statistical district, urban district, traffic area, distance to road, and maximum whole scene entropy.

Table 5.19: OLS regression model for presence of light person injury

(a) Model metrics		(b) Significant variables			
Metrics	Value	Variables	P-value	Coefficient	Significance
R-squared	0.252	z_knr_2	0.000417	-0.4070	***
Adjusted R-squared	-0.004	r_surface_1	0.001389	0.2560	**
F-statistic	0.983	trafficarea_2	0.002254	0.2942	**
Prob(F-statistic)	0.524	curbtype_2	0.003191	0.2256	**
Log-likelihood	-140.020	r_width_5	0.023017	0.1568	*
AIC	432.000	iemin	0.034471	0.3574	*
BIC	712.200	z_knr_4	0.035271	0.1470	*
		z_qnr_2	0.036908	-0.4287	*
		z_knr_9	0.042756	0.2074	*
		speedlimit_3	0.048674	0.8941	*

Significance codes: 0 *** 0.001 ** 0.01 * 0.05

Table 5.20: GAM regression model for presence of light person injury

(a) Model metrics		(b) Significant variables		
Metrics	Value	Variables	P-value	Significance
Pseudo R-squared	0.507	cp	0.000000	***
Log-likelihood	-243.209	cmin	0.000000	***
AIC	739.250	cmax	0.000000	***
AICc	931.483	r_width_value	0.000000	***
GCV	0.608	speedlimit_value	0.000000	***
		curbtype [^]	0.000000	***
		z_qnr [^]	0.000000	***
		z_krn [^]	0.000000	***
		trafficarea [^]	0.000000	***
		r_width [^]	0.000000	***
		r_surface [^]	0.000000	***
		speedlimit [^]	0.000000	***
		mewmax	0.004551	**
		droad	0.011040	*

[^] All categories of the variable.

Significance codes: 0 *** 0.001 ** 0.01 * 0.05

Number of injured persons With respect to the number of injured persons, Table 5.21 presents OLS regression model results, of which the R-squared value is 0.237 and significant variables are urban district, road surface, road width, curb width type, minimum image entropy, and traffic area. Besides, as shown in Table 5.22, GAM regression model has pseudo R-squared value of 0.510, while variables of curb presence, curb numbers, curb width type, road width value and type, speed limit, statistical district, urban district, traffic area, distance to road, maximum value of whole scene entropy, distance to pedestrian crossing, minimum and average values of image entropy, along with distance to stop sign are determined to have a correlation

with the number of injured persons.

Table 5.21: OLS regression model for number of lightly injured person

(a) Model metrics		(b) Significant variables			
Metrics	Value	Variables	P-value	Coefficient	Significance
R-squared	0.237	z_knr_2	0.001014	-0.4567	**
Adjusted R-squared	-0.024	r_surface_1	0.001245	0.3122	**
F-statistic	0.907	curbtype_2	0.014419	0.2253	*
Prob(F-statistic)	0.685	r_width_5	0.019706	0.1943	*
Log-likelihood	-195.570	iemin	0.025343	0.4566	*
AIC	543.100	z_knr_11	0.033367	0.3933	*
BIC	823.300	trafficarea_2	0.041182	0.2360	*

Significance codes: 0 *** 0.001 ** 0.01 * 0.05

Table 5.22: GAM regression model for number of lightly injured person

(a) Model metrics		(b) Significant variables		
Metrics	Value	Variables	P-value	Significance
Pseudo R-squared	0.510	cp	0.000000	***
Log-likelihood	-202.022	cmin	0.000000	***
AIC	656.876	cmax	0.000000	***
AICc	849.109	r_width_value	0.000000	***
GCV	0.864	speedlimit_value	0.000000	***
		curbtype [^]	0.000000	***
		z_qnr [^]	0.000000	***
		z_krn [^]	0.000000	***
		trafficarea [^]	0.000000	***
		r_width [^]	0.000000	***
		r_surface [^]	0.000000	***
		speedlimt [^]	0.000000	***
		droad	0.006802	**
		mewmax	0.013017	*
		dpedcro	0.016521	*
		ie	0.017112	*
		dstopsign	0.020637	*
		iemin	0.047245	*

[^] All categories of the variable.

Significance codes: 0 *** 0.001 ** 0.01 * 0.05

5.6.2.2 Regression for property damage

Presence of property damage According to the Table 5.23, OLS regression model for the presence of property damage has a R-squared value of 0.290. Variables of road surface, statistical district as well as distance to public light are revealed to be correlated with the presence of

property damage. The result from GAM regression is illustrated in Table 5.24, with pseudo R-squared value of 0.579. Correlations between variables of curb presence, curb numbers, road width, speed limit, urban district, statistical district, traffic area, ground scene entropy, whole scene entropy, distance to curb, distance to car parking space, together with traffic demand in morning peak hours and presence of property damage are shown.

Table 5.23: OLS regression model for presence of property damage

(a) Model metrics		(b) Significant variables			
Metrics	Value	Variables	P-value	Coefficient	Significance
R-squared	0.290	r_surface_1	0.031243	0.1856	*
Adjusted R-squared	0.047	z_qnr_11	0.036414	0.2150	*
F-statistic	1.194	dplight	0.046491	0.0719	*
Prob(F-statistic)	0.164	Significance codes: 0 *** 0.001 ** 0.01 * 0.05			
Log-likelihood	-163.55				
AIC	479.100				
BIC	759.300				

Table 5.24: GAM regression model for presence of property damage

(a) Model metrics		(b) Significant variables		
Metrics	Value	Variables	P-value	Significance
Pseudo R-squared	0.579	cp	0.000000	***
Log-likelihood	-233.170	cmin	0.000000	***
AIC	719.173	cmax	0.000000	***
AICc	911.406	r_width_value	0.000000	***
GCV	0.643	speedlimit_value	0.000000	***
		curbtype [^]	0.000000	***
		z_qnr [^]	0.000000	***
		z_krn [^]	0.000000	***
		trafficarea [^]	0.000000	***
		r_width [^]	0.000000	***
		r_surface [^]	0.000000	***
		speedlimt [^]	0.000000	***
		megmax	0.002262	**
		meg	0.003816	**
		mew	0.006699	**
		dcurb	0.013723	*
		mewmax	0.015716	*
		gvm_msp	0.017958	*
		dparkcar	0.035821	*

[^] All categories of the variable.

Significance codes: 0 *** 0.001 ** 0.01 * 0.05

Value of property damage With regard to property damage values, results from OLS linear regression and GAM linear regression are presented in Table 5.25 and Table 5.26 below. OLS regression model for property damage with R-squared value of 0.245 reveals that variables, including statistical district, traffic area, maximum and average values of image entropy, urban district, and traffic area, have significant correlation with property damage value. While the result from GAM regression with pseudo R-squared value of 0.521 shows that presence, width as well as minimum and maximum number of curbs, road width type and value, speed limit type and value, urban district, statistical district, traffic demand in morning peak hours, and distance to curb are significant variables.

Table 5.25: OLS regression model for value of property damage

(a) Model metrics		(b) Significant variables			
Metrics	Value	Variables	P-value	Coefficient	Significance
R-squared	0.245	z_qnr_21	0.004441	2660.5790	**
Adjusted R-squared	-0.014	trafficarea_2	0.006080	2019.0510	**
F-statistic	0.947	iemax	0.009536	2743.7248	**
Prob(F-statistic)	0.601	z_knr_9	0.013566	1939.1458	*
Log-likelihood	-2778.300	trafficarea_3	0.016059	-2135.4976	*
AIC	5709.000	ie	0.034882	-4420.0586	*
BIC	5989.000	Significance codes: 0 *** 0.001 ** 0.01 * 0.05			

Table 5.26: GAM regression model for value of property damage

(a) Model metrics		(b) Significant variables		
Metrics	Value	Variables	P-value	Significance
Pseudo R-squared	0.521	cp	0.000000	***
Log-likelihood	-5019.550	cmin	0.000000	***
AIC	10291.932	cmax	0.000000	***
AICc	10484.165	r_width_value	0.000000	***
GCV	34331076.476	speedlimit_value	0.000000	***
		curbtype^	0.000000	***
		z_qnr^	0.000000	***
		z_krn^	0.000000	***
		trafficarea^	0.000000	***
		r_width^	0.000000	***
		r_surface^	0.000000	***
		speedlimt^	0.000000	***
		gvm_msp	0.011692	*
		dcurb	0.037897	*

^ All categories of the variable.

Significance codes: 0 *** 0.001 ** 0.01 * 0.05

5.7 Prediction Model

A regression model built within the accident variable dataset for different severity was applied to pseudo points, which was designed to examine how severity distributes under the same possibilities of accidents.

5.7.1 Person injury

Predicted presence of person injury The presence of person injury predicted by previously built OLS regression model and GAM regression model was illustrated in Figure 5.15, which shows that most locations of pseudo points were predicted to be prone to person injury. OLS and GAM regression models both predict 97% of the pseudo points are with the presence of person injury.

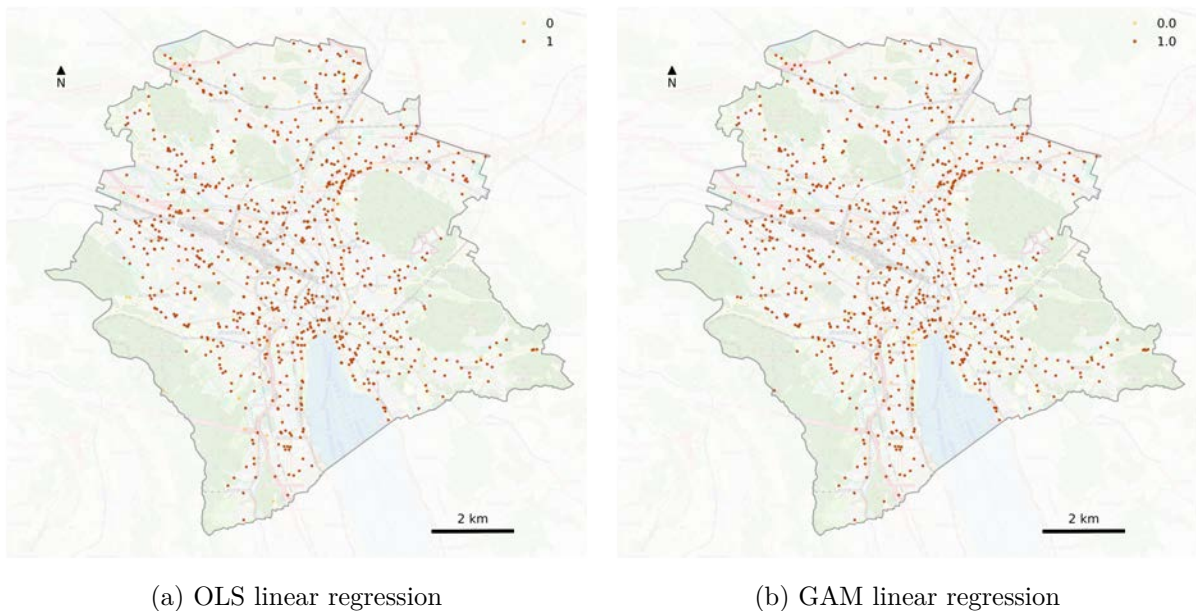
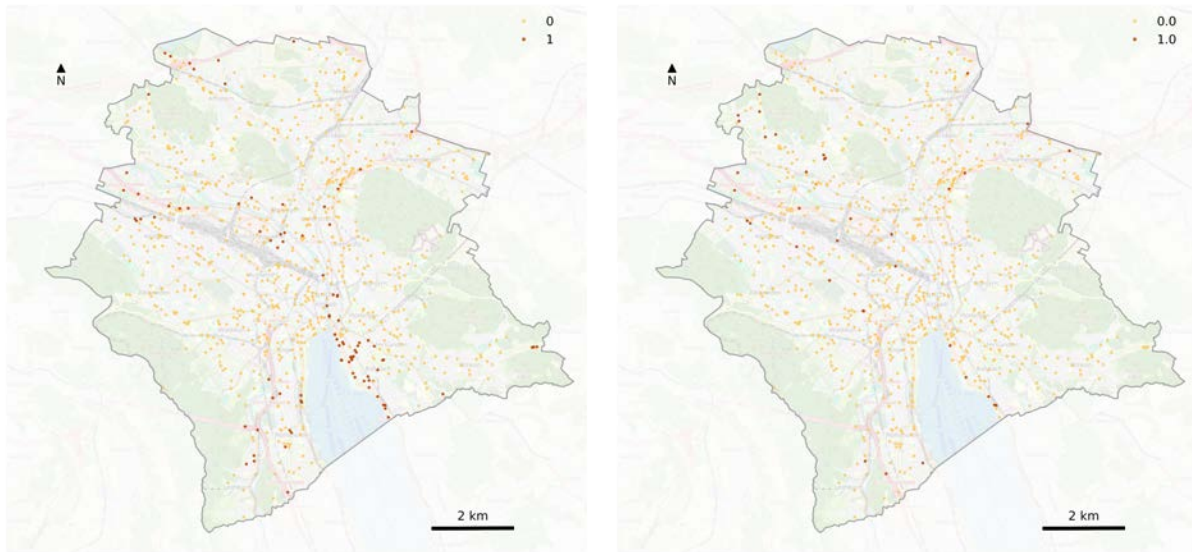


Figure 5.15: Prediction result for presence of person injury

Predicted presence of severe injury Regarding the presence of severe injury, the prediction result is shown below in Figure 5.16, indicating a much smaller distribution compared to the presence of personal injury. Besides, some areas are shown to have a highly dense distribution of points that predict the existence of severe injury. For example, points located close to the eastern shore of Zurich Lake were predicted to likely involve severe injury.

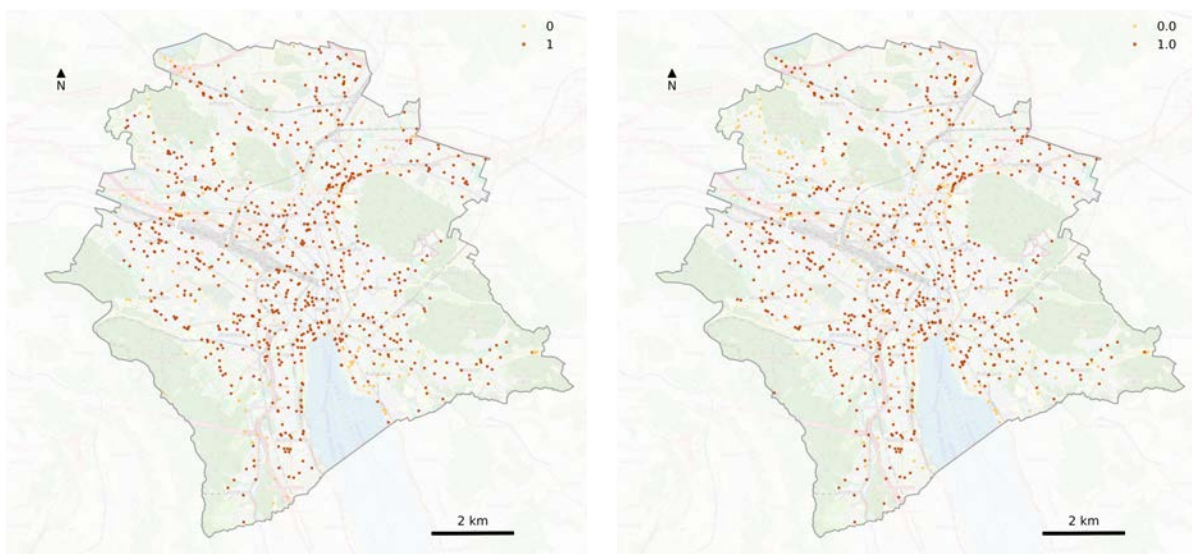
Predicted presence of light injury Different from the prediction result of severe injury, there is a larger distribution of predicted presence of light injury in the result from both regression models, as presented in Figure 5.17.



(a) OLS linear regression

(b) GAM linear regression

Figure 5.16: Prediction result for presence of severe person injury



(a) OLS linear regression

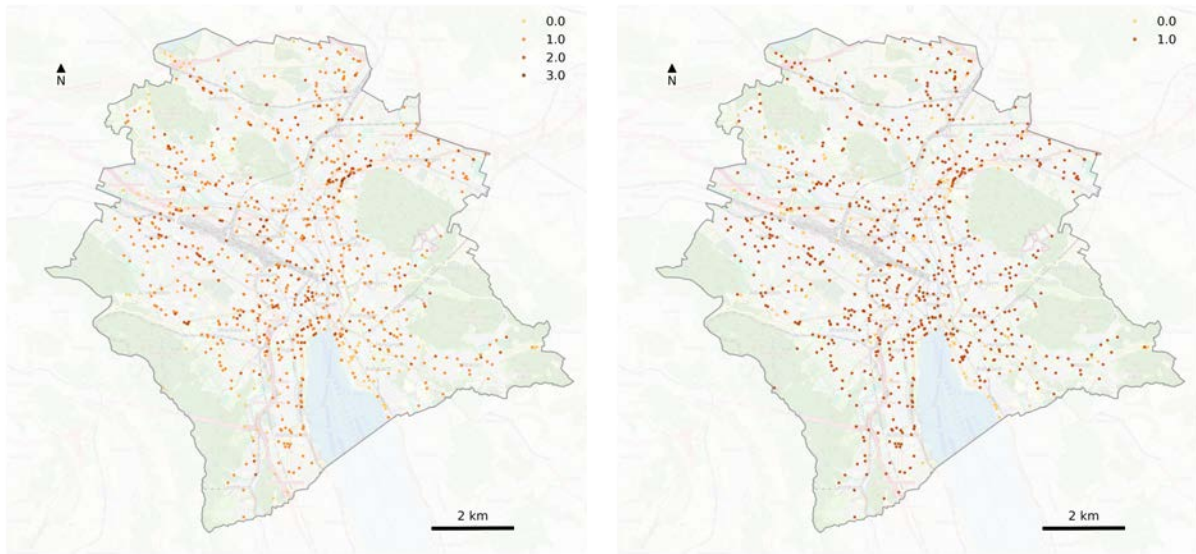
(b) GAM linear regression

Figure 5.17: Prediction result for presence of light person injury

Predicted number of lightly injured person As can be seen from Figure 5.18, while most of locations are predicted to involve one injured person from GAM regression model, most points are expected to be with a probability of over one injured person from OLS regression model.

5.7.2 Property damage

Predicted presence of property damage From Figure 5.19 below, it can be seen that the difference between numbers of points with and without property damage is smaller compared to the prediction result on the presence of person injury. The percentage of points predicted to

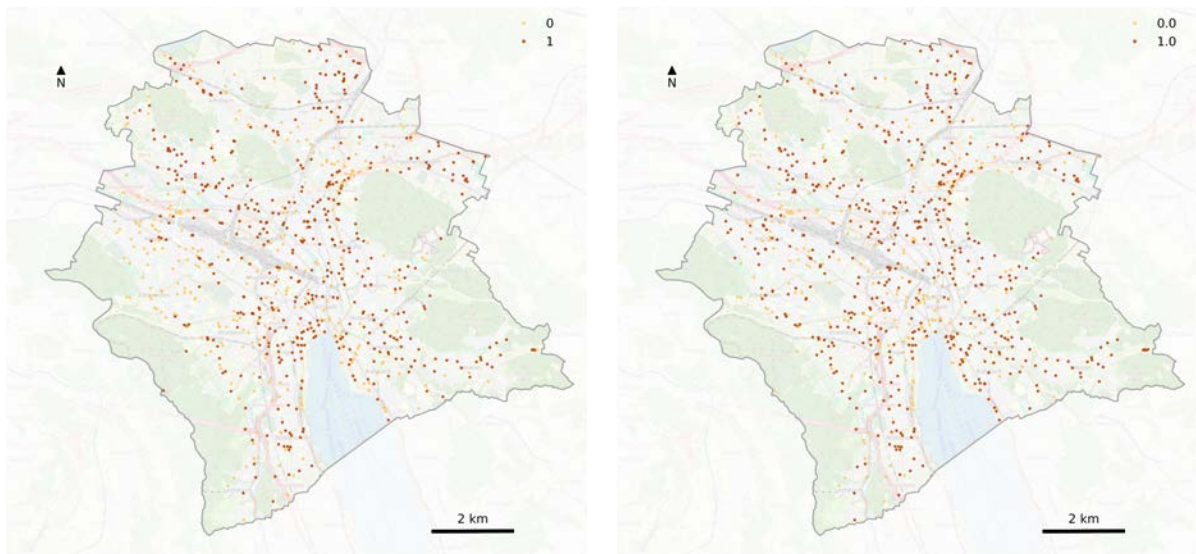


(a) OLS linear regression

(b) GAM linear regression

Figure 5.18: Prediction result for number of lightly injured person

be exposed with likely property damage are 61% from OLS model result and 69% from GAM model result.



(a) OLS linear regression

(b) GAM linear regression

Figure 5.19: Prediction result for presence of property damage

Predicted value of property damage Concerning the value of property damage, ranges of property damage of both OLS and GAM regression models are similar. As displayed in Figure 5.20, values are predicted relatively higher from GAM model than those from OLS model.

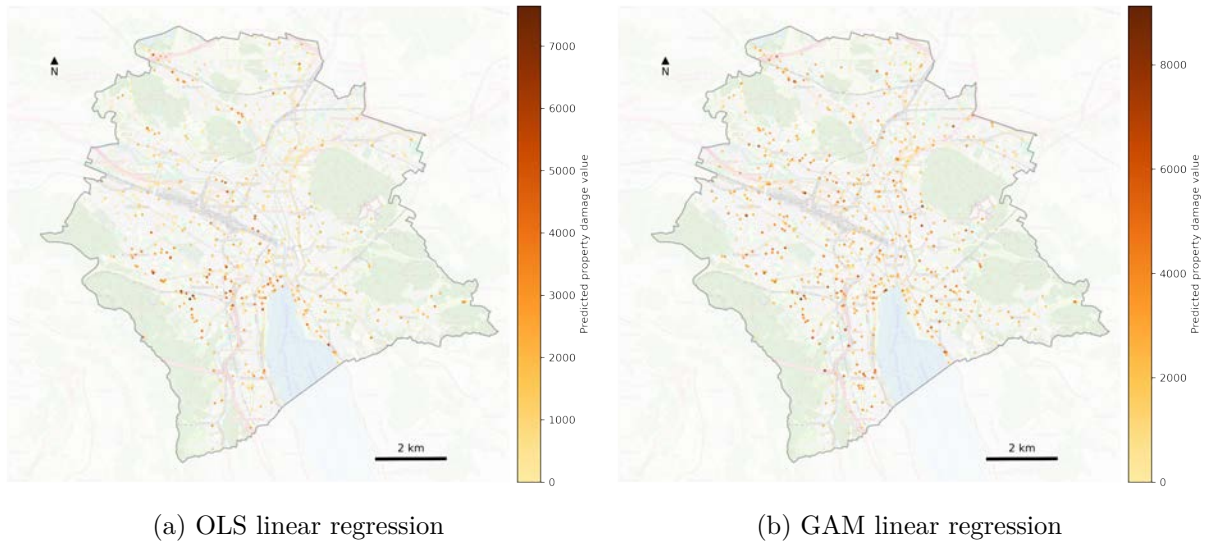


Figure 5.20: Prediction result for value of property damage

5.7.3 Grid-based aggregation of prediction result

To gain insights into the distribution pattern of predicted results and to identify possible areas with high risk in the involvement of personal injury and property damage, predictions for pseudo points were aggregated in square grids. Cell size was set to be about 200 meters (197.12 meters). Aggregation was applied to prediction results from GAM linear regression model, of which the maps are provided in Figure 5.21 as follows.

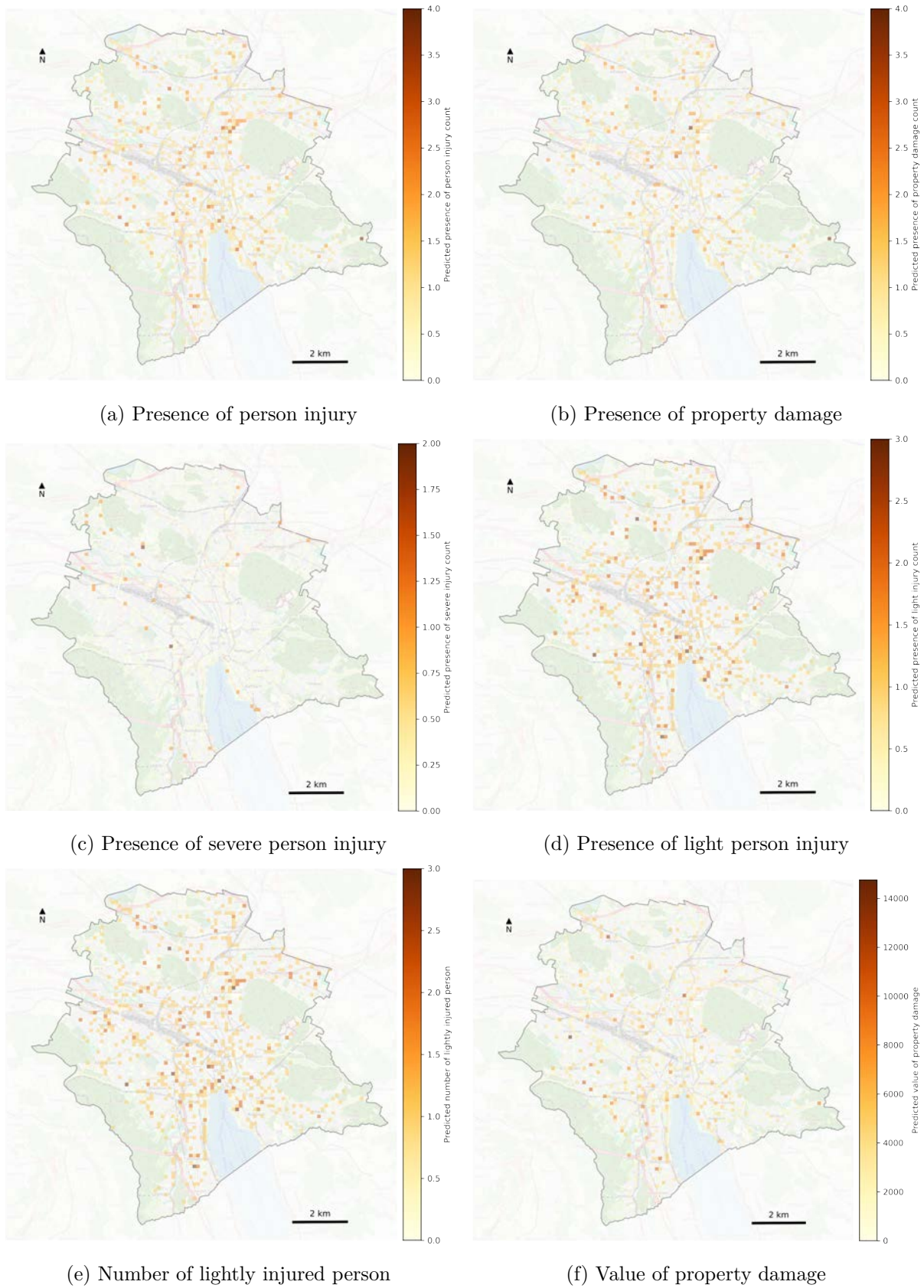


Figure 5.21: Aggregated prediction results

6. Discussion

This chapter aims to discuss the research from four aspects: results interpretation of each research question in Section 6.1, Section 6.2, Section 6.3, comparison with previous research in Section 6.4, assessment of methods in Section 6.5, and limitations in Section 6.6.

6.1 Overview of E-scooter accidents of Zurich

RQ1: What are the spatio-temporal patterns of e-scooter accidents in Zurich? What are the main causes of the accidents?

Overall, 350 e-scooter accidents were recorded by the city police from Year 2019 to 2022, offering an opportunity to gain initial insight into e-scooter safety issues in the city of Zurich. Characteristics and patterns of e-scooter accidents were analyzed from three perspectives: general attributes, spatial distribution, and temporal distribution.

Firstly, as shown in Table 3.1, the majority of the accidents are skidding or self-inflicted accidents, crossing the carriageway, or pedestrian accidents. Most e-scooter accidents have consequences of personal injury and property damage. Among them, although no fatality was recorded, only 46 accidents were recorded as damage-only accidents. Over 70% of the accidents cause light person injury and property damage of less than 500 CHF. Regarding involving persons and objects, most accidents only involve e-scooters or happen between e-scooters and passenger cars. In addition, the predominant age range of e-scooter drivers is from 25 to 64. Concerning infrastructure, all accidents recorded happen in town, while most accidents took place at a straight section on a secondary road, with a maximum of 50 km/h. Moreover, the most common circumstances for e-scooter accidents recorded are good weather, dry road surface, and weak or normal traffic volumes. Among all the e-scooter accidents, 56.6% were skidding or self-inflicted accidents, and 55.2% were mainly caused by the influence of alcohol or other influences related to inattention and distraction.

Secondly, e-scooter accidents were found to be concentrated in the city center in general. According to the result of KDE heat map, areas with a high density of e-scooter accidents in the city of Zurich were found to extend from Sechseläutenplatz north-westwards to Hardbrücke. Relatively less dense areas were located around stations Alstetten and Oerlikon. Besides, an overall increasing tendency of the high-density area was shown by comparing KDE heat map of each year from 2019 to 2022. Additionally, the aggregation of e-scooter accidents on road segments provided a similar spatial pattern, that the streets with the highest number of e-scooter accidents were situated in the city center, such as Bahnhofstrasse and Limmatquai. However, focusing on one single year, the concentration of aggregated accident counts per road segment was not shown obviously, which was probably because of the small size of the accident data amount.

Thirdly, from the exploratory time series analysis, an intuitive pattern was revealed in the time of e-scooter accidents. The number of e-scooter accidents has been increasing steadily from 2019 to 2022. Besides, it was found that obvious differences existed in the number of accidents over smaller time frames, including month, day of week, and hour. E-scooter accidents took place mostly from July to October, and predominantly on weekends. Considering the comparison between weekdays and weekends, the vast majority of e-scooter accidents on weekends happened between 23:00 and 3:00, while accidents on weekdays mostly occurred between 16:00 and 23:00.

6.2 Curb extraction with SAM

RQ2: How could infrastructure features be extracted from SVI by using SAM ?

Extraction of curb was achieved by applying SAM to GSV, generating variables based on properties of image segmentation, and training RF classification model with labels from manual vision interpretation. 7 groups of objects merged from 42 segmentation mask labels were generated. For each segmentation mask, 15 spectral features and 14 geometric attributes of identified contours were calculated, which were prepared to train RF classification model. Moreover, considering the exclusive purpose of detecting curbs, RF was trained and tested with a focus on the lower part of images. Evaluation results showed that the trained RF model had an overall accuracy of 0.838. Additionally, the result of ranking variable importance showed that influential variables for curb extraction were green color channel and red color channel, average color distance between mask color and grey, area, perimeter, equivalent diameter, and position of bottom bounding point. The important contribution of these variables could be explained by the unique characteristics of curbs, including their gray color, long, narrow shape, small size as well, and closeness to the bottom edge of GSV. With the curb extraction model, 278 curbs were identified from GSV images at 295 accident location points. The feasibility of this innovative method for curb extraction was explored and confirmed in this thesis.

6.3 Importance of infrastructure-related variables

RQ3 How do traffic-infrastructure characteristics relate to e-scooter accidents?

Two perspectives of the e-scooter accident were considered to answer this question, which were presence and severity. Presence indicates whether an e-scooter accident occurs or not, while severity means how serious the impact of an e-scooter accident is when it occurs. For each perspective, the relationship between it and traffic-infrastructure characteristics was determined by three steps. First of all, the generation of random pseudo points provided a point dataset that was randomly distributed in the road network without overlapping with accident points. These points could be assumed as random locations with no e-scooter accidents on the one hand and locations that are just situated randomly over the whole road network on the other hand. Subsequently, variables related to traffic-infrastructure characteristics were produced with three focuses, including curb, entropy, and characteristics of both traffic network and transport

infrastructure. Finally, the regression model was applied to the presence of accidents, as well as the severity of accidents, respectively.

Results from regression analysis on accident presence illustrated an acceptable goodness-of-fit with an R-squared value of 0.672. Nine numeric variables were determined to have a statistically significant correlation with the presence of accidents, among which variables of speed limit, curb presence, road width as well as average daily traffic (traffic density/exposure) were negatively related to accident presence. It indicates that accidents might take place more likely at locations with lower speed limit, narrower road, and less traffic density. Besides, distance to traffic area, train railway, stop sign, as well as maximum number of curbs were found to have a positive relationship with e-scooter accidents, which shows the possibility of accidents is higher in areas far from traffic area, railway, tram rails and stop signs. With a focus on curb, curb presence, and maximum number were found to be significant. While the presence of curb reduces the probability of accident presence, a larger maximum number of curbs increases it. It suggested that e-scooter accidents tend to take place at locations without curb compared to locations with curb. However, among locations with curb presence, a higher number of curbs leads to a higher possibility of e-scooter accidents. Furthermore, regarding categorical variables, six of them were found to be significant, such as urban district, statistical district, traffic area, curb width type. It was shown in the result that both types of curb nearby were determined to be positively correlated with accident presence, which could therefore be assumed that the existence of curbs is likely to be related to e-scooter accidents. Curb width type of 25 cm was found to be more significant with a bigger coefficient value compared to curb width type of 15 cm.

Concerning the severity of accidents, the goodness-of-fit of the overall regression models was shown to be lower than regression on accident presence. Nonetheless, significant variables correlated with different content of accident severity were determined from perspectives of both personal injury and property damage. Firstly, for the presence of person injury, OLS regression results illustrated that variables in the presence of both width type of curbs, traffic area, statistical district, as well as distance to road were significant for presence of person injury. Secondly, for the presence of property damage, distance to public light together with statistical district were found to be significant from OLS regression. Furthermore, the specific severity of person injury, including light and severe injury, as well as the value of property damage, were also considered as dependent variables for regression separately. GAM regression model was additionally conducted to be a supplement of OLS regression result.

Comprehensively, results from regression analysis on both the presence and severity of accidents illustrated that the traffic-infrastructure features have an influential impact on understanding e-scooter accidents.

6.4 Comparison with previous studies

The findings in the overview of e-scooter accidents, including main causes and spatial-temporal distribution, are generally consistent with attributes and patterns concluded in previous studies.

Over half of e-scooter accidents were identified to be skidding or self-inflicted accidents in the city of Zurich, which is in agreement with results of e-scooter causes analysis with web content mining in Germany (Brauner et al., 2022). The influence of alcohol was found to be the main cause in this study, which supported the conclusion that driving under alcohol consumption is an indispensable factor in user behavior for e-scooter accidents (Gioldasis et al., 2021). Besides, as for spatial distribution, the concentration of e-scooters in the city center as well as several other important traffic stations revealed in this thesis is associated with findings that e-scooter crashes predominantly happened in city center (Pobudzei et al., 2023) and dense urban settings (Azimian & Jiao, 2022). Furthermore, concerning temporal trend, findings that the majority of e-scooter accidents happened during the weekends support previous research (Stigson et al., 2021). However, the pattern that e-scooter accidents mostly took place from early afternoon to late night was not exactly consistent with previous findings that the majority of e-scooter accidents happened at night or in the evenings (Brauner et al., 2022; Karpinski et al., 2022).

Additionally, the findings of the relationship between traffic infrastructure characteristics and e-scooter accidents confirm that road surface type, riding locations (White et al., 2023) and street type (Pobudzei et al., 2023) are among the most crucial infrastructure factors for e-scooter accidents. Regression results of accident presence that a higher number of curbs leads to a higher possibility of e-scooter accidents, supporting suggested ideas that collision between e-scooters and curbs is one of the common causes of e-scooter accidents.

6.5 Assessment of SAM performance

The performance of image segmentation with the application of SAM is worth discussing since its outstanding performance is confirmed by previous studies as a newly published advanced AI model. In this thesis, both strengths and weaknesses of SAM were observed in its application. Generally, it provided a good performance in image segmentation with an output of about 88 masks in general per image. Performance for segmenting masks was found to be more excellent for several specific object types compared to other types, including vehicles, bicycles, vegetation and humans. Details in components of these objects could also be recognized, such as the wheels of vehicles and the clothes of humans. Besides, an object with a large distance from the photo position could also be detected and segmented, such as a part of a distant mountain. Also, it offered a surprising ability to detect tiny objects and even objects partially obscured by others, such as cobbles on the pavement in Zurich's old town and a faraway building behind trees.

However, limitations and weaknesses of SAM were also found. Firstly, it has a high requirement on computing ability with a consumption of a large amount of time for segmentation. For one single image, the time consumed of SAM was not found to be related to pixel numbers, file sizes of images as well as output number of masks, which ranges from 83 seconds to 282 seconds per image and depends on the computing power of GPU devices. Also, SAM sometimes over segmented areas with rich texture in complex images, which supports the evaluations of SAM (Yilmaz & Kavzoglu, 2024) that limitation of an excessive segmentation exists in complex scenarios with low spatial resolution images. For example, windows on a high glass building and

brick patterns in the old town were found to be easily over segmented.

6.6 Limitations

Several limitations of this study are acknowledged from two perspectives as follows: data availability, coverage, and quality in Section 6.6.1, as well as methodological approach 6.6.2.

6.6.1 Data availability, coverage and quality

Availability, coverage, and quality of the three main data sources used in the thesis are of the greatest importance for the analysis. Fundamentally, the e-scooter accident dataset has a limited data size and potential bias. There were 350 accidents recorded by the city police from 2019 to 2022, on which the entire analysis process was based. The relatively small amount of data might lead to an inadequate understanding of e-scooter accidents. Besides, the e-scooter accidents were only recorded when the police noticed or were informed by the persons involved in an e-scooter accident. It is possible that more e-scooter accidents took place without being registered in this dataset, which could cause the analysis to be not accurate enough. Also, the riding direction of e-scooters was not included in the accident report, which makes it impossible to identify the exact visual environment of drivers. Using the average information from the surrounding four directions of GSV images, it is possible to be mismatched with a true driving view of e-scooter users. Furthermore, the SVI accessed through GSV static API has problems of incomplete coverage, invalid content, and relatively insufficient quality. Since GSV covers the road segments in the city of Zurich partially, streets without GSV were therefore not fully analyzed. Also, GSV includes content such as indoor space, rooftops, and aerial view, which are invalid for this work. And locations with invalid content in GSV were filtered and not included in the analysis for curb extraction and regression on e-scooter accidents. Moreover, it is noteworthy that distortion of objects, the sunlight of overexposure, and shadows exist in some images, which is likely to result in a misunderstanding of the colors and shapes of objects. Last, yet importantly, traffic and transport network datasets obtained from official government datasets also have limitations. Traffic count datasets have an uneven spatial distribution due to the concentration of traffic counting stations on main roads, including traffic census data for individual motorized transport as well as automatic pedestrian and bicycle count data, which causes a bias in traffic count variables in locations other than main roads.

6.6.2 Methodological approach

For **RQ1**, the spatial distribution pattern of e-scooter accidents was firstly visualized by applying kernel density estimation (KDE), of which the selected values of bandwidth and smoother are influential to the result. The optimized bandwidth value was set by Scott's rules, while the default setting for smoother was applied, and therefore, these parameters set with deficient tests might lead to incorrect results. Moreover, the number of e-scooter accidents was aggregated to

the nearby road segments for spatial distribution from the perspectives of the street network. However, the lengths of road segments among the same type of roads are not consistent. Therefore, generating a collection of road segments by cutting the currently used network with the same value of length may be important to have a more accurate understanding of the distribution pattern. Additionally, temporal analysis in this thesis is relatively simple and exploratory, and it would be interesting to analyze the temporal pattern of e-scooter accidents with more methods.

For **RQ2**, limitations of application of SAM are discussed in section 6.5. In addition to that, the filtering functions applied to remove overlapping masks and small-size contours could reduce the number of repetitive and less important masks on the one hand, but also possibly filter out masks for existing curbs. This might cause inadequate extraction of curbs and a smaller number of curbs in comparison to the true number of curbs in the real world.

For **RQ3**, there are three aspects of existing limitations, including variable generation, prediction model design, and regression analysis. To begin with, generated curb variables are limited to their presence and numbers. Other features, such as the portion of curbs in ground infrastructure, would be useful. Additionally, with the lack of riding direction of e-scooters, consecutive points on one e-scooter's driving route are impossible to produce, and therefore, calculating properties of extracted curbs becomes hard to achieve. Secondly, information extracted from GSV of each location is limited by summarising variables of images from all four directions. Information from each of the four GSV images per point is not fully used, which could be an improvement in variable generation to include differences among them or a combination pattern. Regarding transport traffic variables, incorrect results might exist due to the inclusion of unevenly distributed traffic infrastructure data. More transport data such as right of way might also contribute to e-scooter accidents, which should be considered. Concerning the prediction model, only prediction on accident severity was built to define how severity differentiates spatially with the same possibility of accident presence. The prediction of accident presence is not reached with the lack of more points located along the whole road network. It would be interesting to predict accident severity after predicting accident absence first. Additionally, the current aggregation of prediction results on points is based on grids with a size of about 200 meters, which might cause a modifiable areal unit problem without testing grids of more sizes. Moreover, regression analysis in this thesis might be improved by performing models of other regression methods and optimizing the selection of variables.

7. Conclusions

This thesis aims to investigate the influence of traffic infrastructure characteristics on e-scooter accidents in the city of Zurich. With the accident dataset recorded from police reports, this study first performs a spatial-temporal analysis to gain overall knowledge of the distribution pattern of e-scooter accidents. In order to comprehensively understand the impact of infrastructure, especially curb, extraction of curb is carried out by applying SAM to GSV at accident locations. After generating random pseudo points and integrating variables from perspectives in traffic transport, infrastructure, and entropy, the correlation between traffic transport characteristics and e-scooter accidents is determined by regression analysis.

7.1 Main findings

The main findings of this study are concluded into the following points:

- Predominant type of e-scooter accidents is skidding or self-inflicted, with a major cause of alcohol influence as well as inattention and distraction.
- E-scooter accidents concentrate mostly in the city center. Secondary centers of accidents are transport stations with dense urban settings, including Oerlikon and Altstetten.
- An obvious, steadily increasing annual trend has been found in e-scooter accidents. E-scooter accidents take place mostly on weekends. While the majority of accidents occur late at night on weekends, accidents on weekdays happen more from late afternoon to evening.
- Feasibility of extracting curb infrastructure feature from GSV with application of SAM is confirmed.
- There is a strong correlation between traffic infrastructure characteristics and the presence of e-scooter accidents.
- Significant variables of traffic infrastructure are determined to be related to the severity of e-scooter accidents. While curb width types, traffic area, and distance to the road affect the presence of personal injury, distance to public light has an influence on the presence of property damage.

7.2 Contributions and insights

Firstly, this study provides an overview of the main causes, spatial distribution, and temporal pattern of e-scooter accidents, filling the research gap for understanding e-scooter safety issues in

the city of Zurich. Secondly, by applying SAM, feature extraction by calculating segmentation properties and performing a classification model is achieved. The process introduced in this paper could be applied to acquire other interesting features from images, which not only offer a low-cost data collection method but also reduce the difficulty of extracting information from specific objects in traditional methods. Last yet most importantly, correlations are determined between traffic infrastructure and both the presence and severity of e-scooter accidents, which suggests the important influence of traffic infrastructure on e-scooter safety issues. Correlation coefficients of significant variables could be taken into account as a reference for further analysis in e-scooter accidents. Besides, the prediction result of different severity for e-scooter accidents in the city of Zurich presents a primary understanding of the underlying vulnerability of locations to e-scooter accidents.

7.3 Outlook and future research

Due to existing limitations discussed in Section 6.6, modeling the influence with a larger data size of accident data as well as a better SVI with a higher coverage is important to gain a more adequate and unbiased understanding on this problem. It is suggested that pedestrian traffic variables be included since the concentration of accidents is located in the city center, where a dense population exists. Besides, the bias existing in data registered from police reports should be considered and avoided in future research.

Additionally, as found and discussed in this paper, despite the breakthrough made by SAM as one of the most advanced AI models in image segmentation, weaknesses and shortcomings exist. Hence, there is abundant room for further progress in image segmentation. Furthermore, in future investigations, it might be possible and helpful to include more detailed information extracted from features such as measurements by overcoming the limitations of current methods.

Moreover, several questions remain unanswered at present, including how e-scooter accidents are distributed or will occur in rural areas with a predictable growing popularity of micro-mobility and how to thoroughly exclude driver's factor in e-scooter safety issues under the predominant influence of alcohol and distraction recorded so far.

Bibliography

- Abdel-Aty, M., & Wang, X. (2006). Crash estimation at signalized intersections along corridors: Analyzing spatial effect and identifying significant factors. *Transportation Research Record, 1953*(1), 98–111. <https://doi.org/10.1177/0361198106195300112>
- Abduljabbar, R. L., Liyanage, S., & Dia, H. (2021). The role of micro-mobility in shaping sustainable cities: A systematic literature review. *Transportation Research Part D: Transport and Environment, 92*, 102734. <https://doi.org/https://doi.org/10.1016/j.trd.2021.102734>
- Ahmadi, M., Lonbar, A. G., Sharifi, A., Beris, A. T., Nouri, M., & Javidi, A. S. (2023). Application of segment anything model for civil infrastructure defect assessment. <https://doi.org/10.48550/arXiv.2304.12600>
- Alhasoun, F., & Gonzalez, M. (2019). Streetify: Using street view imagery and deep learning for urban streets development. <https://doi.org/10.48550/arXiv.1911.08007>
- Angelov, D., Dulong, C., Filip, D., Frueh, C., Lafon, S., Lyon, R., Ogale, A., Vincent, L., & Weaver, J. (2010). Google street view: Capturing the world at street level. *Computer, 43*(6), 32–38. <https://doi.org/10.1109/MC.2010.170>
- Azimian, A., & Jiao, J. (2022). Modeling factors contributing to dockless e-scooter injury accidents in austin, texas. *Traffic Injury Prevention, 23*, 107–111. <https://doi.org/10.1080/15389588.2022.2030057>
- Badia, H., & Jenelius, E. (2023). Shared e-scooter micromobility: Review of use patterns, perceptions and environmental impacts. *Transport Reviews, 43*(5), 811–837. <https://doi.org/10.1080/01441647.2023.2171500>
- Balaji, S., Karakus, O. K., Balaji, S., Karakus, was, O., & Karakus, was, K. (2024). Unsupervised structural damage assessment from space using the segment anything model (usda-sam): A case study of the 2023 türkiye earthquake. <https://doi.org/10.31223/X5W40V>
- Balali, V., Rad, A. A., & Golparvar-Fard, M. (2015). Detection, classification, and mapping of u.s. traffic signs using google street view images for roadway inventory management. *Visualization in Engineering, 3*. <https://doi.org/10.1186/s40327-015-0027-1>
- Barbet-Massin, M., Jiguet, F., Albert, C. H., & Thuiller, W. (2012). Selecting pseudo-absences for species distribution models: How, where and how many? *Methods in Ecology and Evolution, 3*(2), 327–338. <https://doi.org/10.1111/j.2041-210X.2011.00172.x>
- Biland, G. (2023). *Bicycle accidents in urban zurich: An analysis of temporal patterns, influence of network infrastructure and accident severity* [Master's thesis, Department of Geography, University of Zurich].
- Biljecki, F., & Ito, K. (2021). Street view imagery in urban analytics and gis: A review. *Landscape and Urban Planning, 215*, 104217. <https://doi.org/10.1016/j.landurbplan.2021.104217>
- Bjmskau, T., & Karlseo, K. E-scooter accidents and risk factors - survey results from users of rental e-scooters in norway 2021. In: In *Contributions to the 10th international cy-*

- cling safety conference 2022 (icsc2022)*. Dresden: Technische Universität Dresden, 2022, November, 238–239. <https://doi.org/10.25368/2022.494>
- Bozzi, A. D., & Aguilera, A. (2021). Shared e-scooters: A review of uses, health and environmental impacts, and policy implications of a new micro-mobility service. *Sustainability*, *13*(16). <https://doi.org/10.3390/su13168676>
- Brauner, T., Heumann, M., Kraschewski, T., Prahlow, O., Rehse, J., Kiehne, C., & Breitner, M. H. (2022). Web content mining analysis of e-scooter crash causes and implications in germany. *Accident Analysis and Prevention*, *178*, 106833. <https://doi.org/10.1016/j.aap.2022.106833>
- Breiman, L. (2001). Random forests. *Machine Learning*, *45*, 5–32. <https://doi.org/10.1023/A:1010933404324>
- Bruno, N., & Roncella, R. (2019). Accuracy assessment of 3d models generated from google street view imagery. *The International Archives of the Photogrammetry, Remote Sensing and Spatial Information Sciences*, *XLII-2/W9*, 181–188. <https://doi.org/10.5194/isprs-archives-XLII-2-W9-181-2019>
- Bundesamt für Statistik. (2023a). Mobilitätsverhalten der bevölkerung - ergebnisse des mikrozensus mobilität und verkehr 2021. <https://www.are.admin.ch/are/en/home/mobility/data/mtmc.html>
- Bundesamt für Statistik. (2023b, August). *Mobility and transport*. <https://dam-api.bfs.admin.ch/hub/api/dam/assets/26866731/master>
- Bundesamt für Strassen ASTRA. (2018a). Instruktionen zum ausfüllen des unfallaufnahme-protokolls. <https://www.astra.admin.ch/astra/de/home/dokumentation/daten-informationsprodukte/unfalldaten/grundlagen/unfallerfassung.html>
- Bundesamt für Strassen ASTRA. (2018b). Unfallaufnahmeprotokoll. <https://www.astra.admin.ch/astra/de/home/dokumentation/daten-informationsprodukte/unfalldaten/grundlagen/unfallerfassung.html>
- Button, K., Frye, H., & Reaves, D. (2020). Economic regulation and e-scooter networks in the usa [Journal of the Transportation Research Forum, Volume 57]. *Research in Transportation Economics*, *84*, 100973. <https://doi.org/10.1016/j.retrec.2020.100973>
- Cai, B. Y., Li, X., Seiferling, I., & Ratti, C. (2018). Treepedia 2.0: Applying deep learning for large-scale quantification of urban tree cover. *2018 IEEE International Congress on Big Data (BigData Congress)*, 49–56. <https://doi.org/10.1109/BigDataCongress.2018.00014>
- Cai, Q., Abdel-Aty, M., Zheng, O., & Wu, Y. (2022). Applying machine learning and google street view to explore effects of drivers' visual environment on traffic safety. *Transportation Research Part C: Emerging Technologies*, *135*. <https://doi.org/10.1016/j.trc.2021.103541>
- Campbell, A., Both, A., & Sun, Q. (2019). Detecting and mapping traffic signs from google street view images using deep learning and gis. *Computers, Environment and Urban Systems*, *77*. <https://doi.org/10.1016/j.compenvurbsys.2019.101350>
- Chacra, D. A., & Zelek, J. (2016). Road segmentation in street view images using texture information. *2016 13th Conference on Computer and Robot Vision (CRV)*, 424–431. <https://doi.org/10.1109/CRV.2016.47>

- Chan, T. K., Chin, C. S., Chen, H., & Zhong, X. (2020). A comprehensive review of driver behavior analysis utilizing smartphones. *IEEE Transactions on Intelligent Transportation Systems*, *21*(10), 4444–4475. <https://doi.org/10.1109/TITS.2019.2940481>
- Chao Wang, M. Q., & Ison, S. (2013). A spatio-temporal analysis of the impact of congestion on traffic safety on major roads in the uk. *Transportmetrica A: Transport Science*, *9*(2), 124–148. <https://doi.org/10.1080/18128602.2010.538871>
- Chen, J., Yu, X., Liu, S., Chen, T., Wang, W., Jeon, G., & He, B. (2024). Tunnel sam adapter: Adapting segment anything model for tunnel water leakage inspection. *Geohazard Mechanics*, *2*(1), 29–36. <https://doi.org/10.1016/j.ghm.2024.01.001>
- Cicchino, J. B., Kulie, P. E., & McCarthy, M. L. (2021). Severity of e-scooter rider injuries associated with trip characteristics. *Journal of Safety Research*, *76*, 256–261. <https://doi.org/10.1016/j.jsr.2020.12.016>
- David, L., Zohar, M., & Shimshoni, I. (2023). Geo-referencing and analysis of entities extracted from old drawings and photos using computer vision and deep learning algorithms. *ISPRS International Journal of Geo-Information*, *12*(12). <https://doi.org/10.3390/ijgi12120500>
- Dean, M. D., & Zuniga-Garcia, N. (2023). Shared e-scooter trajectory analysis during the covid-19 pandemic in austin, texas [PMID: 37153185]. *Transportation Research Record*, *2677*(4), 432–447. <https://doi.org/10.1177/03611981221083306>
- Di, C., & Gong, J. (2024). An ai-based approach to create spatial inventory of safety-related architectural features for school buildings. *Developments in the Built Environment*, *17*, 100376. <https://doi.org/10.1016/j.dibe.2024.100376>
- Dias, G., Arsenio, E., & Ribeiro, P. (2021). The role of shared e-scooter systems in urban sustainability and resilience during the covid-19 mobility restrictions. *Sustainability*, *13*(13). <https://doi.org/10.3390/su13137084>
- Diou, C., Lelekas, P., & Delopoulos, A. (2018). Image-based surrogates of socio-economic status in urban neighborhoods using deep multiple instance learning. *Journal of Imaging*, *4*(11). <https://doi.org/10.3390/jimaging4110125>
- Edel, F., Wassmer, S., & Kern, M. (2021). Potential analysis of e-scooters for commuting paths. *World Electric Vehicle Journal*, *12*(2). <https://doi.org/10.3390/wevj12020056>
- Elvik, R. (2004). To what extent can theory account for the findings of road safety evaluation studies? *Accident Analysis and Prevention*, *36*(5), 841–849. <https://doi.org/10.1016/j.aap.2003.08.003>
- Elvik, R., Høyve, A., Vaa, T., & Sørensen, M. (2009, January). Vehicle design and protective devices. Emerald Group Publishing Limited. <https://doi.org/10.1108/9781848552517-010>
- Federal Roads Office. (2023). Transport accidents - overview of all transport modes [Published: 2023-08-09]. <https://www.bfs.admin.ch/bfs/en/home/statistics/mobility-transport/accidents-environmental-impact/transport-accidents.assetdetail.24725632.html>
- Ferreira, M. P., dos Santos, D. R., Ferrari, F., Filho, L. C. T. C., Martins, G. B., & Feitosa, R. Q. (2024). Improving urban tree species classification by deep-learning based fusion of digital aerial images and lidar. *Urban Forestry and Urban Greening*, *94*, 128240. <https://doi.org/10.1016/j.ufug.2024.128240>

- Frank, S., Sator, T., Kinsky, R. M., Frank, J. K., Frank, R., Fialka, C., Mittermayr, R., & Boesmueller, S. (2023). Continuously increasing e-scooter accidents and their possible prevention in a large european city christian fialka auva trauma center vienna meidling. <https://doi.org/10.21203/rs.3.rs-3735009/v1>
- George, Y., Athanasios, T., & George, P. (2017). Investigation of road accident severity per vehicle type [World Conference on Transport Research - WCTR 2016 Shanghai. 10-15 July 2016]. *Transportation Research Procedia*, *25*, 2076–2083. <https://doi.org/10.1016/j.trpro.2017.05.401>
- Gioldasis, C., Christoforou, Z., & Seidowsky, R. (2021). Risk-taking behaviors of e-scooter users: A survey in paris. *Accident Analysis and Prevention*, *163*, 106427. <https://doi.org/10.1016/j.aap.2021.106427>
- Gitelman, V., Doveh, E., & Bekhor, S. (2017). The relationship between free-flow travel speeds, infrastructure characteristics and accidents, on single-carriageway roads [World Conference on Transport Research - WCTR 2016 Shanghai. 10-15 July 2016]. *Transportation Research Procedia*, *25*, 2026–2043. <https://doi.org/10.1016/j.trpro.2017.05.398>
- Gitelman, V., Doveh, E., Carmel, R., & Pesahov, F. The relationship between road accidents and infrastructure characteristics of low-volume roads in israel. In: *Proceedings of second international conference on traffic and transport engineering (ictte)*. Belgrade , Serbia: City Net Scientific Research Center Ltd. Belgrade, 2014, November, 350–358. <https://trid.trb.org/view/1409525>
- Golob, T. F., Recker, W. W., & Alvarez, V. M. (2004). Freeway safety as a function of traffic flow. *Accident Analysis and Prevention*, *36*(6), 933–946. <https://doi.org/10.1016/j.aap.2003.09.006>
- Gong, Z., Ma, Q., Kan, C., & Qi, Q. (2019). Classifying street spaces with street view images for a spatial indicator of urban functions. *Sustainability*, *11*(22). <https://doi.org/10.3390/su11226424>
- Hamim, O. F., & Ukkusuri, S. V. (2024). Towards safer streets: A framework for unveiling pedestrians' perceived road safety using street view imagery. *Accident Analysis and Prevention*, *195*, 107400. <https://doi.org/10.1016/j.aap.2023.107400>
- Hanibuchi, T., Nakaya, T., & Inoue, S. (2019). Virtual audits of streetscapes by crowdworkers. *Health and Place*, *59*, 102203. <https://doi.org/10.1016/j.healthplace.2019.102203>
- Hanson, C. S., Noland, R. B., & Brown, C. (2013). The severity of pedestrian crashes: An analysis using google street view imagery. *Journal of Transport Geography*, *33*, 42–53. <https://doi.org/10.1016/j.jtrangeo.2013.09.002>
- Harbrecht, A., Hackl, M., Leschinger, T., Uschok, S., Wegmann, K., Eysel, P., & Müller, L. P. (2022). What to expect? injury patterns of electric-scooter accidents over a period of one year - a prospective monocentric study at a level 1 trauma center. *European Journal of Orthopaedic Surgery and Traumatology*, *32*, 641–647. <https://doi.org/10.1007/s00590-021-03014-z>
- Harms, P. L. (1993). *Crash injury investigation and injury mechanisms in road traffic accidents*. Her Majesty Stationary Office. <http://worldcat.org/isbn/0115511903>
- Hastie, T. (1990). *Generalized additive models (1st ed.)* Routledge. <https://doi.org/10.1201/9780203753781>

- Hayashi, T., Cimr, D., Fujita, H., & Cimler, R. (2023). Image entropy equalization: A novel preprocessing technique for image recognition tasks. *Information Sciences*, *647*, 119539. <https://doi.org/10.1016/j.ins.2023.119539>
- Haynes, R., Jones, A., Kennedy, V., Harvey, I., & Jewell, T. (2007). District variations in road curvature in England and Wales and their association with road-traffic crashes. *Environment and Planning A*, *39*, 1222–1237. <https://doi.org/10.1068/a38106>
- He, T., Chen, J., Kang, L., & Zhu, Q. (2024). Evaluation of global-scale and local-scale optimized segmentation algorithms in geobias with SAM on land use and land cover. *IEEE Journal of Selected Topics in Applied Earth Observations and Remote Sensing*, *17*, 6721–6738. <https://doi.org/10.1109/JSTARS.2024.3373385>
- He, Y., Wang, J., Zhang, Y., & Liao, C. (2024). An efficient urban flood mapping framework towards disaster response driven by weakly supervised semantic segmentation with decoupled training samples. *ISPRS Journal of Photogrammetry and Remote Sensing*, *207*, 338–358. <https://doi.org/10.1016/j.isprsjprs.2023.12.009>
- Hels, T., & Orozova-Bekkevold, I. (2007). The effect of roundabout design features on cyclist accident rate. *Accident Analysis and Prevention*, *39*(2), 300–307. <https://doi.org/10.1016/j.aap.2006.07.008>
- Hollingsworth, J., Copeland, B., & Johnson, J. X. (2019). Are e-scooters polluters? the environmental impacts of shared dockless electric scooters. *Environmental Research Letters*, *14*(8), 084031. <https://doi.org/10.1088/1748-9326/ab2da8>
- Hosseinzadeh, A., Algomaiah, M., Kluger, R., & Li, Z. (2021). E-scooters and sustainability: Investigating the relationship between the density of e-scooter trips and characteristics of sustainable urban development. *Sustainable Cities and Society*, *66*, 102624. <https://doi.org/10.1016/j.scs.2020.102624>
- Hu, S., Xing, H., Luo, W., Wu, L., Xu, Y., Huang, W., Liu, W., & Li, T. (2023). Uncovering the association between traffic crashes and street-level built-environment features using street view images. *International Journal of Geographical Information Science*, *37*, 2367–2391. <https://doi.org/10.1080/13658816.2023.2254362>
- Huck, S. W., Cross, T. L., & Clark, S. B. (1986). Overcoming misconceptions about z-scores. *Teaching Statistics*, *8*(2), 38–40. <https://doi.org/10.1111/j.1467-9639.1986.tb00624.x>
- Iio, K., Guo, X., & Lord, D. (2021). Examining driver distraction in the context of driving speed: An observational study using disruptive technology and naturalistic data. *Accident Analysis and Prevention*, *153*, 105983. <https://doi.org/10.1016/j.aap.2021.105983>
- International Transport Forum. (2020). Safe micromobility. <https://www.itf-oecd.org/safe-micromobility>
- International Transport Forum. (2021). *Road safety annual report 2021*. <https://doi.org/https://doi.org/10.1787/9cfe972-en>
- International Transport Forum. (2024). Safer micromobility. <https://www.itf-oecd.org/safe-micromobility>
- Ito, K., & Biljecki, F. (2021). Assessing bikeability with street view imagery and computer vision. *Transportation Research Part C: Emerging Technologies*, *132*, 103371. <https://doi.org/10.1016/j.trc.2021.103371>

- Ivan, J. N., Wang, C., & Bernardo, N. R. (2000). Explaining two-lane highway crash rates using land use and hourly exposure. *Accident Analysis and Prevention*, *32*(6), 787–795. [https://doi.org/10.1016/S0001-4575\(99\)00132-3](https://doi.org/10.1016/S0001-4575(99)00132-3)
- Jahangiri, A., Rakha, H., & Dingus, T. A. (2016). Red-light running violation prediction using observational and simulator data. *Accident Analysis and Prevention*, *96*, 316–328. <https://doi.org/10.1016/j.aap.2016.06.009>
- Ji, G.-P., Fan, D.-P., Xu, P., Zhou, B., Cheng, M.-M., & Van Gool, L. (2023). Sam struggles in concealed scenes — empirical study on “segment anything”. *Science China Information Sciences*, *66*(12). <https://doi.org/10.1007/s11432-023-3881-x>
- Ji, W., Li, J., Bi, Q., Liu, T., Li, W., & Cheng, L. (2023). Segment anything is not always perfect: An investigation of sam on different real-world applications. <https://doi.org/10.48550/arXiv.2304.05750>
- JONES, I. (1976). Chapter 1 - the use of accident analysis in determining how vehicle characteristics may contribute to causing accidents. In I. JONES (Ed.), *The effect of vehicle characteristics on road accidents* (pp. 1–33). Pergamon. <https://doi.org/10.1016/B978-0-08-018963-5.50004-6>
- Karpinski, E., Bayles, E., Daigle, L., & Mantine, D. (2022). Characteristics of early shared e-scooter fatalities in the united states 2018–2020. *Safety Science*, *153*, 105811. <https://doi.org/10.1016/j.ssci.2022.105811>
- Kazemzadeh, K., Haghani, M., & Sprei, F. (2023). Electric scooter safety: An integrative review of evidence from transport and medical research domains. *Sustainable Cities and Society*, *89*. <https://doi.org/10.1016/j.scs.2022.104313>
- Kazemzadeh, K., & Sprei, F. (2022). Towards an electric scooter level of service: A review and framework. *Travel Behaviour and Society*, *29*, 149–164. <https://doi.org/10.1016/j.tbs.2022.06.005>
- Keralis, J. M., Javanmardi, M., Khanna, S., Dwivedi, P., Huang, D., Tasdizen, T., & Nguyen, Q. C. (2020). Health and the built environment in united states cities: Measuring associations using google street view-derived indicators of the built environment. *BMC Public Health*, *20*, 215. <https://doi.org/10.1186/s12889-020-8300-1>
- Kim, S., Kim, D., & Choi, S. (2020). Citycraft: 3d virtual city creation from a single image. *The Visual Computer*, *36*, 911–924. <https://doi.org/10.1007/s00371-019-01701-x>
- Kirillov, A., Mintun, E., Ravi, N., Mao, H., Rolland, C., Gustafson, L., Xiao, T., Whitehead, S., Berg, A. C., Lo, W.-Y., Dollár, P., & Girshick, R. (2023). Segment anything. <http://arxiv.org/abs/2304.02643>
- Kita-Wojciechowska, K., & Kidziński, Ł. (2019). Google street view image predicts car accident risk. *Central European Economic Journal*, *6*(53), 151–163. <https://doi.org/doi:10.2478/ceej-2019-0011>
- Kleinertz, H., Ntalos, D., Hennes, F., Nüchtern, J. V., Frosch, K.-H., & Thiesen, D. M. (2021). Accident mechanisms and injury patterns in e-scooter users. a retrospective analysis and comparison with cyclists. *Deutsches Arzteblatt International*, *118*, 117–121. <https://doi.org/10.3238/arztebl.m2021.0019>

- Kong, W., Zhong, T., Mai, X., Zhang, S., Chen, M., & Lv, G. (2022). Automatic detection and assessment of pavement marking defects with street view imagery at the city scale. *Remote Sensing*, *14*. <https://doi.org/10.3390/rs14164037>
- Kononov, J., Bailey, B., & Allery, B. K. (2008). Relationships between safety and both congestion and number of lanes on urban freeways. *Transportation Research Record*, *2083*(1), 26–39. <https://doi.org/10.3141/2083-04>
- Kwon, J.-H., & Cho, G.-H. (2020). An examination of the intersection environment associated with perceived crash risk among school-aged children: Using street-level imagery and computer vision. *Accident Analysis and Prevention*, *146*, 105716. <https://doi.org/10.1016/j.aap.2020.105716>
- Levulytė, L., Baranyai, D., Sokolovskij, E., & Török, Á. (2017). Pedestrians' role in road accidents. *International Journal for Traffic and Transport Engineering*, *7*(3), 328–341. [https://doi.org/10.7708/ijtte.2017.7\(3\).04](https://doi.org/10.7708/ijtte.2017.7(3).04)
- Li, X., Ning, H., Huang, X., Dadashova, B., Kang, Y., & Ma, A. (2022). Urban infrastructure audit: An effective protocol to digitize signalized intersections by mining street view images. *Cartography and Geographic Information Science*, *49*, 32–49. <https://doi.org/10.1080/15230406.2021.1992299>
- Li, Y., Chen, Y., Rajabifard, A., Khoshelham, K., & Aleksandrov, M. (2018). Estimating Building Age from Google Street View Images Using Deep Learning. In S. Winter, A. Griffin, & M. Sester (Eds.), *10th international conference on geographic information science (gis-science 2018)* (40:1–40:7, Vol. 114). Schloss Dagstuhl – Leibniz-Zentrum für Informatik. <https://doi.org/10.4230/LIPIcs.GISCIENCE.2018.40>
Keywords: Building database, deep learning, CNN, SVM, Google Street View.
- Li, Y., Yabuki, N., & Fukuda, T. (2022). Measuring visual walkability perception using panoramic street view images, virtual reality, and deep learning. *Sustainable Cities and Society*, *86*, 104140. <https://doi.org/10.1016/j.scs.2022.104140>
- Liao, F., & Correia, G. (2022). Electric carsharing and micromobility: A literature review on their usage pattern, demand, and potential impacts [doi: 10.1080/15568318.2020.1861394]. *International Journal of Sustainable Transportation*, *16*, 269–286. <https://doi.org/10.1080/15568318.2020.1861394>
- Linhart, C., Jägerhuber, L., Ehrnthaller, C., Schrempf, J., Kußmaul, A. C., Neuerburg, C., Böcker, W., & Lampert, C. (2024). E-scooter accidents—epidemiology and injury patterns: 3-year results from a level 1 trauma center in germany. *Archives of Orthopaedic and Trauma Surgery*. <https://doi.org/10.1007/s00402-024-05209-5>
- Lord, D., Manar, A., & Vizioli, A. (2005). Modeling crash-flow-density and crash-flow-v/c ratio relationships for rural and urban freeway segments. *Accident Analysis and Prevention*, *37*(1), 185–199. <https://doi.org/10.1016/j.aap.2004.07.003>
- Lord, D., Qin, X., & Geedipally, S. R. (2021). Chapter 9 - models for spatial data. In D. Lord, X. Qin, & S. R. Geedipally (Eds.), *Highway safety analytics and modeling* (pp. 299–334). Elsevier. <https://doi.org/10.1016/B978-0-12-816818-9.00009-3>
- Ma, Q., Yang, H., Mayhue, A., Sun, Y., Huang, Z., & Ma, Y. (2021). E-scooter safety: The riding risk analysis based on mobile sensing data. *Accident Analysis and Prevention*, *151*, 105954. <https://doi.org/10.1016/j.aap.2020.105954>

- Mamidala, R. S., Uthkota, U., Shankar, M. B., Antony, A. J., & Narasimhadhan, A. V. (2019). Dynamic approach for lane detection using google street view and cnn. *TENCON 2019 - 2019 IEEE Region 10 Conference (TENCON)*, 2454–2459. <https://doi.org/10.1109/TENCON.2019.8929655>
- Manap, N., Borhan, M. N., Yazid, M. M. R., Manap, N., & Wahid, N. A. (2021). An overview of heavy vehicle accidents characteristic on expressways in malaysia. *IOP Conference Series: Materials Science and Engineering*, 1144(1), 012087. <https://doi.org/10.1088/1757-899X/1144/1/012087>
- Martin, J.-L. (2002). Relationship between crash rate and hourly traffic flow on interurban motorways. *Accident Analysis and Prevention*, 34(5), 619–629. [https://doi.org/10.1016/S0001-4575\(01\)00061-6](https://doi.org/10.1016/S0001-4575(01)00061-6)
- Middel, A., Lukaszcyk, J., Zakrzewski, S., Arnold, M., & Maciejewski, R. (2019). Urban form and composition of street canyons: A human-centric big data and deep learning approach. *Landscape and Urban Planning*, 183, 122–132. <https://doi.org/10.1016/j.landurbplan.2018.12.001>
- Milton, J., & Mannering, F. (1998, November). The relationship among highway geometrics, traffic-related elements and motor-vehicle accident frequencies. <https://doi.org/10.1023/A:1005095725001>
- Minaee, S., Boykov, Y., Porikli, F., Plaza, A., Kehtarnavaz, N., & Terzopoulos, D. (2022). Image segmentation using deep learning: A survey. *IEEE Transactions on Pattern Analysis and Machine Intelligence*, 44(7), 3523–3542. <https://doi.org/10.1109/TPAMI.2021.3059968>
- Mitropoulos, L., Stavropoulou, E., Tzouras, P., Karolemeas, C., & Kepaptsoglou, K. (2023). E-scooter micromobility systems: Review of attributes and impacts. *Transportation Research Interdisciplinary Perspectives*, 21, 100888. <https://doi.org/10.1016/j.trip.2023.100888>
- More, A. S., & Rana, D. P. (2017). Review of random forest classification techniques to resolve data imbalance. *2017 1st International Conference on Intelligent Systems and Information Management (ICISIM)*, 72–78. <https://doi.org/10.1109/ICISIM.2017.8122151>
- Narváez, Y. V., Sierra, V. P., Cárdenas, F. P., Ramos, L. R., González, B. Z., Martínez, J. I. V., & Aranda, O. M. (2019). Road risk behaviors: Pedestrian experiences [PMID: 30971147]. *Traffic Injury Prevention*, 20(3), 303–307. <https://doi.org/10.1080/15389588.2019.1573318>
- Navin, F., Zein, S., & Felipe, E. (2000). Road safety engineering: An effective tool in the fight against whiplash injuries. *Accident Analysis and Prevention*, 32(2), 271–275. [https://doi.org/10.1016/S0001-4575\(99\)00077-9](https://doi.org/10.1016/S0001-4575(99)00077-9)
- Niemann, M., Braun, K. F., Otto, E., Tiefenbrunner, M., Wüster, J., Stöckle, U., Ahmad, S. S., Märdian, S., & Graef, F. (2023). Dangers of e-mobility: A systematic review and meta-analysis of sustained injury patterns and injury severity. *Safety Science*, 167, 106283. <https://doi.org/10.1016/j.ssci.2023.106283>
- Ning, H., Ye, X., Chen, Z., Liu, T., & Cao, T. (2022). Sidewalk extraction using aerial and street view images. *Environment and Planning B: Urban Analytics and City Science*, 49, 7–22. <https://doi.org/10.1177/2399808321995817>

- Noland, R. B., & Oh, L. (2004). The effect of infrastructure and demographic change on traffic-related fatalities and crashes: A case study of illinois county-level data. *Accident Analysis and Prevention*, *36*(4), 525–532. [https://doi.org/10.1016/S0001-4575\(03\)00058-7](https://doi.org/10.1016/S0001-4575(03)00058-7)
- Noland, R. B., & Quddus, M. A. (2005). Congestion and safety: A spatial analysis of london. *Transportation Research Part A: Policy and Practice*, *39*(7), 737–754. <https://doi.org/10.1016/j.tra.2005.02.022>
- Oeschger, G., Carroll, P., & Caulfield, B. (2020). Micromobility and public transport integration: The current state of knowledge. *Transportation Research Part D: Transport and Environment*, *89*, 102628. <https://doi.org/10.1016/j.trd.2020.102628>
- Ogawa, M., & Aizawa, K. (2019). Identification of buildings in street images using map information. *2019 IEEE International Conference on Image Processing (ICIP)*, 984–988. <https://doi.org/10.1109/ICIP.2019.8803066>
- O’Hern, S., & Estgfaeller, N. (2020). A scientometric review of powered micromobility. *Sustainability*, *12*(22). <https://doi.org/10.3390/su12229505>
- Oscro, L. P., Wu, Q., de Lemos, E. L., Gonçalves, W. N., Ramos, A. P. M., Li, J., & Marcato, J. (2023). The segment anything model (sam) for remote sensing applications: From zero to one shot. *International Journal of Applied Earth Observation and Geoinformation*, *124*, 103540. <https://doi.org/10.1016/j.jag.2023.103540>
- Paleti, R., Eluru, N., & Bhat, C. R. (2010). Examining the influence of aggressive driving behavior on driver injury severity in traffic crashes. *Accident Analysis and Prevention*, *42*(6), 1839–1854. <https://doi.org/10.1016/j.aap.2010.05.005>
- Papadimitriou, E., Filtness, A., Theofilatos, A., Ziakopoulos, A., Quigley, C., & Yannis, G. (2019). Review and ranking of crash risk factors related to the road infrastructure. *Accident Analysis and Prevention*, *125*, 85–97. <https://doi.org/10.1016/j.aap.2019.01.002>
- Pljakić, M., Jovanović, D., & Matović, B. (2022). The influence of traffic-infrastructure factors on pedestrian accidents at the macro-level: The geographically weighted regression approach. *Journal of Safety Research*, *83*, 248–259. <https://doi.org/10.1016/j.jsr.2022.08.021>
- Pobudzei, M., Tießler, M., Sellaouti, A., & Hoffmann, S. E-scooter and bicycle accidents: Spatial, temporal, and demographic characteristics in munich, germany. In: In *Transportation research board 102nd annual meeting*. Washington DC, United States, 2023, January. <https://trid.trb.org/View/2117763>
- Präsidialdepartement. (2022). Zürich in zahlen [Accessed: 2024-04-02]. *Stadt Zürich*. https://www.stadt-zuerich.ch/portal/de/index/portraet_der_stadt_zuerich/zuerich_in_zahlen.html
- Präsidialdepartement. (2024). Stadt zürich 2023: Zunahme der bevölkerungszahl, rückgang der geburten [Accessed: 2024-04-02]. *Stadt Zürich*. https://www.stadt-zuerich.ch/content/prd/de/index/statistik/publikationen-angebote/publikationen/webartikel/2024-02-13_Stadt-Zuerich-2023-Zunahme-der-Bevoelkerungszahl-Rueckgang-der-Geburten.html
- Rahman, M. M., Sainju, A. M., Yan, D., & Jiang, Z. (2021). Mapping road safety barriers across street view image sequences: A hybrid object detection and recurrent model. *Proceedings of the 4th ACM SIGSPATIAL International Workshop on AI for Geographic Knowledge Discovery, GeoAI 2021*, 47–50. <https://doi.org/10.1145/3486635.3491074>

- Reck, D. J., & Axhausen, K. W. (2021). Who uses shared micro-mobility services? empirical evidence from zurich, switzerland. *Transportation Research Part D: Transport and Environment*, 94. <https://doi.org/10.1016/j.trd.2021.102803>
- Reck, D. J., Haitao, H., Guidon, S., & Axhausen, K. W. (2021). Explaining shared micromobility usage, competition and mode choice by modelling empirical data from zurich, switzerland. *Transportation Research Part C: Emerging Technologies*, 124. <https://doi.org/10.1016/j.trc.2020.102947>
- Ren, M., Zhang, X., Chen, X., Zhou, B., & Feng, Z. (2023). Yolov5s-m: A deep learning network model for road pavement damage detection from urban street-view imagery. *International Journal of Applied Earth Observation and Geoinformation*, 120. <https://doi.org/10.1016/j.jag.2023.103335>
- Riggs, W., Kawashima, M., & Batstone, D. (2021). Exploring best practice for municipal e-scooter policy in the united states. *Transportation Research Part A: Policy and Practice*, 151, 18–27. <https://doi.org/10.1016/j.tra.2021.06.025>
- Rita, L., Peliteiro, M., Bostan, T.-C., Tamagusko, T., & Ferreira, A. (2023). Using deep learning and google street view imagery to assess and improve cyclist safety in london. *Sustainability*, 15(13). <https://doi.org/10.3390/su151310270>
- Rodionova, M., Skhvediani, A., & Kudryavtseva, T. (2022). Prediction of crash severity as a way of road safety improvement: The case of saint petersburg, russia. *Sustainability*, 14(16). <https://doi.org/10.3390/su14169840>
- Romero, L. M., Guerrero, J. A., & Romero, G. (2021, November). Road curb detection: A historical survey. <https://doi.org/10.3390/s21216952>
- Sainju, A. M., & Jiang, Z. (2020). Mapping road safety features from streetview imagery: A deep learning approach. *ACM/IMS Trans. Data Sci.*, 1(3). <https://doi.org/10.1145/3362069>
- Scott, D. (2015). *Multivariate density estimation: Theory, practice, and visualization*. Wiley. <https://books.google.ch/books?id=pIAZBwAAQBAJ>
- Şengül, B., & Mostofi, H. (2021). Impacts of e-micromobility on the sustainability of urban transportation—a systematic review. *Applied Sciences (Switzerland)*, 11. <https://doi.org/10.3390/app11135851>
- Shah, N. R., Aryal, S., Wen, Y., & Cherry, C. R. (2021). Comparison of motor vehicle-involved e-scooter and bicycle crashes using standardized crash typology. *Journal of Safety Research*, 77, 217–228. <https://doi.org/10.1016/j.jsr.2021.03.005>
- Shaheen, S., & Cohen, A. (2019). Shared micromobility policy toolkit: Docked and dockless bike and scooter sharing. *UC Berkeley: Transportation Sustainability Research Center*. <https://doi.org/10.7922/G2TH8JW7>
- Shankar, V., Mannering, F., & Barfield, W. (1995). Effect of roadway geometrics and environmental factors on rural freeway accident frequencies. *Accident Analysis and Prevention*, 27(3), 371–389. [https://doi.org/10.1016/0001-4575\(94\)00078-Z](https://doi.org/10.1016/0001-4575(94)00078-Z)
- Shankar, V., Mannering, F., & Barfield, W. (1996). Statistical analysis of accident severity on rural freeways. *Accident Analysis and Prevention*, 28(3), 391–401. [https://doi.org/10.1016/0001-4575\(96\)00009-7](https://doi.org/10.1016/0001-4575(96)00009-7)
- Shannon, C. E. (1948). A mathematical theory of communication. *The Bell System Technical Journal*, 27(3), 379–423. <https://doi.org/10.1002/j.1538-7305.1948.tb01338.x>

- Shivangi Srivastava, S. L., John E. Vargas Muñoz, & Tuia, D. (2020). Fine-grained landuse characterization using ground-based pictures: A deep learning solution based on globally available data. *International Journal of Geographical Information Science*, *34*(6), 1117–1136. <https://doi.org/10.1080/13658816.2018.1542698>
- Singh, H., & Kathuria, A. (2021). Analyzing driver behavior under naturalistic driving conditions: A review. *Accident Analysis and Prevention*, *150*, 105908. <https://doi.org/10.1016/j.aap.2020.105908>
- Singh, P., Jami, M., Geller, J., Granger, C., Geaney, L., & Aiyer, A. (2022). The impact of e-scooter injuries: A systematic review of 34 studies. *3*(9), 674–683. <https://doi.org/10.1302/2633-1462.39.BJO-2022-0096.R1>
- Sohail, A., Cheema, M. A., Ali, M. E., Toosi, A. N., & Rakha, H. A. (2023). Data-driven approaches for road safety: A comprehensive systematic literature review. *Safety Science*, *158*, 105949. <https://doi.org/10.1016/j.ssci.2022.105949>
- Solero, L. (2001). Nonconventional on-board charger for electric vehicle propulsion batteries. *IEEE Transactions on Vehicular Technology*, *50*(1), 144–149. <https://doi.org/10.1109/25.917904>
- Steinmetz-Wood, M., El-Geneidy, A., & Ross, N. A. (2020). Moving to policy-amenable options for built environment research: The role of micro-scale neighborhood environment in promoting walking. *Health and Place*, *66*, 102462. <https://doi.org/10.1016/j.healthplace.2020.102462>
- Stigson, H., Malakuti, I., & Klingegård, M. (2021). Electric scooters accidents: Analyses of two swedish accident data sets. *Accident Analysis and Prevention*, *163*, 106466. <https://doi.org/10.1016/j.aap.2021.106466>
- Stiles, J., Li, Y., & Miller, H. J. (2022). How does street space influence crash frequency? an analysis using segmented street view imagery. *Environment and Planning B: Urban Analytics and City Science*, *49*(9), 2467–2483. <https://doi.org/10.1177/23998083221090962>
- Sultan, R. I., Li, C., Zhu, H., Khanduri, P., Brocanelli, M., & Zhu, D. (2024). Geosam: Fine-tuning sam with sparse and dense visual prompting for automated segmentation of mobility infrastructure. <https://doi.org/10.48550/arXiv.2311.11319>
- Tanishita, M., Sekiguchi, Y., & Sunaga, D. (2023). Impact analysis of road infrastructure and traffic control on severity of pedestrian–vehicle crashes at intersections and non-intersections using bias-reduced logistic regression. *IATSS Research*, *47*(2), 233–239. <https://doi.org/10.1016/j.iatssr.2023.03.004>
- United Nations. (2015). Transforming our world: The 2030 agenda for sustainable development. <https://wedocs.unep.org/20.500.11822/9814>
- United Nations. (2020). Improving global road safety : Resolution / adopted by the general assembly. *UN. General Assembly (74th sess.:2019-2020)*. <https://digitallibrary.un.org/record/3879711>
- Useche, S. A., Gonzalez-Marin, A., Faus, M., & Alonso, F. (2022). Environmentally friendly, but behaviorally complex? a systematic review of e-scooter riders' psychosocial risk features. *PLOS ONE*, *17*(5), 1–20. <https://doi.org/10.1371/journal.pone.0268960>

- Vlahogianni, E. I., Yannis, G., & Golias, J. C. (2012). Overview of critical risk factors in power-two-wheeler safety. *Accident Analysis and Prevention*, *49*, 12–22. <https://doi.org/10.1016/j.aap.2012.04.009>
- Wang, B., Hallmark, S., Savolainen, P., & Dong, J. (2017). Crashes and near-crashes on horizontal curves along rural two-lane highways: Analysis of naturalistic driving data. *Journal of Safety Research*, *63*, 163–169. <https://doi.org/10.1016/j.jsr.2017.10.001>
- Wang, C., Quddus, M. A., & Ison, S. G. (2013). The effect of traffic and road characteristics on road safety: A review and future research direction. *Safety Science*, *57*, 264–275. <https://doi.org/10.1016/j.ssci.2013.02.012>
- Wang, Y., Liu, D., & Luo, J. (2022). Identification and improvement of hazard scenarios in non-motorized transportation using multiple deep learning and street view images. *International Journal of Environmental Research and Public Health*, *19*(21). <https://doi.org/10.3390/ijerph192114054>
- Waskom, M. L. (2021). Seaborn: Statistical data visualization. *Journal of Open Source Software*, *6*(60), 3021. <https://doi.org/10.21105/joss.03021>
- White, E., Guo, F., Han, S., Mollenhauer, M., Broaddus, A., Sweeney, T., Robinson, S., Novotny, A., & Buehler, R. (2023). What factors contribute to e-scooter crashes: A first look using a naturalistic riding approach. *Journal of Safety Research*, *85*, 182–191. <https://doi.org/10.1016/j.jsr.2023.02.002>
- World Health Organization. (2021). Global plan for the decade of action for road safety 2021–2030. *Safety and Mobility*. <https://www.who.int/publications/m/item/global-plan-for-the-decade-of-action-for-road-safety-2021-2030>
- World Health Organization. (2023, December 13). Road traffic injuries. <https://www.who.int/news-room/fact-sheets/detail/road-traffic-injuries>
- Xia, J., Gong, G., Liu, J., Zhu, Z., & Tang, H. (2023). Pedestrian accessible infrastructure inventory: Assessing zero-shot segmentation on multi-mode geospatial data for all pedestrian types. <https://doi.org/10.48550/arXiv.2310.09918>
- Yang, C., Forest, J., Einhorn, M., & Cleland, T. A. (2023). Automated behavioral analysis using instance segmentation. <https://doi.org/10.48550/arXiv.2312.07723>
- Yang, H., Ma, Q., Wang, Z., Cai, Q., Xie, K., & Yang, D. (2020). Safety of micro-mobility: Analysis of e-scooter crashes by mining news reports. *Accident Analysis and Prevention*, *143*, 105608. <https://doi.org/10.1016/j.aap.2020.105608>
- Yang, R., He, G., Yin, R., Wang, G., Zhang, Z., Long, T., & Peng, Y. (2024). Weakly-supervised extraction of rooftop photovoltaics from high-resolution images based on segment anything model and class activation map. *Applied Energy*, *361*, 122964. <https://doi.org/https://doi.org/10.1016/j.apenergy.2024.122964>
- Ye, Y., Zeng, W., Shen, Q., Zhang, X., & Lu, Y. (2019). The visual quality of streets: A human-centred continuous measurement based on machine learning algorithms and street view images. *Environment and Planning B: Urban Analytics and City Science*, *46*(8), 1439–1457. <https://doi.org/10.1177/2399808319828734>
- Yencha, C. (2019). Valuing walkability: New evidence from computer vision methods. *Transportation Research Part A: Policy and Practice*, *130*, 689–709. <https://doi.org/10.1016/j.tra.2019.09.053>

- Yeo, I.-K., & Johnson, R. A. (2000). A new family of power transformations to improve normality or symmetry. *Biometrika*, *87*(4), 954–959. <https://doi.org/10.1093/biomet/87.4.954>
- Yilmaz, E. O., & Kavzoglu, T. (2024). Quality assessment for multi-resolution segmentation and segment-anything model using worldview-3 imagery. *The International Archives of the Photogrammetry, Remote Sensing and Spatial Information Sciences*, *XLVIII-4/W9-2024*, 383–390. <https://doi.org/10.5194/isprs-archives-XLVIII-4-W9-2024-383-2024>
- Yu, Q., Wang, C., McKenna, F., Yu, S. X., Taciroglu, E., Cetiner, B., & Law, K. H. (2020). Rapid visual screening of soft-story buildings from street view images using deep learning classification. *Earthquake Engineering and Engineering Vibration*, *19*, 827–838. <https://doi.org/10.1007/s11803-020-0598-2>
- Yu, X., Ma, J., Tang, Y., Yang, T., & Jiang, F. (2024). Can we trust our eyes? interpreting the misperception of road safety from street view images and deep learning. *Accident Analysis and Prevention*, *197*, 107455. <https://doi.org/10.1016/j.aap.2023.107455>
- Zhang, C., Liu, L., Cui, Y., Huang, G., Lin, W., Yang, Y., & Hu, Y. (2023). A comprehensive survey on segment anything model for vision and beyond. <http://arxiv.org/abs/2305.08196>
- Zhang, L., Pei, T., Wang, X., Wu, M., Song, C., Guo, S., & Chen, Y. (2020). Quantifying the urban visual perception of chinese traditional-style building with street view images. *Applied Sciences*, *10*(17). <https://doi.org/10.3390/app10175963>
- Zhang, Y., Shen, Z., & Jiao, R. (2024). Segment anything model for medical image segmentation: Current applications and future directions. *Computers in Biology and Medicine*, *171*, 108238. <https://doi.org/10.1016/j.combiomed.2024.108238>
- Zheng, H., Zhang, C., Guan, K., Deng, Y., Wang, S., Rhoads, B. L., Margenot, A. J., Zhou, S., & Wang, S. (2023). Segment any stream: Scalable water extent detection with the segment anything model. *NeurIPS 2023 Computational Sustainability: Promises and Pitfalls from Theory to Deployment*. <https://openreview.net/forum?id=BaZZzH7EgA>
- Zhou, M., & Sisiopiku, V. P. (1997). Relationship between volume-to-capacity ratios and accident rates. *Transportation Research Record*, *1581*(1), 47–52. <https://doi.org/10.3141/1581-06>

Personal declaration

I hereby declare that the submitted thesis is the result of my own, independent work.

All external sources are explicitly acknowledged in the thesis.

A handwritten signature in black ink, appearing to read 'Yelu He', is centered on the page. The signature is written in a cursive style.

Yelu He

Zurich, 30.04.2024